THESIS

This is to certify that the

dissertation entitled

Biochemical Mechanisms of
Acetaminophen Nephrotoxicity

presented by

John F. Newton, Jr.

has been accepted towards fulfillment
of the requirements for

Ph.D. degree in Environmental Toxicology/
Pharmacology

Major professor

Date April 19, 1983

BIOCHEMICAL MECHANISMS OF ACETAMINOPHEN NEPHROTOXICITY

By

John F. Newton, Jr.

A DISSERTATION

Submitted to
Michigan State University
in partial fulfillment of the requirements
for the degree of

DOCTOR OF PHILOSOPHY

Department of Pharmacology and Toxicology

1983

me
of
re
wi
45
re
el
te
va
co

Cr
li
A
fo
ad
ig

ABSTRACT

BIOCHEMICAL MECHANISMS OF ACETAMINOPHEN NEPHROTOXICITY

By

John F. Newton, Jr.

Metabolism of acetaminophen (APAP) to a reactive arylating intermediate has been postulated to be a requisite step in the pathogenesis of APAP-induced renal cortical necrosis. At least two different mechanisms for the generation of reactive intermediates from APAP within the renal cortex have been suggested: (1) Direct cytochrome P-450-dependent activation; or (2) deacetylation prior to the renal metabolism of the deacetylated product, p-aminophenol (PAP), to an electrophilic intermediate. The purpose of this investigation was to test the hypothesis that PAP formation and subsequent metabolic activation are requisite steps in the pathogenesis of APAP-induced renal cortical necrosis.

Urinary PAP excretion, measured as an index of PAP formation, increased with increasing doses of APAP. In addition, APAP was metabolized to PAP in isolated kidneys and in renal cortical homogenates. A reactive arylating intermediate was detected subsequent to PAP formation from APAP in renal cortical 10,000 x g supernatants. PAP administration to F344 rats resulted in renal lesions qualitatively identical to those observed following APAP administration. However,

PAP w

funct

necro

appro

neph

ates

F344

phat

of P

F344

with

an ob

PAP was 5-10 times more nephrotoxic than APAP as determined by renal functional and histopathological evaluations.

The relevance of PAP formation to APAP-induced renal cortical necrosis was established with three different types of experimental approaches: (1) Strain differences in susceptibility to APAP-induced nephrotoxicity were related to the formation of arylating intermediates *in vivo* by a deacetylase-dependent mechanism; (2) pretreatment of F344 rats with the deacetylase inhibitor, bis-(p-nitrophenyl)phosphate, reduced the nephrotoxicity of acetaminophen and the formation of PAP; and (3) administration of specifically labelled [^{14}C]-APAP to F344 rats indicated that a large portion of arylating intermediates within the kidney originated from PAP.

These investigations support the hypothesis that deacetylation is an obligatory event in the pathogenesis of APAP-induced renal necrosis.

My m

With

this

dedi

advi

see-

deep

to e

and

for

than

Brod

deep

intel

the

Ken

and

Hook,

throu

ACKNOWLEDGEMENTS

The following pages are a culmination of the unwavering support my mother and father have provided me over the past twenty-six years. Without their constant guidance, love and comfort it is my belief that this thesis would not have been possible. Therefore, this thesis is dedicated to my mother and father for they have been my most important advisors, my greatest fans and my financial support throughout my seemingly endless years of education. Words alone cannot express how deeply grateful I am for all my parents have done for me. I also wish to express my appreciation to my brother and sisters Reed, Christine and Mary Ellen and to my Aunt, Shirley Hespelt.

I would like to express appreciation to the Monsanto Foundation for the financial support of my graduate training. I would like to thank Drs. Robert Roth, Emmett Braselton, Philip Watanabe and Theodore Brody for constructive criticism of the dissertation research. I am deeply grateful to Drs. Gilbert Mudge and Mark Gemborys for their intellectual guidance throughout the project. I would like to thank the many collaborators involved in this research, Drs. Jay Bernstein, Ken Yoshimoto, Steve Kuo, and Glenn Rush and Dale Pasino, Diane Hoefle and Marc Bailie. I am deeply indebted to my mentor, Dr. Jerry B. Hook, for the financial and moral support and intellectual guidance throughout my undergraduate and graduate studies.

I w

of chick

like to

Erickson

excellen

A v

deep fri

their st

Diane, w

through

I would like to thank Diane Hummel for the excellent translation of chicken scrawl in the preparation of this thesis. I would also like to thank Bruce Hook, Carmel Clarke, Julie Baughman-Howe, David Erickson, Julie Eldredge, Debra Finucan, and Gay DeShone for their excellent technical assistance.

A very special thanks goes to Diane and the Short Boys for the deep friendship over the many years. These people never wavered in their staunch support of me. For this I am sincerely grateful. To Diane, who often bore the brunt of many of the difficult times throughout the past three years, I am especially thankful.

TABLE OF CONTENTS

TABLE OF C

B.

RESULTS---

A.

B.

C.

TABLE OF CONTENTS (continued)

TABLE OF CONTENTS (continued)

Table

1

2

3

4

5

6

7

8

9

10

11

12

13

14

LIST OF TABLES

LIST O

Table

LIST OF TABLES (continued)

Figure

1

2

3

4

5

6

7

8

9

10

11

12

13

14

15

LIST OF FIGURES

LIST

Fig

16

17

18

19

20

21

22

23

24

25

26

27

28

29

LIST OF FIGURES (continued)

LIST OF

Figure

LIST OF FIGURES (continued)

AP
AP
AP
AP
APA
APA
APA
APA
APA
APA
APE
BNP
BPA
BUN
F344
GSH
GSSG
HEX
IPK
MFOs
N-OH
NPSH
PAH

LIST OF ABBREVIATIONS

APAP	4-hydroxyacetanilide; (acetaminophen)
APAP-CONJ	sum of APAP-GLUC and APAP-SO_3
APAP-CYS	3-(5'-acetamido-2-'-hydroxyphenyl)-2-aminopropanoic acid; (3-cysteinylacetaminophen)
APAP-GLUC	4'-acetamidophenyl-β-D-glucopyranosideuronic acid; (acetaminophen glucuronide)
APAP-GSH	S-(5'-acetamido-2'-hydroxyphenyl)glutathione; (3-glutathionylacetaminophen)
APAP-MAP	sum of APAP-CYS, APAP-GSH, APAP-NAC, APAP-SCH_3 and APAP-$SOCH_3$
APAP-NAC	2-acetamido-3-(5'-acetamido-2'-hydroxyphenylthio)propanoic acid; (acetaminophen-3-mercapturate)
APAP-SCH_3	4-hydroxy-3-methylthioacetanilide; (3-methylthioacetaaminophen)
APAP-SO_3	4'-acetamidophenyl sulfate; (acetaminophen sulfate)
APAP-$SOCH_3$	methyl 2-hydroxy-5-acetamidophenyl sulfoxide; (acetaminophen-3-methylsulfoxide
APBQI	N-acetyl-p-benzoquinoneimine
BNPP	bis-(p-nitrophenyl)-phosphate
BPAP	4-hydroxybutyranilide; (butyryl-p-aminophenol)
BUN	blood urea nitrogen
F344	Fischer 344
GSH	reduced glutathione
GSSG	oxidized glutathione
HEX	cycloheximide
IPK	isolated perfused kidney
MFOs	mixed function oxidases
N-OH-APAP	N,4-dihydroxyacetanilide; (N-hydroxy-acetaminophen)
NPSH	non-protein sulfhydryl
PAH	p-aminohippurate

LIST

PAP

PAP-M

PBB

PES

PGG_2

PGH_2

PIP BU

SD

SSPT

TEA

TMC

LIST OF ABBREVIATIONS (continued)

PAP	4-hydroxyaniline; (p-aminophenol)
PAP-NAC	2-acetamido-3-(5'-amino-2'-hydroxyphenylthio)propanoic acid; (p-aminophenol-3-mercapturate)
PBB	polybrominated biphenyls
PES	prostaglandin endoperoxide synthetase
PGG_2	prostaglandin G_2
PGH_2	prostaglandin H_2
PIP BUT	piperonyl butoxide
SD	Sprague-Dawley
SGPT	serum glutamic pyruvic transaminase
TEA	tetraethylammonium
3MC	3-methylcholanthrene

INTRODUCTION

N-acetyl-p-aminophenol (APAP), commonly known as acetaminophen or paracetamol, is an antipyretic analgesic that today is present in a large number of pharmaceutical preparations. In 1978, APAP sales accounted for approximately 29% and 75% of the analgesic market in the United States and Great Britain, respectively (Rumach, 1978). APAP was first introduced into therapy as an analgesic by von Mering in 1893, but gained popularity only since 1949 (Flower et al., 1980). Several reasons have been suggested for the increase in popularity: 1) APAP has antipyretic analgesic properties similar to aspirin yet does not cause gastrointestinal bleeding (Czapels, 1976); 2) APAP is the major active metabolite of the more toxic coal tar analgesics phenacetin and acetanilid (Smith and Williams, 1949a); and 3) APAP has been available in the United States without prescription since 1955 (Flower et al., 1980).

Even though APAP has proven to be safe at therapeutic doses, large acute overdoses or long-term abuse of moderate doses often results in toxicity. There are four clinical manifestations of APAP intoxication (Duggin and Mohandas, 1982): 1) hepatic centrilobular necrosis following an acute overdose (Proudfoot and Wright, 1970; Prescott et al., 1971; Williams and Davis, 1977); 2) renal cortical

necro

overd

activ

peutic

and 4

by re

chron

(Dugg

nephr

(Dugg

renal

decade

E

induce

the es

bioche

fracti

nism t

glutat

tive i

ly, no

result

betwee

of APA

<u>vitro</u>

differ

necrosis, often associated with hepatic damage, following an acute overdose (Boyer and Rouff, 1971; Kleinman et al., 1980); 3) an active hepatitis-like syndrome associated with chronic high therapeutic intake in susceptible individuals (Bonkowsky et al., 1978); and 4) the chronic renal disease, analgesic nephropathy, characterized by renal papillary necrosis and interstitial nephritis following chronic abuse of combination analgesic preparations containing APAP (Duggin, 1980; Stylges and Iuliucci, 1981; Murray, 1982). Analgesic nephropathy is the major clinical problem resulting from APAP abuse (Duggin, 1980); however, APAP overdoses resulting in acute hepatic and renal failure have increased at an alarming rate over the past two decades (Meredith et al., 1981).

Extensive literature exists on the biochemical mechanism of APAP-induced hepatic necrosis (for review see Hinson, 1980). Basically, the essential features that have emerged from investigations into the biochemical mechanism of APAP hepatotoxicity are as follows: A small fraction of APAP is metabolized by a cytochrome P-450 dependent mechanism to an arylating intermediate which combines with intracellular glutathione (GSH). If cellular stores of GSH are reduced, the reactive intermediate then arylates cellular macromolecules. Consequently, normal cellular functions are impaired and cellular necrosis results. Several investigators have demonstrated a direct correlation between hepatic necrosis and the loss of hepatic GSH, covalent binding of APAP to hepatic macromolecules in vivo or activation of APAP in vitro using inducers and inhibitors of cytochrome P-450 and species differences in the constitutive forms of cytochrome P-450 responsible

for activating APAP (Mitchell et al., 1973a,b; Jollow et al., 1973; Potter et al., 1973; Davis et al., 1974).

Although extensive clinical literature exists on the role of APAP in analgesic nephropathy, few investigations have dealt with the biochemical mechanisms of APAP renal cortical and papillary necrosis. However, it has been emphasized repeatedly that the renal lesion resulting from acute overdose of APAP is markedly different than that resulting from chronic abuse. Therefore, the biochemical mechanisms of the nephropathies may be radically different, depending upon the time course of drug administration.

A. Role of APAP in Analgesic Nephropathy

Analgesic nephropathy is an important medical problem worldwide; a large proportion of chronic renal failure and end-stage renal disease is thought to be due to analgesic nephropathy (Murray, 1982; Kincaid-Smith, 1978). Approximately 20% of patients in the Australian dialysis and transplant program suffered from analgesic-induced renal disease (Duggin, 1980). Comparable figures reported from other countries include: South Africa 20%, Switzerland 15%, United Kingdom 10%, Canada 6%, and Western Europe 2-3%. Studies in the United States suggest that between 5 and 20% of patients with chronic renal failure and end-stage renal disease abused analgesics (Murray, 1982).

Analgesic nephropathy was first recognized as a disease entity in 1953 by Spuhler and Zollinger. These investigators described interstitial nephritis and papillary necrosis in individuals that abused the analgesic preparation Saridon^{R} (Saridon is composed of 150 mg of isopropyl antipyrine, 250 mg of phenacetin and 250 mg of caffeine).

Ninety percent of patients suffering from analgesic nephropathy have abnormal intravenous pyelograms, markedly shrunken kidneys and non-specific calyceal abnormalities. Classic pyelonephritic scars have also been reported (Murray, 1982). Patients often exhibit reduced inulin or creatinine clearances, and increases in plasma creatinine indicative of decreased glomerular filtration rates (Bengtsson, 1975; Burry and Dieppe, 1976; Schreiner, 1978). Since almost 50% of renal function must be lost before plasma creatinine is elevated above normal ranges (Duggin, 1980), extensive papillary disease with considerable scarring is often present before a change in creatinine clearance is evident (Bengtsson, 1975). The inability to excrete a concentrated urine, which may occur prior to histological lesions, is consistently associated with analgesic nephropathy (Angervall and Bengtsson, 1968; Abel, 1971; Dubach et al., 1975; Murray, 1982). In addition to renal disease, analgesic nephropathy patients often demonstrate peptic ulceration, psychiatric instability, anemia, hypertension and myocardial infarction. Furthermore, there is increasing evidence to support a causal relationship between analgesic nephropathy (and perhaps heavy analgesic use without overt nephropathy) and renal pelvic carcinoma (Kincaid-Smith, 1978).

The conclusion that there is a causal relationship between analgesic abuse and the subsequent development of renal disease appears irrefutable. Four different types of studies provided support for this association (Murray, 1982). Several studies indicated that both chronic renal disease and papillary necrosis developed more often in individuals that abuse analgesics than those that do not (Larsen and

Mall
gati
in p
dise
gato
abus
1959
coun
coun
dise
Cont
expe
ship
1972

know
its
man
Smit
necr
the
beer
1982
indi
in a
Papi

Møller, 1959; Grimlund, 1963; Dubach et al., 1975). Other investigations suggested that a history of analgesic abuse was more prevalent in patients who had papillary necrosis than those who did not have the disease (Olafsson et al., 1966; Bengtsson, 1962). Several investigators have demonstrated a correlation between the extent of analgesic abuse and the incidence or severity of renal disease (Lindeneg et al., 1959; Gault et al., 1971). The incidence of analgesic nephropathy per country paralleled the per capita consumption of phenacetin in that country (Murray and Goldberg, 1976). In fact, the incidence of renal disease in Sweden has decreased since the availability of phenacetin-containing analgesics was restricted (Nordenfalt, 1972). Lastly, experiments performed in certain animal models suggested a relationship between renal disease and analgesic consumption (Kincaid-Smith, 1978).

The precise drug responsible for analgesic nephropathy is unknown. Phenacetin and its metabolite, APAP, as well as aspirin and its metabolite, salicylate, all produce renal papillary necrosis in man and experimental animals (Duggin, 1980; Murray, 1982; Kincaid-Smith, 1978). While aspirin consistently resulted in papillary necrosis in experimental animals, the doses required often exceeded the lethal dose (Duggin, 1980). However, analgesic nephropathy has been reported in individuals that consumed only aspirin (Murray, 1982). On the other hand, a far larger number of clinical cases indicated that phenacetin alone results in analgesic nephropathy. Yet in animal studies, even large doses of phenacetin or APAP produced papillary necrosis only inconsistently. However, combination

analgesics containing APAP or phenacetin resulted in a striking incidence of renal disease, possibly suggesting synergistic toxicity (Duggin, 1980). Therefore, it appears that the presence of phenacetin, and possibly its metabolite APAP, in combination or alone, is essential for the development of most cases of analgesic nephropathy.

Several lines of evidence support the possibility that the role of phenacetin in analgesic nephropathy may be mediated, not by the parent drug itself, but by the major metabolite, APAP. At moderate oral doses, the first-pass metabolic conversion of phenacetin in the liver is so effective that phenacetin concentrations in the peripheral circulation are extremely low (Raaflaub and Dubach, 1975). Localization of the lesion to the renal papilla in analgesic nephropathy has been suggested to be a consequence of a high intracellular drug concentration in the papilla. Several elegant studies by Duggin and Mudge have demonstrated that APAP, but not phenacetin, was concentrated intracellularly in the renal papilla and that intracellular papillary APAP concentration was related to urine flow. This is consistent with aggravation of analgesic nephropathy during oliguria or dehydration. Therefore, it appears that APAP is the primary agent present in renal cells following phenacetin administration. Thus, it is APAP and not phenacetin that undoubtedly plays a role in analgesic nephropathy subsequent to phenacetin or combination analgesic abuse. However, the exact biochemical mechanism of APAP-induced pathophysiology in the renal papilla is not known.

B.

dev
197
occ
tio
liv
(Pr
wit
Jef
fai
of a
also
et a
velo
cell

an i
and
Cobd
chal
indi
(Jeff
usual
sever
diate

B. APAP-Induced Acute Renal Failure

As many as ten percent of all documented APAP overdose cases develop acute renal failure (Clark et al., 1973; McJunkin et al., 1976). However, the appearance of renal failure is variable and may occur at different times after APAP ingestion. Human APAP intoxication can be roughly divided into three clinical outcomes. Fulminant liver damage often occurs without detectable renal insufficiency (Prescott et al., 1971; Clark et al., 1973). Renal failure coupled with fulminant hepatic damage may result (Boyer and Rouff, 1971; Jeffrey and Lafferty, 1981). However, the onset and duration of renal failure may be different than that of hepatic failure. Several cases of acute renal failure in the absence of fulminant hepatic damage have also been reported (Cobden et al., 1982; Curry et al., 1981; Kleinman et al., 1980; Prescott et al., 1971). Such differences in the development of renal and hepatic toxicity after APAP suggest that the cellular mechanisms within each organ may not be the same.

Acute renal failure following APAP overdose is characterized by an increase in serum creatinine and blood urea nitrogen concentrations and a decrease in creatinine clearance (Jeffrey and Lafferty, 1981; Cobden et al., 1982). Progressive oliguria, often despite a fluid challenge, with a marked rise in the fractional excretion of sodium is indicative of the onset of renal failure in APAP-overdose victims (Jeffrey and Lafferty, 1981). Prognosis of APAP-overdose victims is usually good, as most renal function tests return to normal after several days of high urine output which, characteristically, immediately follows the period of progressive oliguria (Kleinman et al.,

1980; Jeffrey and Lafferty, 1981; Curry et al., 1981). The renal histopathologic lesion after APAP overdose was restricted to the cortex; extensive focal coagulation necrosis of the proximal tubule was primary although some distal tubule lesions have been reported (Kleinman et al., 1980; Cobden et al., 1982). Ultrastructural damage, similar to that found with other forms of toxic nephropathy, includes loss of luminal brush borders, mitochondrial disarray, sloughing of cells and disruption of the tubular basement membrane (Kleinman, et al., 1980).

Several mechanisms for acute renal failure following APAP overdose have been proposed. Hypotension is a plausible mechanism of acute renal failure in patients that demonstrate extensive hepatic damage and/or coma (Boyer and Rouff, 1971). However, hypotension was not detected in many patients that developed acute renal failure following APAP consumption (Jeffrey and Lafferty, 1981; Kleinman et al., 1980; Gabriel et al., 1982). Wilkinson and coworkers have suggested that renal failure in APAP overdose victims was related to the release of an endotoxin that cannot be cleared by the diseased liver (Wilkinson et al., 1977). Support for their hypothesis included evidence that the occurrence of renal failure was similar in APAP overdose patients with fulminant liver failure and in patients with liver failure from other causes. However, the numerous reports of renal failure without apparent hepatic damage following APAP-overdose argue against the hypothesis set forth by Wilkinson and coworkers (Prescott et al., 1971; Kleinman et al., 1980; Curry et al., 1981; Cobden et al., 1982). In fact, acute renal failure after therapeutic

doses of APAP has been reported (Gabriel et al., 1982). A more likely explanation of acute renal failure is a direct nephrotoxic action of APAP and/or a metabolite. Strong evidence for this mechanism is provided by investigations of APAP-induced renal cortical necrosis in the rat (Mitchell et al., 1977; McMurtry et al., 1978). If APAP nephrotoxicity is due to a direct action of APAP and/or metabolites, then differences in renal and hepatic toxicity suggest that the biochemical mechanism of renal and hepatic drug-induced injury is different.

Until recently, elucidation of the exact biochemical mechanism of APAP-induced nephrotoxicity was hampered by the lack of an appropriate animal model. High doses of APAP did not produce histopathological changes in kidneys of Sprague-Dawley (SD) rats or mice (Mitchell et al., 1973). In Wistar rats, APAP at a dose of 3710 mg/kg resulted in generalized proximal tubular dilation, but not necrosis (Arnold et al., 1973). Renal damage was not evident in hooded rats that were administered APAP (Calder et al., 1971). Hart and coworkers (1982) demonstrated APAP-induced renal proximal tubular necrosis in female 3-methylcholanthrene pretreated, but not naive, SD rats following an oral dose of 2250 mg/kg APAP. Administration of APAP to New Zealand White female rabbits resulted in some renal biochemical, but not histopathological, abberations (Hennis et al., 1981). However, Mitchell and coworkers demonstrated that administration to male Fischer 344 (F344) rats of a single sublethal dose of APAP consistently resulted in acute necrosis of the proximal convoluted tubules of the inner renal cortex (Mitchell et al., 1977; McMurtry et al.,

1978). The APAP-induced renal lesion in the F344 rat was similar to that found in APAP overdose victims (McMurtry et al., 1978; Kleinman et al., 1980). The identification of an appropriate animal model for acute APAP-induced renal necrosis was an important initial step in the elucidation of the biochemical mechanism of this disease.

C. Role of Metabolism in APAP-Induced Renal Damage

A myriad of mechanisms have been proposed for the renal lesions produced by APAP (Shelley, 1978). Recently, APAP metabolism to reactive intermediates in papillary tissue was suggested to be the initial obligatory biochemical event in the pathogenesis of papillary necrosis (Mudge et al., 1978; Duggin, 1980). For certain xenobiotics, correlations between the binding of metabolites to kidney and renal necrogenesis have been reported (Ilett et al., 1973; Reid, 1973). The correlation between papillary binding of APAP and papillary necrogenesis is not as extensive. However, covalent binding of APAP to papilla is many times the binding in non-target tissues (Mudge et al., 1978; Mudge, 1982) and was increased by dehydration, a known aggravating factor in the etiology of analgesic nephropathy (Mudge et al., 1978; Duggin, 1980).

Extensive experimental evidence supports the involvement of metabolic activation in APAP-induced renal cortical necrosis. Arylation of renal protein and depletion of renal cortical GSH produced by APAP appears to be much greater in F344 rats than SD rats which are sensitive and insensitive to APAP-induced nephrotoxicity, respectively (McMurtry et al., 1978; Mudge et al., 1978). Following a dose of 750

mg/kg (i.p.) APAP to SD rats, Mudge and coworkers (1978) reported a 20 percent decrease in renal cortical GSH and covalent binding of approximately 0.1 nmol APAP/mg renal cortical protein. In contrast, McMurtry and coworkers (1978) reported a 50 percent decrease in renal cortical GSH and covalent binding of approximately 0.75 nmol APAP/mg renal cortical protein following a dose of 750 mg/kg (s.c.) APAP to F344 rats. In addition, agents such as cobaltous chloride and piperonyl butoxide, that reduced APAP-induced cortical necrosis also reduced covalent binding to renal cortical protein (Mitchell et al., 1977; McMurtry et al., 1978). Finally, autoradiographic analysis of kidneys from F344 rats following ^{3}H-APAP administration indicated that most of the radioactivity was associated with necrotic areas in the kidney and liver (Mitchell et al., 1977).

The instability of reactive intermediates generally precludes passage across cellular membranes suggesting that reactive intermediates are formed in close proximity to the site of macromolecular arylation (Nelson, 1982). The presence of covalently bound APAP metabolites within the kidney, therefore, suggests that APAP activation occurs directly in the kidney. There is additional evidence which is consistent with the conclusion that the reactive intermediate of APAP which arylates renal macromolecules is formed in situ and not in the liver. 3-Methylcholanthrene (3MC) enhanced APAP-induced hepatic necrosis but had no effect on APAP-induced renal necrosis (McMurtry et al., 1978). In addition, covalent binding of APAP to renal macromolecules was not altered by total hepatectomy (Breen et al., 1982). Lastly, Emslie and coworkers (1981a) have demonstrated covalent binding of APAP in the isolated perfused kidney (IPK).

Therefore, it appears that arylation of renal macromolecules could be the initial biochemical event in APAP-induced renal cortical and papillary necrosis, although the evidence is much more extensive in APAP-induced renal cortical necrosis. Furthermore, the metabolism of APAP to a reactive intermediate probably occurs within the kidney. At least three different biochemical mechanisms have been proposed and/or demonstrated for the generation of a reactive intermediate from APAP. Localization of these enzyme systems to specific areas of the kidney, however, may preclude their involvement in one or both types of APAP-induced renal disease.

1. Cytochrome P-450 Activation of APAP

Many investigators have suggested that the biochemical mechanism of APAP activation within the kidney is similar to the hepatic mechanism of APAP activation demonstrated by Brodie and co-workers (Mitchell et al., 1977; McMurtry et al., 1978). That is, APAP could be metabolized by a cytochrome P-450 dependent reaction to a chemically reactive arylating agent which could bind covalently to cellular macromolecules resulting in pathological changes (Figure 1; McMurtry et al., 1978). However, the restricted localization of cytochrome P-450 to the renal cortex dictates that this mechanism of metabolic activation, if applicable, is involved only in acute necrosis, not analgesic nephropathy.

The structural and immunological similarities between renal and hepatic microsomal P-450 suggest a similar mechanism of APAP activation. The actual reactive intermediate that arylates tissue protein is generally accepted to be N-acetyl-p-benzoquinoneimine

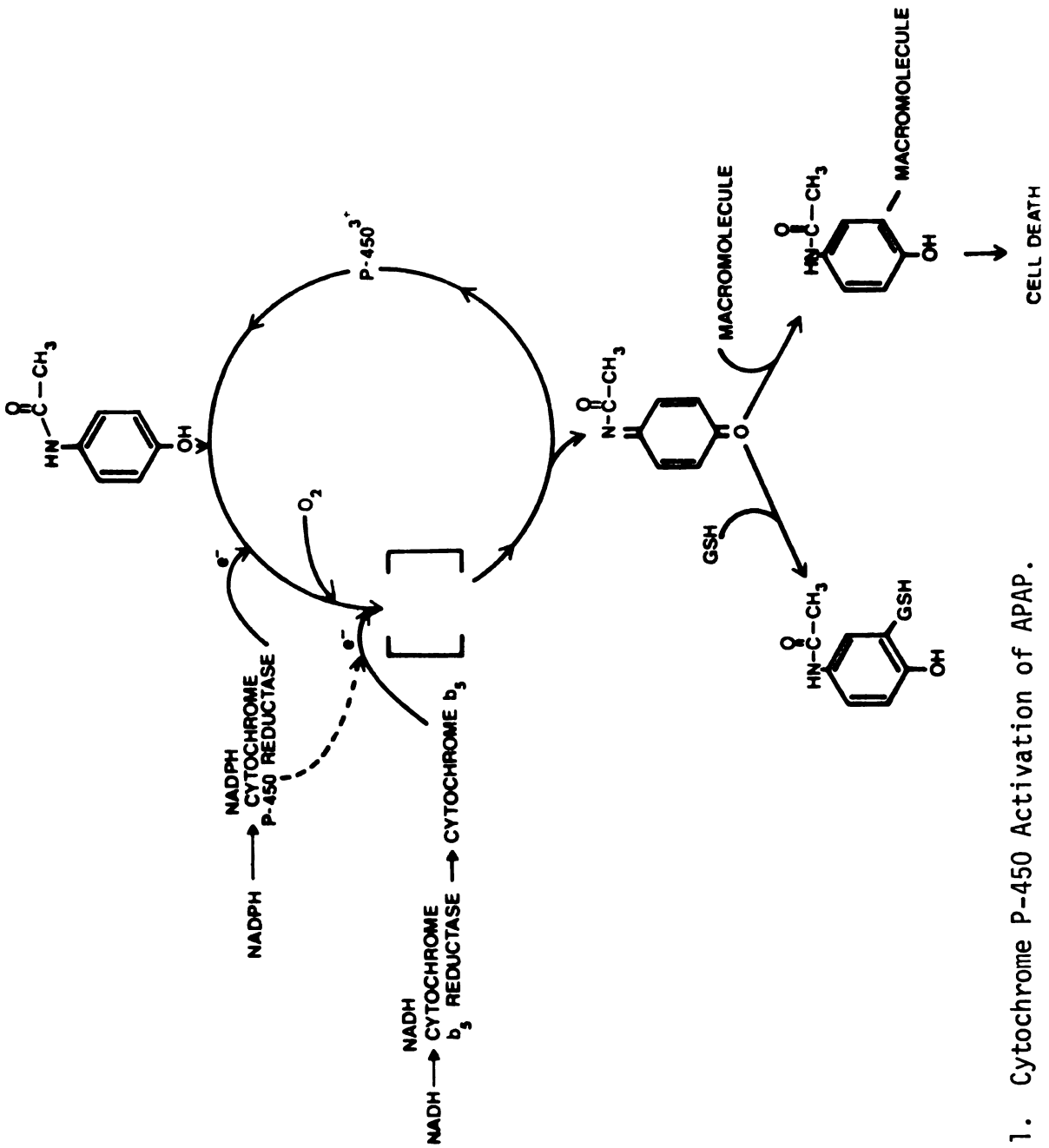

Figure 1. Cytochrome P-450 Activation of APAP.

(APBQI) (Miner and Kissinger, 1979; Hinson, 1980; Gemborys et al., 1980). However, the exact sequence of oxidation or oxygenation reactions that result in APBQI is not known. Originally, a P-450 dependent N-hydroxylation of APAP was thought to be the initial step in the formation of APBQI. The resulting N-hydroxy acetaminophen (N-OH-APAP) could then dehydrate to APBQI. However, subsequent in vitro experiments demonstrated that N-OH-APAP was not formed by a P-450 dependent reaction (Hinson et al., 1979; Nelson et al., 1980). Furthermore, N-OH-APAP was not a urinary metabolite of APAP even though N-OH-APAP is surprisingly stable in biological fluids (Gemborys and Mudge, 1981; Gemborys et al., 1980).

At least two possibilities can be envisioned whereby APBQI is formed directly from APAP without an intermediate N-hydroxylation (Figure 2). P-450 acting as a peroxidase rather than an oxygenase may oxidize APAP. P-450 metabolizes a variety of compounds by peroxidative as well as oxygenative processes (Hrycay and O'Brien, 1972; Nordblom et al., 1976). Furthermore, APAP is metabolized to an arylating intermediate by horseradish peroxidase (Nelson et al., 1981). The exact mechanism of the peroxidative metabolism of APAP by P-450 has not been defined. However, a ferryl oxyradical complex, because of its structural similarities to peroxidase Compound I, can be envisioned to initiate radical abstraction resulting in a radical cage complex of ferric cytochrome-hydroxyl radical and an APAP radical (Figure 2). This radical, be it a resonance-stabilized semiquinone or nitrenium radical, could easily be oxidized by a rapid second electron transfer to produce APBQI and a hydrated ferric P-450 complex (Nelson

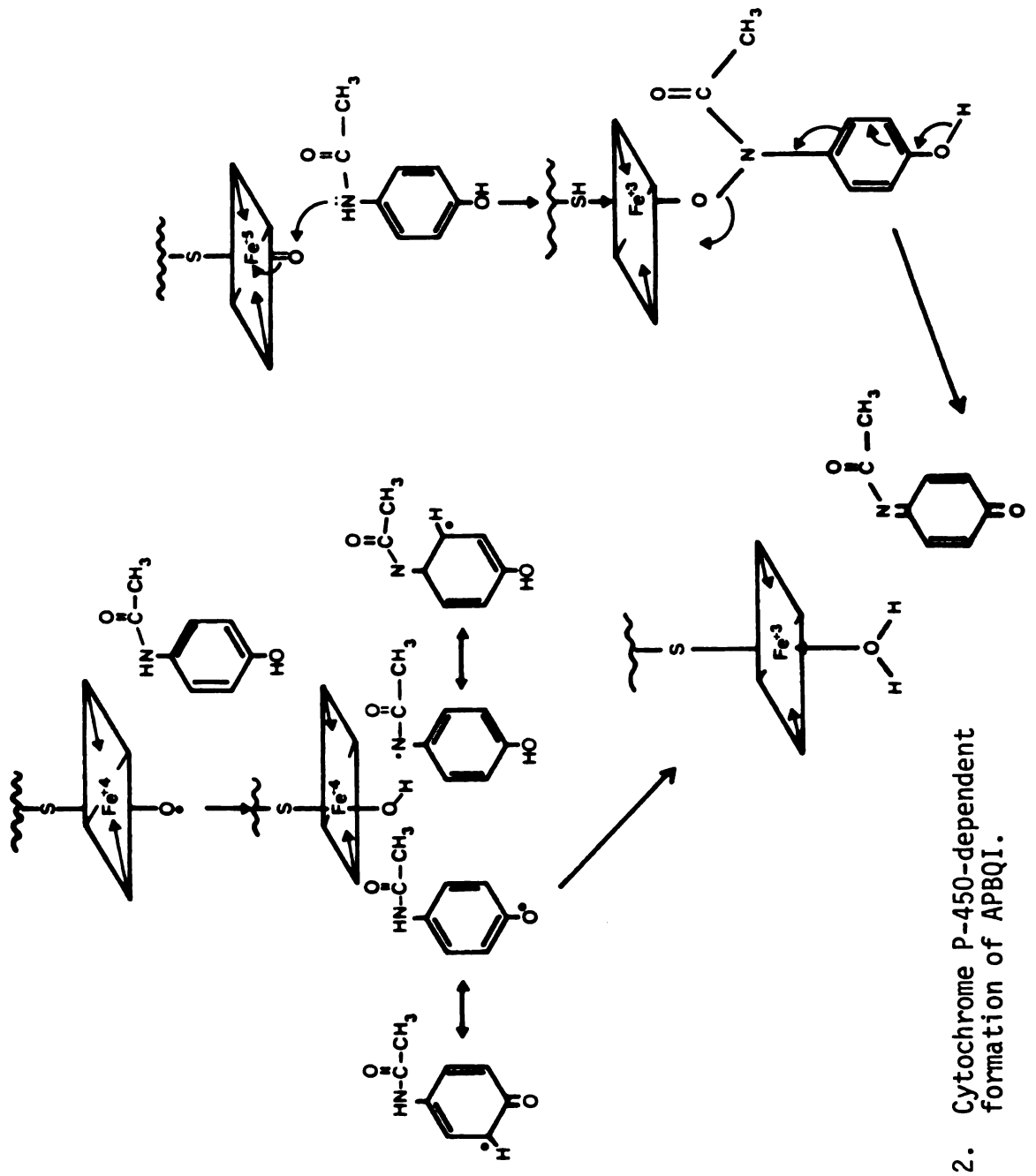

Figure 2. Cytochrome P-450-dependent formation of APBQI.

et al., 1981). Many of the characteristics of the arylating intermediate formed by horseradish peroxidase and P-450 are similar. However, an APAP-radical can be detected in horseradish peroxidase but not microsomal incubations (Nelson et al., 1981).

Alternatively, APBQI may result from P-450 reactions without the intermediate formation of radicals (Figure 2). This reaction would be initiated by the reaction of APAP with the perferryl form of P-450 resulting in a ferric oxyamide complex. This complex could decompose at the N-O bond or at the O-Fe bond. In the case of APAP, the N-O bond is more likely to break with oxygen retaining a pair of electrons due to the resonance stabilizing influence of the phenolic group on the incipient nitrenium ion. Rapid ionization of the phenolic group would result in formation of APBQI (Hinson et al., 1980). Such a mechanism is an attractive explanation of the preferential N-hydroxylation of phenacetin but not APAP. Phenacetin, lacking the ionizable phenolic group, would not be resonance stabilized to the same degree as APAP, resulting in cleavage at the O-Fe bond with subsequent formation of N-hydroxy metabolites (Hinson et al., 1979).

Several different types of experimental approaches have provided support for P-450 dependent renal metabolic activation of APAP and its toxicological relevance. Localization of APAP-induced renal lesions to the same discrete area of the kidney that contains the highest P-450 concentration supports the concept of P-450 dependent metabolic activation (Mitchell et al., 1977). Furthermore, McMurtry and coworkers (1978) demonstrated a correlation between loss of renal GSH, covalent binding of APAP metabolites to renal tissue and

APAP-induced renal cortical necrosis, using cytochrome P-450 inducers and inhibitors. Isolated renal proximal tubular cells and perfused kidneys metabolized APAP to its mercapturic acid (APAP-NAC), presumably via the intermediate formation of a glutathione adduct of APAP (APAP-GSH) resulting from direct conjugation with a reactive intermediate of APAP (Jones et al., 1979; Ross et al., 1980; Emslie et al., 1981a). The metabolism of APAP to APAP-NAC was induced by the cytochrome P-450 inducer, 3MC (Jones et al., 1979; Emslie et al., 1981b). In addition, McMurtry and coworkers (1978) demonstrated NADPH-dependent covalent binding of APAP in renal microsomes that was inhibited by carbon monoxide, nitrogen, boiling and 0°C. Furthermore, a correlation between renal P-450 content and susceptibility to APAP-induced nephrotoxicity has been suggested (Mitchell et al., 1977).

While it is apparent from in vitro studies that P-450 dependent metabolic activation of APAP does occur within the kidney, the toxicological relevance of this mechanism of activation to APAP-induced renal necrosis is unclear. Several points should be taken into consideration when evaluating the above mentioned studies. First, experiments using inducers or inhibitors of P-450 do not necessarily provide an indication of metabolic activation in the constitutive (uninduced) state. Furthermore, alternative pathways of metabolism may also be induced by xenobiotic treatment. For example, 3MC pretreatment increases the formation of APAP-NAC in isolated cells and kidneys yet has no effect on in vitro covalent binding of APAP or APAP nephrotoxicity (Jones et al., 1979; Emslie et al., 1981b; McMurtry et al., 1978). Therefore, the apparent 3MC-dependent increase

in P-450 activation of APAP may actually be due to the increased metabolism of the reactive intermediate (i.e., conjugation with GSH). In addition, inducers or inhibitors may alter the distribution of APAP into the kidney. For example, cobaltous chloride, a P-450 inhibitor, reduced APAP-induced nephrotoxicity which was interpreted to result from cobaltous chloride's inhibitory effect on renal P-450 (McMurtry et al., 1978). However, further validation of this interpretation is required following the recent demonstration that cobaltous chloride markedly reduced delivery to the kidney in vivo of the structurally similar aromatic amine, p-aminophenol (Calder et al., 1979). Extreme care, therefore, must be used in evaluating the toxicological relevance of renal P-450 activation from experiments utilizing inducers or inhibitors of mixed function oxidases.

Experiments in non-induced animals suggest that, in addition to P-450 activation, there may be another mechanism of APAP metabolic activation. This hypothesis is supported by covalent binding of ^{3}H-APAP to tissue macromolecules in vivo. After a nephrotoxic dose of APAP, binding to liver and kidney was roughly equal in the two organs even though P-450 on a nmol/mg protein basis was 10 times higher in liver than in kidney (McMurtry et al., 1978). In vitro kinetic parameters of P-450 dependent covalent binding of APAP also indicated that in vivo arylation of hepatic macromolecules should be much greater than arylation of renal macromolecules (McMurtry et al., 1978). Nevertheless, in vitro studies indicated that P-450 activation of APAP occurred within renal cortical cells. However, the quantitative

contribution of this type of metabolic activation to APAP-induced renal cortical necrosis is unknown.

2. Prostaglandin Endoperoxide Synthetase Activation of APAP

Recently, APAP was demonstrated to be metabolized to an arylating metabolite *in vitro* via an arachidonic acid-dependent pathway by prostaglandin endoperoxide synthetase (PES) (Moldeus and Rahimtula, 1980; Mohandas *et al.*, 1981; Boyd and Eling, 1981). Prostaglandin endoperoxide synthetase (PES) is a hemoprotein involved in the biosynthesis of eicosanoids (Samuelsson *et al.*, 1975; Nugteren and Hazelhof, 1973; Hamberg and Samuelsson, 1974). This enzyme catalyzes the oxygenation of polyunsaturated fatty acids (primarily arachidonic acid) to the hydroxyendoperoxide PGH_2. PES is found in highest concentration in seminal vesicle, platelets and kidney medulla (Christ and Van Dorp, 1972; Marcus, 1972; Samuelsson *et al.*, 1978). Marnett *et al.* (1975) observed that during the conversion of arachidonic acid to PGH_2, some structurally unrelated chemicals can be cooxygenated. For example, luminol, diphenylisobenzofuran, oxyphenylbutazone, benzidine and benzo(a)pyrene have been shown to be cooxygenated by this mechanism (Marnett *et al.*, 1975; Zenser *et al.*, 1979; Marnett, 1981; Rapp *et al.*, 1980).

In the kidney, PES exhibits a papillary to cortical gradient (highest in the papilla) which is in sharp contrast to renal mixed-function oxidases (Zenser *et al.*, 1979). Cyclooxygenase has been localized to the renal vascular endothelial cells, collecting tubules and medullary interstitial cells by immunohistochemical techniques and was not detected in cells of proximal tubules, thick ascending limbs

of Henle's loop or distal tubules (Smith and Bell, 1978). Arachidonic acid-dependent in vitro covalent binding of APAP was greatest in the papilla and least in the cortex whereas NADPH-dependent binding was greatest in the cortex and undectectable in the papilla. Microsomes from the outer medulla were capable of activating APAP by either a PES- or NADPH-dependent pathway (Mohandas et al., 1981a).

PES-dependent covalent binding of APAP to rabbit medullary microsomes was reduced by inhibitors of PES (aspirin, indomethacin, and ethoxyquin) and antioxidants (butylated hydroxyanisole and ascorbic acid) (Mohandas et al., 1981a; Boyd and Eling, 1981; Moldeus et al., 1982). GSH also reduced PES-dependent covalent binding of APAP, some of which could be accounted for by the generation of a GSH conjugate (Moldeus et al., 1982). However, a larger portion of the reduction in covalent binding could be accounted for by the oxidation of reduced GSH. Linolenic acid hydroperoxide can act as a substrate for the hydroperoxidase component of PES. However, linolenic acid hydroperoxide-dependent covalent binding of APAP was not dependent on oxygen or inhibited by indomethacin (Moldeus et al., 1982). Thus, the peroxidase component of PES, which catalyzes the reduction of PGG_2 to PGH_2, appeared to be responsible for the metabolic activation of APAP.

The exact mechanism of PES-dependent APAP activation remains speculative. The reaction probably involves a one electron oxidation reaction which could result in hydrogen abstraction with formation of the phenoxy radical of APAP (Figure 3) (Moldeus et al., 1982). The inhibitory effect of antioxidants and the rapid oxidation of GSH support the hypothesis that a radical of APAP is formed. The APAP

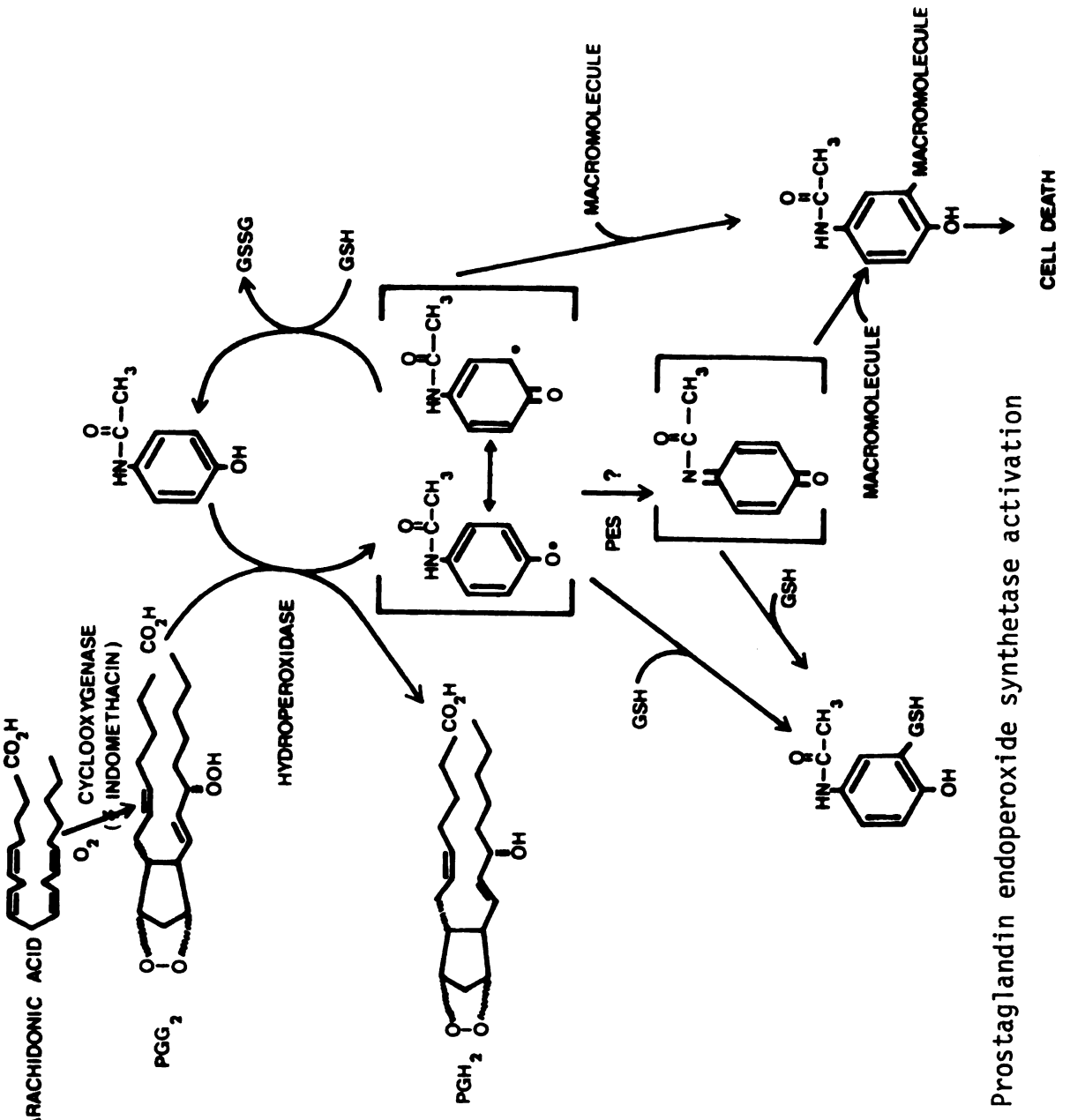

Figure 3. Prostaglandin endoperoxide synthetase activation of APAP.

radical may be conjugated directly with GSH or after further oxidation to the APBQI (Figure 3). GSH is presumably oxidized upon the reduction of the phenoxy radical back to APAP (Moldeus et al., 1982). This mechanism of APAP oxidation is similar to the horseradish peroxidase-dependent oxidation of APAP recently reported by Nelson and coworkers (1981).

APAP, at certain concentrations, inhibited prostaglandin synthesis in kidney medulla (Duggin and Mohandas, 1982). This may explain the low rates of renal PES-dependent activation of APAP in comparison to that found in ram seminal vesicles. However, Duggin and Mohandas (1982) demonstrated that inhibition of prostaglandin biosynthesis by APAP was concentration-dependent; at low APAP concentrations, prostaglandin biosynthesis was actually stimulated while at higher concentrations it was inhibited. The toxicological implications of the arachidonic acid-dependent pathway are as yet unclear; however, localization of PES to the inner medulla suggests that this mechanism may be involved in analgesic nephropathy but probably not proximal tubular necrosis produced by acute high doses of APAP. Furthermore, renal concentrations of APAP following an overdose are probably many times the 2 mM concentration of APAP required to inhibit completely prostaglandin synthesis in vitro.

3. Deacetylase-Dependent Activation of APAP

Theoretically, stable metabolites of APAP could be formed that would have greater nephrotoxic potential than the parent drug. The relationship of molecular structure of several APAP and phenacetin derivatives to nephrotoxicity has been determined by several

investigators (Calder et al., 1971, 1975). Of the structural analogues that were more nephrotoxic than APAP, only the deacetylated derivative p-aminophenol (PAP) could feasibly be formed in vivo. Deacetylation of arylacetamido compounds has been observed in vitro in liver and extrahepatic tissues. The subcellular distribution of deacetylases is highly variable, depending upon the species, organ or substrate investigated. For example, renal microsomes deacetylated acetanilide to a greater extent than p-acetamidobenzoic acid while the converse was true in renal cytosol (Franklin et al., 1969).

While deacetylation had been demonstrated for structural analogues such as phenacetin and acetanilide, the deacetylation of APAP in vitro or in vivo was never unequivocally demonstrated (Brodie and Axelrod, 1949; Smith and Williams, 1949b; Franklin et al., 1969). However, there was extensive evidence which hinted at this possibility. For example, Smith and Griffiths (1976) demonstrated that approximately 6% of [carbonyl-^{14}C]-APAP was excreted as ^{14}C-carbon dioxide, suggesting that a significant amount of APAP was deacetylated to PAP. Furthermore, Welch and coworkers (1966) reported excretion of a free diazotizable aromatic amine following APAP administration. Large amounts were excreted by cats and trace amounts by humans. The amine was not identified, and although it was claimed that is was not PAP, the possibility cannot be excluded that it was a phenolic conjugate of PAP (Mudge, 1982).

Direct evidence for PAP formation in vivo was first provided by Gemborys and Mudge (1981). Following development of special derivatization and concentration techniques, PAP was identified as a

metabolite of APAP in hamster urine. Subsequently, Hart and coworkers (1982) identified the phenolic sulfate conjugate of PAP in the urine of SD rats following APAP administration. Carpenter and Mudge (1981) earlier had demonstrated in vitro deacetylation of APAP to PAP in mouse renal cortical slices and homogenates. Recently, the tissue and subcellular distribution of APAP deacetylation was quantitated in homogenates of rat tissue. Deacetylase activity was in the rank order liver > kidney cortex > kidney medulla. Deacetylase activity appears to reside primarily in the soluble fraction, since it is unaffected by removal of the microsomal or mitochondrial fractions (Mudge, 1982).

PAP is a potent, selective nephrotoxicant that, like APAP, damages the latter third of the proximal tubule (Green et al., 1969; Calder et al., 1971; Cottrell et al., 1976). Unlike APAP, PAP did not result in hepatic histopathologic changes (Green et al., 1969). Similar biochemical sequelae have also been noted following APAP and PAP. Both compounds reduced renal GSH concentrations and arylated renal macromolecules; however, whether assessing biochemical or histopathological lesions, PAP appeared to have much greater nephrotoxic potential than APAP (Calder et al., 1971, 1975). This conclusion is tenuous as PAP nephrotoxicity has never been determined in an animal susceptible to APAP-induced nephrotoxicity such as the F344 rat. Certainly, the strain differences in APAP-induced nephrotoxicity suggest caution in the extrapolation of the nephrotoxic potential of PAP between strains. Nevertheless, an alternative biochemical mechanism of APAP-induced nephrotoxicity in the F344 rat can be envisioned: deacetylation of APAP to PAP which would then produce renal damage

subsequent to its own metabolic activation (Figure 4). Such a mechanism would be consistent with APAP-induced depletion of GSH and arylation of renal proteins reported by McMurtry and coworkers (1978), since PAP has been reported to produce similar effects in other strains of rats (Crowe et al., 1979).

PAP-induced nephrotoxicity, like APAP hepatotoxicity, is believed to be dependent upon metabolism to an arylating agent (Calder et al., 1979). Several biological oxidation systems such as ceruloplasmin and cytochrome c oxidase can oxidize PAP (Frieden and Hsieh, 1976; Borei and Bjorklund, 1953). However, the relevance of these systems to intrarenal generation of reactive intermediates from PAP is unknown. Another enzyme system responsible for the oxidation of PAP to an arylating intermediate is localized to renal microsomes. The activity of this enzyme system was much greater than that found in hepatic microsomes, which correlated with the arylation of renal and hepatic macromolecules by PAP in vivo (Calder et al., 1979; Crowe et al., 1979). The actual enzyme system present within renal microsomes responsible for PAP oxidation is unknown. However, it required molecular oxygen and was inhibited by ascorbate, NADPH and GSH, suggesting that a radical intermediate was formed during PAP oxidation (Calder et al., 1979) (Figure 4). Furthermore, PAP oxidation does not appear to be mediated by P-450 as several inhibitors of P-450, such as piperonyl butoxide, cobaltous chloride and SKF-525A, did not affect in vitro renal microsomal covalent binding of PAP. In addition to the undetermined enzymatic oxidation of PAP in renal microsomes, Andersson and coworkers (1982) have recently demonstrated PES-dependent

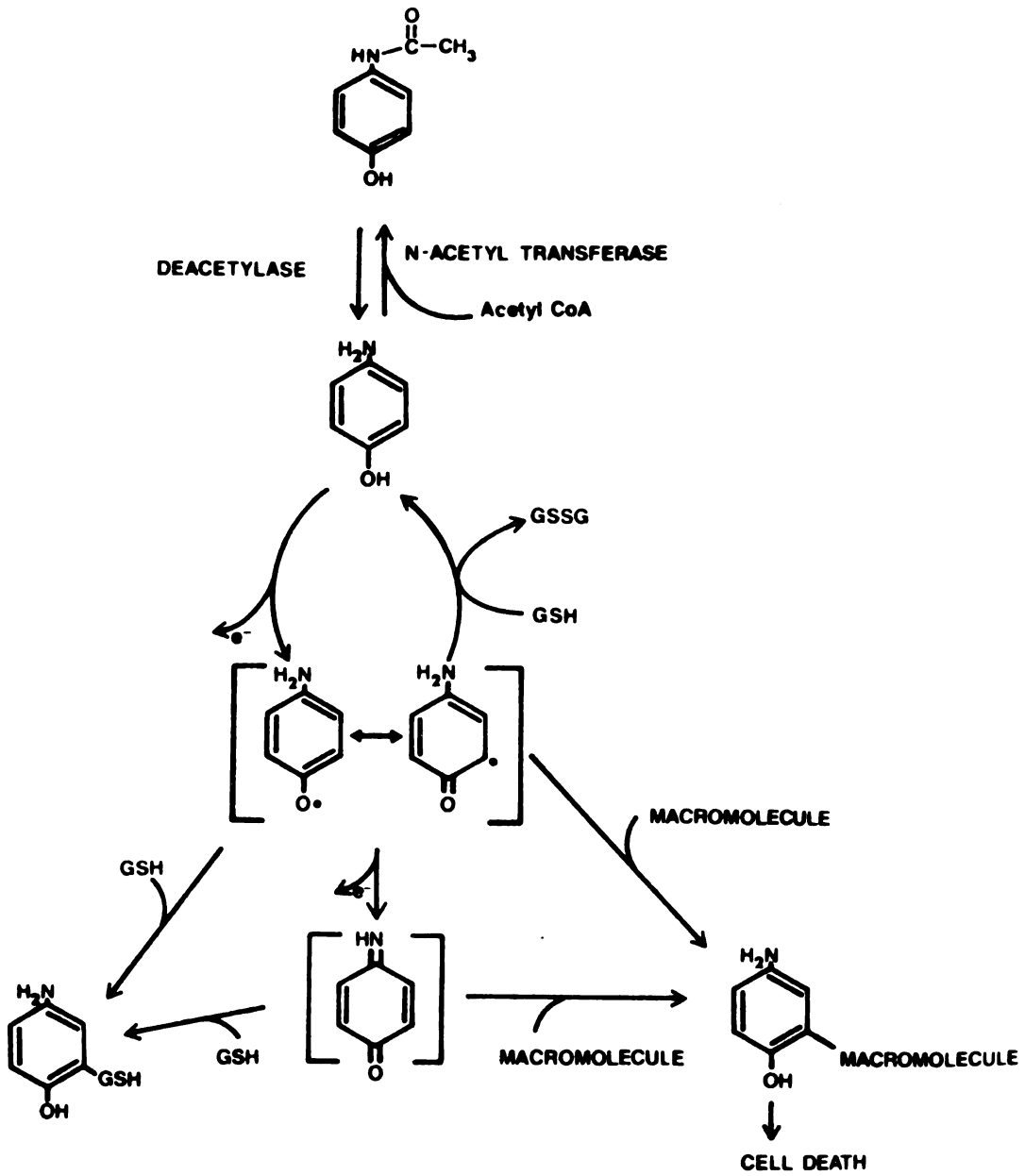

Figure 4. Deacetylase-dependent activation of APAP.

activation of PAP in ram seminal vesicle microsomes as well as rabbit renal medullary microsomes. Furthermore, the arylating intermediate resulting from PES-dependent activation of PAP, unlike that resulting from APAP, was of sufficient stability to induce DNA strand breaks in human fibroblasts (Andersson et al., 1982).

Therefore, PAP can be formed in many tissues within the body. Most important to APAP-induced renal disease, however, is the formation of PAP by subcellular fractions of renal cortex and medulla. Furthermore, at least two systems of PAP metabolic activation can take place in the kidney; one is localized in the cortex and requires only molecular oxygen and another is localized in the renal medulla and requires oxygen and arachidonic acid. This suggests that deacetylation could play a significant role in the eventual renal metabolic activation of APAP and, by implication, acute and chronic APAP-induced renal disease.

D. Purpose

The primary purpose of this investigation was to test the hypothesis that metabolic activation is involved in the pathogenesis of chemically-induced renal injury. The mechanism of APAP-induced acute renal cortical necrosis was the focus because the drug induces a reproducible renal lesion in a specific animal model.

Although there is extensive evidence that suggests APAP may be metabolically activated by mixed-function oxidases (MFOs), there is now evidence suggesting alternative means of APAP activation. In an organ such as the kidney, that contains variable amounts of MFOs in a heterogeneous mixture of cell types, such alternative mechanisms of

metabolic activation may play an important role in the pathogenesis of chemically-induced renal injury. The study of non-MFO metabolic activation would be important not only when concerned with renal cortex but also within areas of the urinary tract where MFOs are not detectable such as the renal papilla and perhaps the urinary bladder.

At least two mechanisms of metabolic activation could be envisioned to generate reactive intermediates from APAP within the renal cortex, following an acute sublethal dose. These include the P-450-dependent (Figure 1) and deacetylase-dependent activation (Figure 4) of APAP. It was therefore essential to document the presence of each pathway of metabolic activation within the renal cortex. Furthermore, the toxicological relevance of each mechanism was evaluated using strain differences in APAP-induced nephrotoxicity as well as specific inhibitors of deacetylation. Finally, attempts were made to quantitate the generation of reactive intermediates in vivo by each pathway and their relationship to the pathogenesis of APAP-induced cortical necrosis.

Elucidation of the mechanism of renal cortical APAP metabolic activation and its relationship to toxicity may provide a framework from which to study the mechanism of pathogenesis of the more clinically relevant analgesic nephropathy.

E. Objectives

The specific objectives of this investigation were:

1) To document APAP- and PAP-induced nephrotoxicity in the F344 rat.

2) To quantify deacetylation of APAP *in vivo* and *in vitro* in subcellular fractions and intact kidneys.

3) To compare APAP nephrotoxicity and metabolism in SD and F344 rats. In contrast to F344 rats, APAP-induced renal lesions have not been reported in SD rats.

4) To compare PAP nephrotoxicity and metabolism in SD and F344 rats.

5) To determine the biochemical mechanisms of APAP metabolic activation in the renal cortex *in vitro* by a group of experiments using isolated cell fragments and specifically labelled APAP fortified with various cofactors.

6) To quantify the effect of the deacetylase inhibitor, bis-(p-nitrophenyl)phosphate (BNPP), on the nephrotoxicity and metabolism of APAP and PAP in the F344 rat.

7) To identify the exact compound, PAP or APAP, that arylates renal and hepatic macromolecules *in vivo* in experiments that compare the covalent binding of [acetyl-^{14}C]-APAP and [ring-^{14}C]-APAP.

8) To determine the relationship of arylation to APAP-induced cortical necrosis in F344 and SD rats.

METHODS

A. Specific Methods

1. Animals

Male F344 (200-250 g) and SD (200-250 g) were purchased from Harlan Industries, Inc. of Indianapolis, IN and Haslett, MI, respectively. Animals were housed in sanitary, ventilated animal rooms with controlled temperature (24-25°C) and humidity (40-50%) and regular light cycles (7 a.m.-7 p.m.). Animals were allowed free access to food (Wayne Lab-Blox, Allied Mills, Inc., Chicago, IL) and water until use.

2. Toxicity tests

Rats were killed by cervical dislocation and decapitated 24 hr after APAP administration and 24 or 48 hr after PAP administration; blood was collected and the kidneys were excised and placed in ice-cold saline. The blood was allowed to clot for 60 min at room temperature, centrifuged and the serum was collected for measurement of serum glutamic pyruvic transaminase (SGPT) activity (Reitman and Frankel, 1957) with a commercial reagent kit (Sigma Chemical Co., St. Louis, MO); the activity was expressed as Sigma-Frankel (SF) units/ml. One SF unit of SGPT forms 4.82×10^{-4} μmmol glutamate/min in phosphate buffer (pH 7.5) at 25°C. Blood urea nitrogen (BUN) was determined

spectrophotometrically (Kaplan, 1965) with a commercial reagent kit (Sigma Chemical Co.).

Thin renal cortical slices were prepared and incubated in 4.0 ml of phosphate-buffered medium (Cross and Taggart, 1950) which contained 7.4×10^{-5}M PAH and 1.0×10^{-5}M [^{14}C]TEA (specific activity 2.0 Ci/mole). Incubations were carried out in a Dubnoff metabolic shaker at 25°C under a gas phase of 100% O_2 for 90 min. After incubation, the slices were removed, weighed and homogenized in 10 ml of 3% trichloroacetic acid. Two ml of incubation medium was treated similarly. After centrifugation, the supernatant was assayed for PAH and [^{14}C]TEA concentrations. PAH was determined by the method of Smith et al. (1945). One ml of slice or medium supernatant was added to 10 ml of ACS counting cocktail (Amersham, Arlington Heights, IL). Accumulation of PAH and TEA in renal cortical slices was expressed as a slice-to-medium (S/M) concentration ratio, where S represents mg of PAH or TEA per gram of tissue and M represents mg of PAH or TEA per ml of medium.

3. Histopathology

Specimens of kidney were cut longitudinally through the hilum and fixed in Lillie's "B5" solution (sodium acetate 1.25%, mercuric chloride 6%, formalin 10%). Blocks were dehydrated in graded alcohols, cleared in xylene, and embedded in paraffin by standard procedures. Sections were stained with hematoxylin and eosin and with periodic acid-schiff reagent. Sections were coded and examined without other information. Sections were evaluated for necrosis, tubular protein precipitates and casts, and tubular protein resorption droplets. Histopathologic changes were graded on an arbitrary scale of

negative, mild, moderate and severe (0-3+), and the area of cortex involved by tubular necrosis was estimated visually.

4. Determination of renal and hepatic non-protein sulfhydryl (NPSH) content

In order to avoid diurnal changes in tissue NPSH content, animals were killed before 12 noon. NPSH content was measured according to the method of Ellman (1959) with a few modifications. Kidneys and liver were quickly excised and immediately homogenized in 20 volumes of ice-cold 6% trichloroacetic acid (TCA) and centrifuged at 10,000 x g for 20 min. After an adequate dilution with 6% TCA, 0.5 ml of the diluted supernatant was added to 2 ml of 0.3 m Na_2PO_4 solution, pH 8.2. A solution (0.5 ml) of 0.04%, 5,5'-dithiobis-(2-nitrobenzoic acid) in 10% sodium citrate was then added, and the absorbance at 412 nm measured immediately after mixing.

5. Isolated perfused kidney (IPK)

The recirculating perfusion apparatus, perfusion medium and operative technique has been described in detail elsewhere (Newton and Hook, 1981). Bovine serum albumin (Fraction V) was obtained from either Sigma Chemical Company (St. Louis, MO) or Miles Biochemicals (Elkhart, IN) and used in the perfusates at concentrations of 6% and 7%, respectively. After perfusion was initiated, a 15-minute period of equilibration was allowed, followed by nine 10-min periods of urine collection. When APAP perfusate concentrations greater than 2.0 mM were used, APAP was dissolved in the perfusate (total volume, 225 ml) prior to perfusion. At lower concentrations, APAP was added to the perfusate after the first period of urine collection. When experiments

were designed to quantify urinary excretion of PAP, urine was collected into 500 µl of 10 mM N-acetylcysteine/50 mM sodium acetate (pH 5.0). At APAP perfusate concentrations greater than 2.0 mM three consecutive urine samples taken between 30 and 60 min after equilibration were combined for analysis. At APAP perfusate concentrations less than 2.0 mM urine samples, urine samples from the last eight collection periods were combined.

In certain cases, at the termination of the perfusion renal non-protein sulfhydryl content was determined. Both the perfused kidney and the contralateral nonperfused kidney (placed in ice-cold saline after the initiation of perfusion) were dissected into cortical, medullary and papillary (white medulla and papilla) sections, homogenized in 6% trichloroacetic acid and centrifuged to collect the denatured protein. Nonprotein sulfhydryl concentrations were estimated in the supernatant fraction by the method of Ellman (1959). Greater than 90% of nonprotein sulfhydryl in the kidney of the naive F344 rat has been determined to be glutathione (GSH) (W.M. Kluwe, personal communication). Percentage of depletion of GSH in the IPK was determined by the following formula: {1-([GSH] perfused kidney/[GSH] nonperfused kidney)} x 100.

In most cases, APAP did not affect renal function in the IPK. However, the highest concentration of APAP (10 mM) resulted in increased urine flow and reduced sodium reabsorption compared to IPKs perfused without APAP.

6. Quantitation of urinary metabolites of APAP and PAP from intact animals

After APAP or PAP dosing, rats were placed individually in stainless steel metabolism cages with free access to food and water. Urine collection bottles contained 10 ml of 10 mM N-acetylcysteine/50 mM sodium acetate (pH 4.5) with a crystal of thymol. In most cases, 23 hr after dosing animals were injected i.p. with furosemide (20 mg/kg) to facilitate uniform voidings and urine collections. Twenty-four hr after APAP dosing, the cages were rinsed with warm degassed water and the washings were combined with urine and diluted prior to analysis.

APAP, several thioether metabolites (3-glutathionyl acetaminophen, APAP-GSH; 3-cysteinyl acetaminophen, APAP-CYS; acetaminophen-3-mercapturate, APAP-NAC; 3-methylthioacetaminophen, APAP-SCH_3; 3-methylsulfoxideacetaminophen, APAP-$SOCH_3$) and the phenolic conjugates of each (glucuronide and sulfate) were analyzed by HPLC following dilution and clarification by filtration (pore size, 0.2 μm). Amounts of phenolic conjugates were calculated from the differences of non-conjugated metabolites before and after enzymatic hydrolysis. Enzymatic hydrolysis was carried out in the following manner: 5.0 ml of buffer (10 mM N-acetylcysteine/500 mM sodium acetate/20 mM barium chloride; pH 5.0) was added to 1.0 ml of diluted urine followed by a drop of chloroform and 100 μl of β-glucuronidase (Type H-2, Sigma Chemical Co., St. Louis, MO); incubation was carried out for 18 hr at 37°C.

Unconjugated PAP excreted following APAP administration was quantified following conversion to 4-hydroxybutyranilide (BPAP) by the method of Gemborys and Mudge (1981) with the following modifications: 2.0 ml of 1 M Na_2HPO_4 (pH 7.0) was added to 3.0 ml of urine followed by 100 µl of n-butyric anhydride. 4.0 ml of 1 M Na_2HPO_4 (pH 7.0) was added to 1.0 ml of urine when unconjugated PAP was determined following PAP administration. After continuous agitation for 1 hr, the solution was passed through a Sep Pak (Waters Associates, Milford, MA) and eluted with 4.0 ml of methanol. The amount of BPAP was then determined by HPLC. This procedure was slightly modified to determine the total amount of PAP after enzymatic hydrolysis by adding 2.0 ml of 1 M Na_2HPO_4 (pH 7.0) to 5.6 ml of hydrolysate. Hydrolysis also produced a small amount of BPAP proportional to the APAP concentration in the hydrolysate. This was not seen in samples of urine incubated without added enzyme and may be attributed to deacetylation of APAP catalyzed by contaminants in the β-glucuronidase. Experimental assays of PAP were corrected according to the concentration of APAP in the hydrolysate.

APAP and metabolites were quantified on an HPLC system consisting of a model M6000-A solvent delivery system, a model 440 UV detector set at 254 nm, a model U6K injector, a Data Module™, and a model RCM-100 radial compression module (Waters Associates, Inc., Milford, MA). Dedicated 5 µ Radial Pak™ reverse phase cartridges (8 mm x 10 cm) were used for all analyses. BPAP was quantified using a solvent system consisting of 15.5% acetonitrile/10.0 mM NaH_2PO_4 (pH 7.0) at a flow rate of 2.5 ml/min. APAP, APAP-NAC, APAP-CYS,

APAP-GSH, APAP-$SOCH_3$, and APAP-SCH_3 in the urine from intact animals, were quantified using a solvent system consisting of 6.5% dioxane/1% acetic acid at a flow rate of 2.5 ml/min. Solvents were clarified by filtration (pore size, 0.2 μm) prior to analysis. Metabolites were quantified by extrapolation from peak area calibration curves of unmanipulated synthesized standards (Gemborys and Mudge, 1981). Recovery experiments with PAP revealed 60-70 percent recovery from unhydrolyzed samples and 55-65 percent recovery from hydrolyzed samples over concentration ranges encountered in these studies. Therefore, quantified BPAP was corrected for these expected recoveries. APAP and its acetylated metabolites were not corrected for recovery. The urinary excretory pattern has been described in terms of percent of recovered dose, defined as the amount of a compound factored by the sum of the parent drug plus total metabolites, all on a molar basis.

7. Quantitation of urinary metabolites of APAP from IPKs

The four major metabolites of APAP, APAP-SO_3, APAP-GLUC, APAP-NAC and PAP were quantified by HPLC. At APAP perfusate concentrations less than 2.0 mM the following methodology was used. Before HPLC analysis urine samples from the last eight collection periods were combined, dissolved in eight volumes of methanol and concentrated under nitrogen. Urine samples were first chromatographed on a Waters radial compression module with a 10 μ radial pak A reverse phase cartridge (8 mm x 10 cm) with methanol-water-acetic acid (13:86:1, v/v/v) solvent system at a flow rate of 3.0 ml/min. The fractions of eluent corresponding to the elution volumes of synthesized standards

(Gemborys and Mudge, 1981) were collected, concentrated and injected on separate solvent systems which were optimized for the separated metabolites. All three of the metabolites were quantified at a flow rate of 3.0 ml/min using an acetonitrile/water solvent system containing 5 mM tetrabutylammonium phosphate. The ratio of acetonitrile/water (v/v) was varied with the metabolite fraction chromatographed (APAP-SO_3, 17.5:82.5; APAP-NAC, 15:85; APAP-GLUC, 12.5:87.5).

At APAP perfusate concentrations greater than 2.0 mM, metabolites were quantified directly, without concentration, on a 5 μ radial pak A reverse phase cartridge (8 mm x 10 cm) using a solvent system consisting of 12% dioxane/5.0 mM tetrabutylammonium phosphate at a flow rate of 2.5 ml/min.

Unconjugated PAP was determined in the urine of the IPK by methods described above. In all cases quantification of metabolites was by extrapolation from peak area calibration curves of unmanipulated synthesized standards. Furthermore, all samples and solvents were clarified by filtration (pore size, 0.2 μM) prior to analysis.

8. Quantitation of APAP and metabolites in liver, kidney and plasma

Rats were killed by cervical dislocation and decapitation 0.5, 1, 2, 3 or 5 hr after APAP (900 mg/kg) administration. Blood was collected in heparinized tubes and the liver and kidneys excised and weighed. Samples (1 g) of kidney cortex were rinsed with ice-cold saline and homogenized (Potter-Elvehjem homogenizer with a teflon pestle) in 4 volumes of water. Aliquots (0.25 ml) of tissue homogenates or plasma were combined with 2.5 ml of methanol and centrifuged at 3,000 x g for 10 min. The supernatant was removed and the

pellet extracted twice with 1.0 ml methanol. All supernatants were combined and dried under N_2 at 40°C. Extracts were reconstituted in 1.0 ml 10 mM N-acetylcysteine/50 mM sodium acetate buffer (pH 4.5). Enzymatic hydrolysis of APAP-CONJ was carried out as described previously except that only 0.5 ml of sample was hydrolyzed. APAP, APAP-NAC, APAP-CYS, APAP-GSH and APAP-SCH_3 in plasma and tissue extracts were quantified on a dedicated 5 μ Radial Pak™ reverse phase cartridge (8 mm x 10 cm) using a solvent system consisting of 6.5% dioxane/1% acetic acid/4 mM hexane sulfonic acid/1 mM octane sulfonic acid at a flow rate of 2.5 ml/min. All samples and solvents were clarified by filtration (pore size, 0.2 μm) prior to analysis. Metabolites were quantified by extrapolation from peak area calibration curves of unmanipulated synthesized standards (Gemborys and Mudge, 1981). Recovery experiments with plasma, and renal cortical and hepatic homogenates spiked with APAP and synthetic metabolites (APAP-CONJ, APAP-CYS, APAP-GSH and APAPNAC) revealed greater than 85 percent recovery over concentration ranges encountered in these studies. APAP and its acetylated metabolites were not corrected for recovery.

9. Preparation of renal cortical and hepatic subcellular fractions

Subcellular fractions were prepared from livers and kidneys of rats killed by cervical dislocation. Livers and kidneys were quickly excised and placed in ice-cold 1.15% KCl. Kidneys were bisected and papillary and white medullary tissue discarded. After being weighed, tissues were minced and homogenized (Potter-Elvehjem

homogenizer with a teflon pestle) in 3 volumes of 0.1 M sodium phosphate buffer (pH 7.4). The homogenate was centrifuged at 10,000 x g for 20 min and, when appropriate, the postmitochondrial supernatant was centrifuged at 105,000 x g for 60 min. The resulting microsomal pellet was resuspended in 0.1 M sodium phosphate buffer (pH 7.4) to a final concentration of 15-25 mg protein per ml. Protein concentrations of all subcellular fractions were determined by the method of Lowry et al. (1951).

10. In vitro microsomal mixed function oxidase activities

Reaction mixtures contained microsomes (1-2 mg/ml for kidney and 0.25-0.50 mg/ml for liver) and 1 ml of 0.1 M sodium phosphate buffer (pH 7.8) containing 4.5 μM glucose-6-phosphate, 0.3 μM NADP, 0.3 μM NADH, 0.1 μM NADPH, 163 μM $MgCl_2$ and 1 unit of glucose-6-phosphate dehydrogenase. After 3 minutes preincubation, the reaction was initiated by addition of substrate. The deethylation of ethoxycoumarin, measured by the method of Atio (1978), was linear with respect to time and protein concentration. Cytochrome P-450 (P-450) concentrations were determined from the dithionite reduced CO difference spectra (Omura and Sato, 1964). All spectral measurements were made on a Beckman dual beam spectrophotometer (Model No. UV 5260). Microsomal protein was determined by the method of Lowry et al. (1951).

11. In vitro APAP deacetylation

Liver and kidney cortex was homogenized as above with 3 volumes of ice-cold sodium phosphate buffer (0.067 M; pH 7.0 when the pH of the final incubation had to be adjusted; 0.1 M, pH 7.4 in all

other situations) and the homogenate centrifuged for 20 min at 10,000 x g at 4°C. The assay system contained 0.5 ml of the tissue supernatant and 0.7 ml of sodium phosphate buffer (0.2 M, at the desired pH when the pH of the final incubation had to be adjusted; 0.1 M, pH 7.4 in all other situations) in which APAP (final concentration, 10 mM) was dissolved. In certain cases, microsomal or cystolic suspensions were substituted (12 mg protein/ml) for 10,000 x g supernatants. Incubation was at 37°C, usually for 30 min. Deacetylation within renal and hepatic homogenates was determined to be linear for approximately 1 hr at 10 mM APAP. Reactions were terminated by the addition of 0.6 ml 10% TCA followed by centrifugation for 10 min at 3,000 x g. One ml of supernatant was used for PAP analysis by the alkaline phenol method with minor modifications (Frings and Saloom, 1979). Enzyme activities were expressed as micromoles of PAP generated per hour per gram, wet weight of initial tissue or nmoles of PAP generated per mg protein per hour.

12. Cytochrome P-450-dependent binding of APAP to microsomal protein in vitro

Reactions contained microsomes (2.5 mg/ml, unless indicated) and 2.0 ml of 0.1 M sodium phosphate buffer (pH 7.4) containing an NADPH regenerating system (Potter et al., 1974). After 2 minutes preincubation, the reaction was initiated by the addition of 4.0 μmole of [ring-^{14}C]-APAP or [acetyl-^{14}C]-APAP (500 dpm/nmole). The reaction was terminated, usually 10 min later, by addition of 1.0 ml 10% trichloroacetic acid (TCA) and the tubes were centrifuged at 3,000 x g for 10 min. The resulting precipitate was washed twice with 3 ml 10%

TCA followed by repeated washings with aqueous 80% methanol and centrifugation until radioactivity could no longer be extracted from the pellet. Protein pellets were then dissolved in 1.0 ml 1 N NaOH and analyzed for radioactivity and protein content (Lowry et al., 1951).

13. Binding of PAP to microsomal protein in vitro

Reactions contained microsomes (4.0 mg/ml, unless indicated) and 1.2 ml 0.1 M sodium phosphate buffer (pH 7.4). After 2 minutes preincubation, the reaction was initiated by the addition of 1.2 μmole [ring-^{14}C]-PAP (500 dpm/nmole). The reaction was terminated, usually 10 min later, by addition of 0.6 ml 10% trichloroacetic acid (TCA) and tubes were centrifuged at 3,000 x g for 10 min. Covalent binding was determined as indicated above.

14. Deacetylase-dependent binding of APAP in vitro

Reactions contained tissue (10-14 mg/ml, unless indicated) and 1.2 ml 0.1 M sodium phosphate buffer (pH 7.4), when indicated, reaction mixtures also contained a NADPH regenerating system (Potter et al., 1974). After 2 minutes preincubation, the reaction was initiated by the addition of 2.4 μmoles [ring-^{14}C]-APAP or [acetyl-^{14}C]-APAP (500 dpm/nmole). The reaction was terminated, usually 120 min later, by addition of 0.6 ml 10% TCA and tubes were centrifuged at 3,000 x g for 10 min. Covalent binding was determined as indicated above.

15. Determination of covalent binding of APAP in vivo

Rats were killed by CO_2 asphyxiation and decapitated; blood was collected in heparinized tubes and kidneys, liver and muscle (gastronemius) were quickly excised and placed in ice-cold saline.

Kidneys were bissected and papillary and white medullary tissue discarded. Approximately 1 g of the remaining renal tissue was homogenized in 4 volumes of water; liver was treated similarly. Muscle was minced with a Polytron prior to homogenization.

For distribution studies, 250 µl of tissue homogenate or whole blood were added to scintillation vials containing 1 ml of Soluene 350™ and allowed to stand overnight. Following decolorization, 10 ml of ACS was added to each vial for analysis of radioactivity. The amount of covalently bound APAP was determined in the following manner. Three ml of 10% TCA was added to 1 ml of tissue homogenate in a 15 ml screw cap tube and the tubes were centrifuged at 3,000 x g for 10 min. The resulting precipitate was washed twice with 3 ml of 10% TCA followed by repeated washings with aqueous 80% methanol and centrifugation until radioactivity could no longer be extracted from the pellet. Protein pellets were then dissolved in 1.0 ml of 1 N NaOH and analyzed for radioactivity and protein content (Lowry et al., 1951).

16. Radiolabelled substrate preparation

[Ring-^{14}C]-APAP and [acetyl-^{14}C]-APAP were purified prior to use by HPLC on a µBondapak™ C_{18} prep column (6.8 mm x 30 cm) using 21% methanol/0.15% phosphoric acid as a solvent system at a flow rate of 4.5 ml/min. The HPLC system consisted of a model M6000-A solvent delivery system, a model 440 UV detector set at 254 nm, a model U6K injector, and a Data Module™ (Waters Associates, Inc., Milford, MA). Approximately 1 mg of [ring-^{14}C]-APAP (182 µCi/mg) and 3.5 mg of [acetyl-^{14}C]-APAP (53 µCi/mg) were purified in individual runs at a

recovery

APAP, sy

ceutical

New Engl

and [ace

systems.

mm x 10

2.5 ml/

mm x 30

rate of

for puri

with the

^{14}C]-APA

from Pat

purity o

phenyl c

$NaPO_4$, p

counts w

determir

17.

randomiz

test or

1960).

signific

recovery of approximately 73% and 81%, respectively. [Ring-^{14}C]-APAP, synthesized by Tracer labs, was the kind gift of McNeil Pharmaceuticals (Fort Washington, PA). [Acetyl-^{14}C]-APAP was purchased from New England Nuclear (Boston, MA).

The radiochemical purity of HPLC purified [ring-^{14}C]-APAP and [acetyl-^{14}C]-APAP was verified by HPLC on two different solvent systems. One system utilized a 5 μ C_{18} radial compression column (5 mm x 10 cm) eluted with 4.5% dioxane/1% acetic acid at a flow rate of 2.5 ml/min. Another system utilized a μBondapak™ phenyl column (3.9 mm x 30 cm) eluted with 13% methanol/0.15% phosphoric acid at a flow rate of 1.8 ml/min. Approximately one million counts were injected for purity analysis. In both systems, 99.95% of radioactivity eluted with the UV absorbing APAP peak for both [ring-^{14}C]-APAP and [acetyl-^{14}C]-APAP.

[Ring-^{14}C]-PAP, in its hydrochloride form, was purchased from Pathfinder Laboratories (St. Louis, MO). The radiochemical purity of [ring-^{14}C]-PAP was verified by HPLC with a μBondapak™ phenyl column (3.9 mm x 30 cm) eluted with 4% acetonitrile/10 mm $NaPO_4$, pH 7.0 at a flow rate of 1.5 ml/min. Approximately one million counts were injected for purity analysis. Radiochemical purity was determined to be >99.0%.

17. Statistics

Data were analyzed by analysis of variance (completely randomized design) and treatment means were compared using Tukey's test or the least significant difference test (Steel and Torrie, 1960). The 0.05 level of probability was used as the criterion of significance in all instances.

B.

glu
per
3x
and

the
(P
sta
min
pre
Pot
rem
dig
wer

me
pro
vi
Ap

to
add

B. Individual Experiments

1. APAP-induced GSH depletion and metabolism in the IPK

First, experiments were designed to quantify the change in glutathione content in three discrete areas of the kidney after perfusion for 80 min with various concentrations of APAP ranging from $3x10^{-8}$ to $3x10^{-5}$M. In addition, renal function (sodium reabsorption and inulin clearance) was also evaluated.

The second series of experiments were designed to determine the role of drug metabolism in GSH depletion. Piperonyl butoxide (PIP BUT), used as an inhibitor of renal drug metabolism, was administered as a single i.p. dose (1000 mg/kg, dissolved in peanut oil) 90 min before initiation of perfusion. Kidneys from naive and PIP BUT pretreated animals were perfused with either 0 or $3x10^{-5}$M APAP. Polybrominated biphenyls (PBB, Firemaster BP-6), used as inducer of renal drug metabolism, was administered daily by gavage (90 mg/kg, dissolved in peanut oil) for 2 days; 24 hr after the last dose kidneys were perfused with either 0 or $3x10^{-8}$M APAP.

In the third series of experiments, the excretion of APAP metabolites was quantified in IPKs from naive F344 rats or F344 rats pretreated with PBB in a manner identical to that indicated previously. In these experiments all IPKs were perfused with $3x10^{-5}$M APAP for 80 min.

2. APAP and PAP nephrotoxicity and metabolism in the F344 rat

In the first series of experiments, various doses of APAP (0 to 900 mg/kg, i.p.) as a warmed (40°C) suspension (35 mg/ml) were administered to male F344 rats. Animals were placed in metabolism

cages for collection of urine for 24 hr and then killed. Nephrotoxicity was evaluated by quantification of changes in BUN; hepatotoxicity was evaluated by quantification of changes in SGPT. Urinary excretion of PAP was also determined in these animals as well as in IPKs from naive F344 rats perfused with 2.5-10 mM APAP.

In the next series of experiments, various doses of PAP (0-200 mg/kg, s.c.) in its hydrochloride form as an aqueous solution (100 mg/ml) were administered to male F344 rats under light ether anesthesia. Rats were killed 24 or 48 hr after PAP administration and nephrotoxicity and hepatotoxicity was evaluated by quantification of changes in BUN, PAH and TEA accumulation by cortical slices and SGPT.

In an attempt to determine the relationship of aminophenol structure to nephrotoxicity, several isomeric forms of PAP were evaluated for their nephrotoxic and hepatotoxic potential. Male F344 rats received 1.37 nmol/kg (s.c.) of PAP, o-aminophenol or m-aminophenol dissolved in 0.5 mM HCl in isotonic saline (20 mg/ml). Nephrotoxicity was determined 24 hr later by quantification of changes in KW/BW ratio, BUN and PAH accumulation; hepatotoxicity was determined by quantification of changes in SGPT.

In the next series of experiments, the effect of inducers of renal MFOs on PAP-induced nephrotoxicity was evaluated. To induce MFOs a group of male F344 rats were treated daily with a gavage of PBB (Firemaster BP-6, 90 mg/kg for 2 days) or β-naphthoflavone (BNF, 100 mg/kg for 4 days) dissolved in corn oil and were then administered PAP (0, 100 or 200 mg/kg, s.c.) 24 hr after the last dose of inducer. Twenty-four hr after PAP administration, BUN and PAH accumulation by renal cortical slices were determined.

3. Comparison of APAP nephrotoxicity and metabolism in F344 and SD rats

Various doses of APAP (0 to 900 mg/kg, i.p.) as a warmed (40°C) suspension (35 mg/ml) were administered to weight-matched F344 and SD rats. Animals were placed in metabolism cages for collection of urine for 24 hr and then killed. Nephrotoxicity was evaluated by quantification of changes in histopathology, BUN and PAH accumulation by cortical slices. Urinary excretion of APAP and metabolites was also determined in these animals as well as in IPKs from naive F344 and SD rat kidneys perfused with 5 or 10 mM APAP. In a separate series of experiments, strain differences in in vitro renal and hepatic APAP deacetylation, mixed function oxidase activities and NADPH-dependent APAP activation were determined.

4. Comparison of PAP nephrotoxicity and metabolism in F344 and SD rats

Various doses of PAP (0 to 400 mg/kg, s.c.) in its hydrochloride form as an aqueous solution (100 mg/ml) were administered to weight-matched F344 and SD rats. Animals were placed in metabolism cages for collection of urine for 24 hr and then killed. Nephrotoxicity was evaluated by quantification of changes in histopathology, BUN and PAH accumulation by renal cortical slices. In addition, urinary excretion of PAP and metabolites was determined in these animals. In a separate group of experiments, strain differences in renal and hepatic NPSH content and renal PAP activation in vitro were determined.

5. In vitro activation of APAP

In the first series of experiments, cytochrome P-450 dependent covalent binding of [ring-^{14}C]-APAP to renal and hepatic microsomes from F344 rats was determined at optimal protein concentrations and incubation durations. In addition, the covalent binding of [ring-^{14}C]-PAP to renal and hepatic microsomes from F344 rats was also determined at optimal protein concentrations and incubation durations.

In the second series of experiments, in vitro incubation conditions were optimized in an attempt to identify a deacetylase-dependent mechanism of APAP activation. Therefore, the subcellular localization of APAP deacetylation and deacetylase-dependent APAP activation was determined. Specifically, labelled [^{14}C]-APAP and specific inhibitors of APAP deacetylation and PAP activation were employed to substantiate deacetylase-dependent APAP activation.

6. Effect of Bis-(p-nitrophenyl)phosphate (BNPP) on APAP and PAP nephrotoxicity and metabolism

In the first series of experiments, rats were divided into 10 groups of 6 rats each. Five groups received BNPP pretreatment (100 mg/kg, i.p.); the remaining 5 groups were pretreated with water 30 min prior to the administration of APAP or PAP. Two groups (pretreated with water or BNPP) served as controls while the other groups received APAP (750 or 900 mg/kg, i.p.) or PAP (150 or 300 mg/kg, i.p.). Animals were placed in metabolism cages for collection of urine for 24 hr and then killed. Nephrotoxicity was evaluated by quantification of changes in histopathology, BUN and TEA and PAH accumulation by renal cortical slices. Urinary excretion of APAP or PAP and metabolites was

also determined. In addition, the effect of BNPP on renal APAP deacetylation and deacetylase-dependent covalent binding in vitro was determined.

For tissue distribution studies, 2 groups of 30 rats each were used. One group received BNPP pretreatment (100 mg/kg, i.p.) while the other received water 30 min prior to APAP administration; all animals received 900 mg/kg APAP. Animals were killed at various times following APAP administration (0.5, 1, 2, 3, 5 hr) and tissue concentrations of APAP and metabolites determined.

7. In vivo covalent binding of APAP

In the first series of experiments, the time course of [ring-^{14}C]-APAP arylation of renal cortical, hepatic and muscle protein was determined. Male F344 rats received a single i.p. dose of [ring-^{14}C]-APAP (900 mg/kg, approximately 50 dpm/nmole) between 6 a.m. and 8 a.m. Animals were killed 3, 6 or 9 hr later and arylation of protein and tissue distribution of radioactivity determined.

In a separate series of experiments, the covalent binding of [acetyl-^{14}C]-APAP and [ring-^{14}C]-APAP to renal cortical, hepatic, and muscle protein was determined in male F344 and SD rats. Animals were pretreated with either water or cycloheximide (1 mg/kg, i.p.) 60 min prior to and 3.0 hr after APAP administration. Animals received a single i.p. dose of either [ring-^{14}C]-APAP or [acetyl-^{14}C]-APAP (900 mg/kg, approximately 50 dpm/nmole) between 6 and 8 a.m. Animals were killed 6 hr following APAP administration and arylation of protein and tissue distribution of radioactivity determined.

RESULTS

A. APAP-Induced Glutathione Depletion and Metabolism in the IPK

1. APAP-induced glutathione depletion

Perfusion alone significantly depleted glutathione (GSH) concentrations in the cortex, medulla and papilla. However, APAP further reduced the GSH content in all areas of the perfused kidney over a concentration range of $3x10^{-8}$ to $3x10^{-5}$M. The highest concentration of APAP used produced significant depletion of GSH concentrations in all three areas of the kidney (Figure 5). No alterations in function (glomerular filtration rate, urine flow, sodium reabsorption) were evident at any concentrations of APAP used (data not shown).

2. Role of APAP metabolism in glutathione depletion

Treatment of rats with PBB did not alter the GSH concentrations in kidneys perfused without APAP. However, PBB enhanced the ability of $3x10^{-8}$M APAP to deplete cortical and medullary GSH contents. In contrast, PBB failed to result in a reduction in GSH content in the papilla of IPKs perfused with $3x10^{-8}$M APAP (Figure 6). PIP BUT treatment alone did not significantly alter GSH concentrations in perfused kidneys. Perfusion with $3x10^{-5}$M APAP significantly lowered GSH concentrations in all three areas of the kidney. PIP BUT treatment reduced the ability of $3x10^{-5}$M APAP to deplete cortical and medullary, but not papillary, GSH concentrations (Figure 7).

Figure 5. APAP-induced depletion of GSH concentration in the IPK. Five concentrations of APAP in the perfusate were used [0 (control), $3x10^{-8}$, $3x10^{-7}$, $1x10^{-6}$ and $3x10^{-5}$M]. Each point represents the mean ± S.E.M. of five IPKs from male F344 rats. Percentage of depletion of GSH was expressed relative to GSH concentration in the contralateral unperfused kidney. Values for contralateral unperfused kidney for cortex, medulla and papilla were 3.73±0.28, 2.89±0.41 and 1.51±0.13 μmol/g of wet tissue, respectively. *Significantly greater depletion compared to control (perfused without APAP) IPKs.

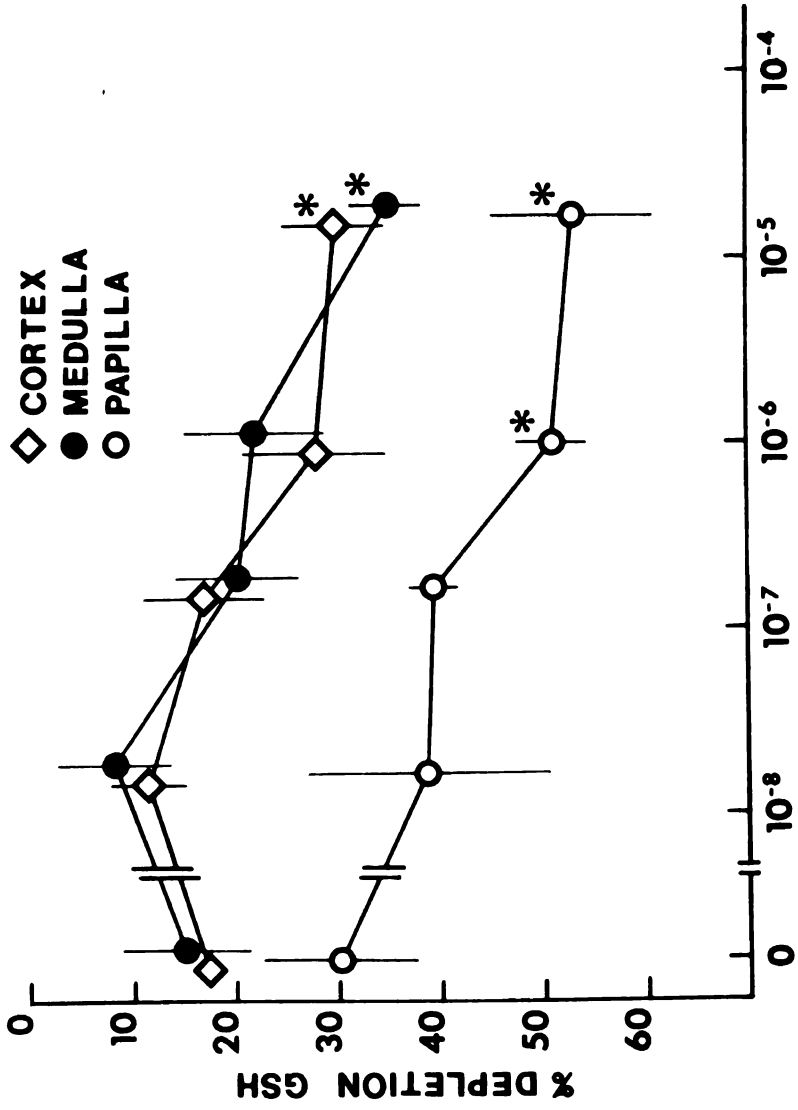
◇ CORTEX
● MEDULLA
○ PAPILLA
% DEPLETION GSH
0
10
20
30
40
50
60
0
10⁻⁸
10⁻⁷
10⁻⁶
10⁻⁵
10⁻⁴
APAP in Perfusate (molar)
*
*
*
*

Figure 5

Figure 6. Effect of PBB on APAP-induced depletion of GSH concentration in the IPK. Animals were treated daily with a gavage of PBB (Firemaster BP-6, 90 mg/kg for 2 days) dissolved in peanut oil and were used for perfusion 24 hr after the last dose. Reduction in GSH concentration was quantified in IPKs from control or PBB pretreated F344 rats perfused with either 0 or $3x10^{-8}$M APAP. Each bar represents the mean $\pm$ S.E.M. of five IPKs. *Significantly greater depletion compared to IPKs from animals treated with vehicle and perfused with the same concentration of APAP.

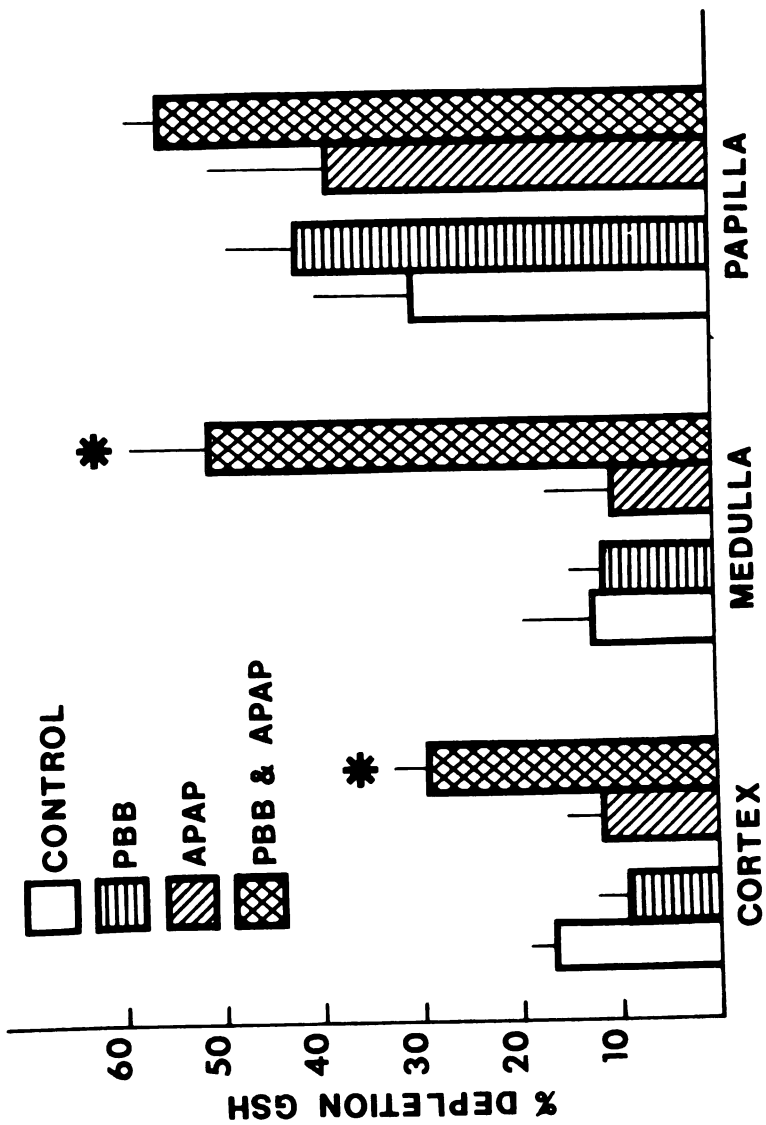
% DEPLETION GSH
60
50
40
30
20
10
CONTROL
PBB
APAP
PBB & APAP
CORTEX
MEDULLA
PAPILLA
*
*

Figure 6

Figure 7. Effect of PIP BUT on APAP-induced depletion of GSH concentration in the IPK. PIP BUT was administered as a single i.p. dose (1000 mg/kg, dissolved in peanut oil) 90 min before initiation of perfusion. Reduction in GSH concentration was quantified in IPKs from control or PIP BUT pretreated F344 rats perfused with either 0 or $3x10^{-5}$M APAP. Each bar represents the mean $\pm$ S.E.M. of five IPKs. *Significantly less depletion compared to IPKs from animals treated with vehicle perfused with the same concentration of APAP.

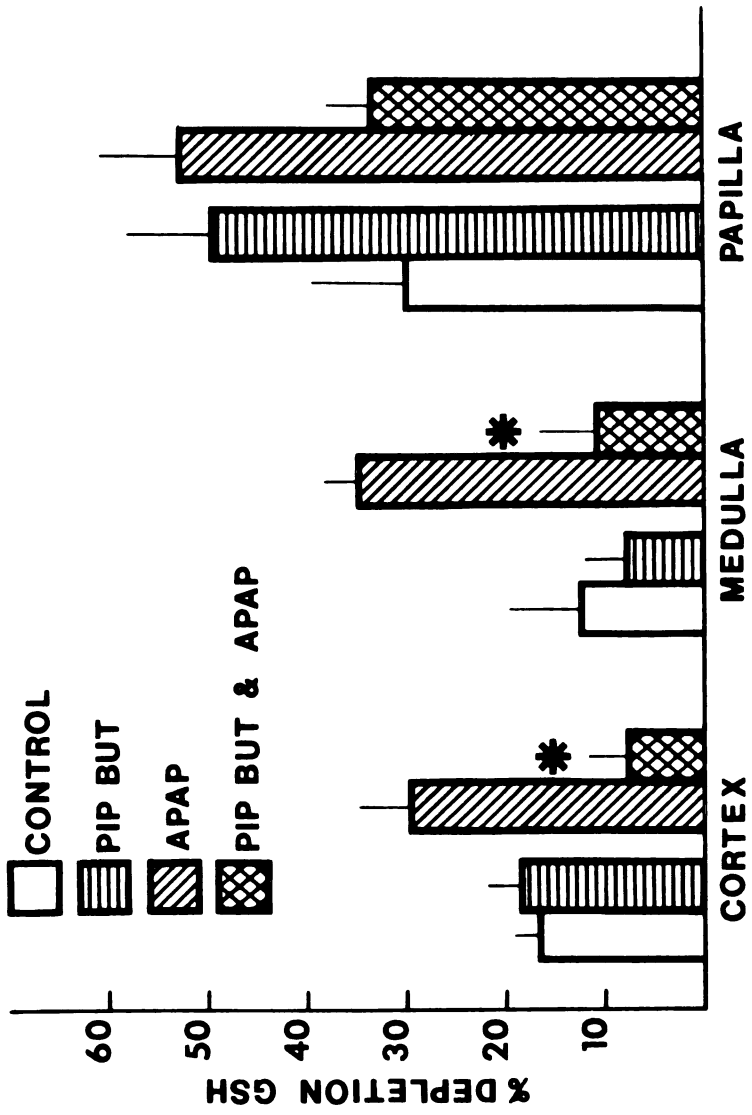
% DEPLETION GSH
60
50
40
30
20
10
CONTROL
PIP BUT
APAP
PIP BUT & APAP
CORTEX
MEDULLA
PAPILLA
*
*

Figure 7

3. Metabolism of APAP by the IPK

Metabolites of APAP were not detectable in the perfusate of the IPK. APAP-GLUC, APAP-SO_3 and APAP-NAC were detectable in the urine of the IPK after perfusion with $3x10^{-5}$M APAP (Figure 8). During the 80-min perfusion, IPKs excreted 272±50 and 772±142 ng/g of APAP-GLUC and APAP-SO_3, respectively. In addition, a reactive metabolite of APAP conjugated GSH in the IPK as demonstrated by the excretion of the APAP-NAC (44±12 ng/g). Conversion to all three metabolites over 80 min accounted for less than 0.2% of the total APAP present in the perfusion medium and approximately 1% of APAP found in the urine. Approximately 23% of the filtered load of APAP was excreted. Treatment with PBB failed to alter the excretion of APAP-GLUC (220±40 ng/g kidney) or APAP-SO_3 (571±136 ng/g kidney). However, PBB treatment increased the excretion of APAP-NAC 391% (172±54 ng/g of kidney).

B. PAP-Induced Nephrotoxicity in the F344 Rat

1. PAP excretion after APAP administration

Urinary excretion of total PAP (free and conjugated) increased with increasing dose of APAP up to 750 mg/kg (Table 1). At all doses the amount of unconjugated PAP excreted accounted for approximately ten percent of the total (free and conjugated) amount of PAP excreted. After 900 mg/kg APAP, the urinary excretion of total PAP decreased in parallel with the fall in urine flow, which probably occurred as a consequence of nephrotoxicity.

IPKs from F344 rats also converted APAP to PAP (Table 2). In addition, APAP was metabolized by the IPK to APAP-SO_3 and APAP-NAC.

Figure 8. Excretion of the major metabolites of APAP by the IPK. APAP-GLUC, APAP-NAC and APAP-SO_3 excretion was quantified in IPKs perfused with $3x10^{-5}$M APAP from F344 rats treated with PBB or vehicle. Animals were treated daily with a gavage of either peanut oil or PBB (Firemaster BP-6, 90 mg/kg for 2 days) dissolved in peanut oil and were used for perfusion 24 hr later after the last dose. Each bar represents the mean $\pm$ S.E.M. of four IPKs. *Significantly greater excretion of metabolite compared to IPKs from animals treated with vehicle.

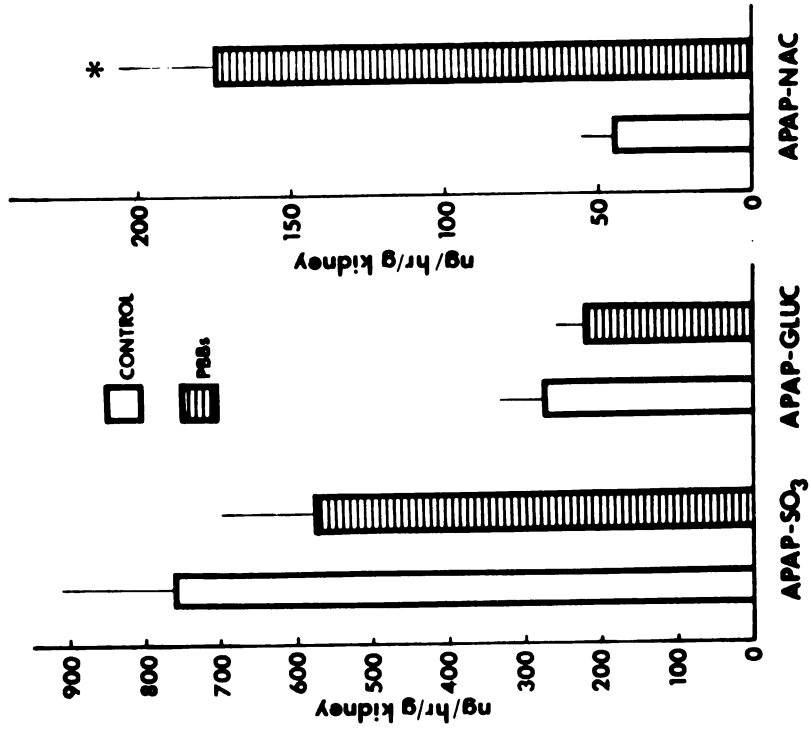
ng/hr/g kidney
0
100
200
300
400
500
600
700
800
900
APAP-SO3
APAP-GLUC
APAP-NAC
CONTROL
PBS
ng/hr/g kidney
0
50
100
150
200
*

Figure 8

TABLE 1

PAP Excretion, Blood Urea Nitrogen and Serum Glutamic Pyruvic Transaminase Activity Following APAP Administration to F344 Rats[a]

	Dose of APAP (mg/kg)[a]				
	0	250	500	750	900
PAP Excreted (mg/kg)[b]	N.D.[c]	4.70±0.46	10.66±0.90	16.71±0.85	9.94±1.20
BUN (mg %)	30±3	28±4	24±3	99±21[d]	173±27[d]
SGPT (units/ml)	33±2	139±6[d]	272±21[d]	740±79[d]	1680±190[d]

[a]Values are means ± SEM for four animals. Animals were killed 24 hr after APAP administration.

[b]Includes free and conjugated PAP excreted over a 24 hr period.

[c]Not detected.

[d]Significantly different from control (0 mg/kg APAP), $p<0.05$.

TABLE 2

APAP Metabolism by the IPK[a]

Metabolite Excreted	Concentration of APAP in Perfusion Medium (mM)		
	2.5	5.0	10.0
	nmoles metabolite excreted/minute/gram wet kidney weight		
APAP-SO_3	0.82±0.09	1.43±0.12	1.31±0.15
APAP-NAC	0.44±0.04	0.99±0.09	0.81±0.09
PAP[b]	0.024±0.009	0.209±0.076	0.315±0.047

[a]Values are means ± SEM for four isolated kidneys from male F344 kidneys.

[b]Includes only free, unconjugated PAP.

Biotransformation of APAP to PAP increased nearly 10-fold when APAP concentration in the perfusate was increased from 2.5 to 5.0 mM while other metabolic pathways were only minimally increased. Metabolites were detected only in the urine of the IPK; no metabolites were detected in the perfusate. However, this does not necessarily indicate that metabolites were preferentially excreted in the urine. Rather, dilution of metabolites in the large volume of perfusate could have been such that the metabolite concentration was below the limit of detection by HPLC.

2. Effect of PAP on renal and hepatic function in the F344 rat

PAP produced dramatic changes in renal function at doses much lower than required for APAP. At the higher doses of PAP, the kidneys exhibited small circular blanched areas on the capsular surface and extensive necrosis along the cortical-medullary junction. Measurements of renal function also indicated extensive renal damage. Blood urea nitrogen (BUN) was elevated at 24 hr at doses of PAP as low as 100 mg/kg; BUN was even higher at 48 hr (Figure 9). Absolute kidney weights and kidney to body weight ratios were also markedly increased at doses as low as 100 mg/kg PAP 24 hr after administration (data not shown). Similarly, accumulation of p-aminohippurate (PAH) and tetraethylammonium (TEA) by thin renal cortical slices was reduced (Figure 10). Twenty-four hours after PAP administration, PAH accumulation was depressed at doses as low as 50 mg/kg while TEA was not affected until doses of 200 mg/kg.

PAP administration had little effect on hepatic function as estimated by serum glutamic pyruvic transaminase activities (Figure

Figure 9. Effect of PAP on BUN in F344 rats. Animals received an s.c. dose of PAP and were killed 24 or 48 hr later. Data are represented as the mean + S.E.M. of four rats. *Significantly different from control ($\overline{0}$ mg/kg PAP), $p<0.05$.

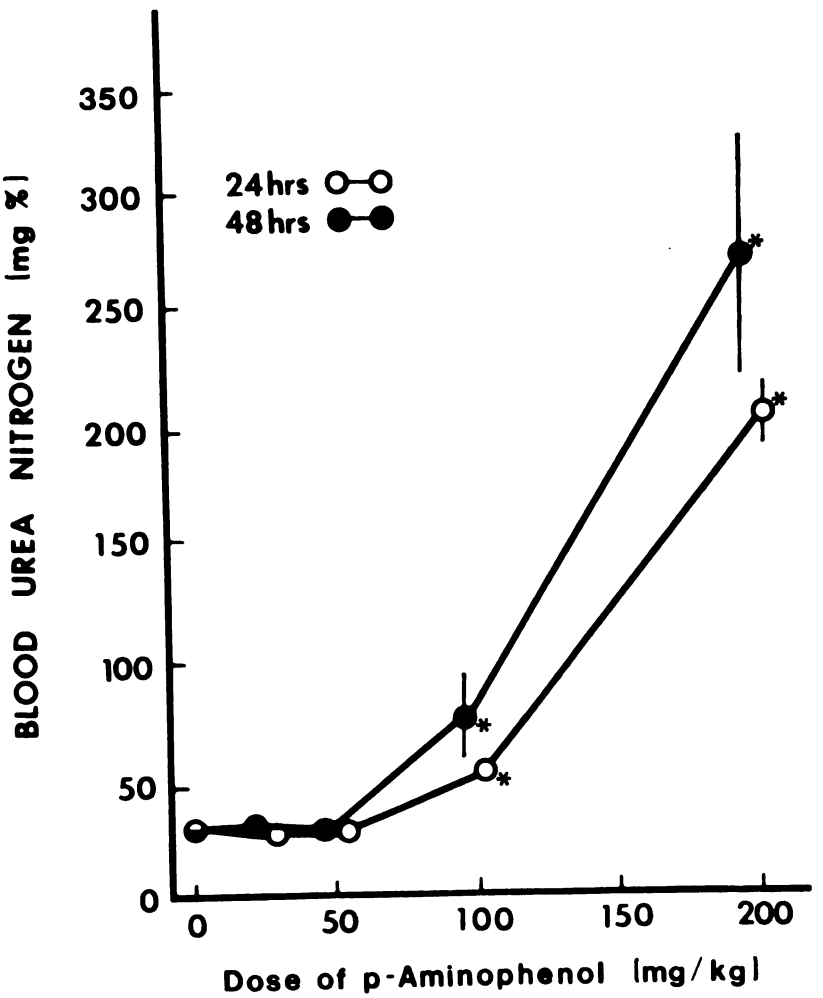
BLOOD UREA NITROGEN (mg %)
350
300
250
200
150
100
50
0
24hrs
48hrs
*
*
*
*
0
50
100
150
200
Dose of p-Aminophenol (mg/kg)

Figure 9

Figure 10. Accumulation of PAH and TEA by renal cortical slices from F344 rats 24 hr after PAP (s.c.) administration. Data are presented as the mean ± S.E.M. of four rats. *Significantly different from control (0 mg/kg PAP), $p<0.05$.

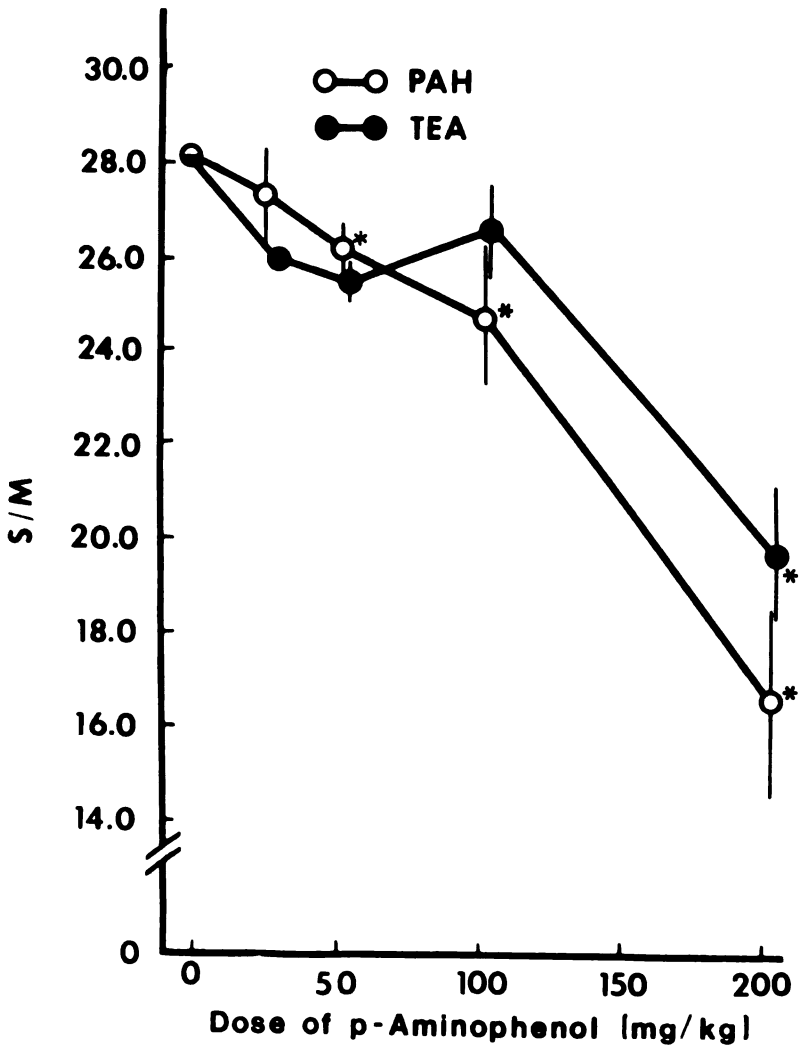
PAH
TEA
30.0
28.0
26.0
24.0
22.0
20.0
18.0
16.0
14.0
0
S/M
0
50
100
150
200
Dose of p-Aminophenol (mg/kg)

Figure 10

11). Only at the dose of 200 mg/kg PAP 24 hours after administration was there a trivial increase in SGPT activity. However, this effect was no longer present at 48 hours. In addition, liver weight or liver weight/body weight ratios were not altered by any dose of PAP either 24 or 48 hr after administration (data not shown).

3. Nephrotoxicity and hepatotoxicity of aminophenol isomers

Equimolar doses of PAP, o-aminophenol and m-aminophenol produced markedly different effects on renal and hepatic function (Table 3). Trivial increases in SGPT were produced by both m-aminophenol and p-aminophenol. Only PAP produced a significant elevation of BUN and KW/BW ratio while markedly reducing the accumulation of PAH by renal cortical slices.

4. Effect of inducers of renal mixed function oxidases on PAP nephrotoxicity

Animals were pretreated with either corn oil, β-naphthoflavone (BNF) or polybrominated biphenyls (PBB) and then treated with 0, 100, or 200 mg/kg PAP. Pretreatment with MFO inducers appeared to protect from PAP-induced nephrotoxicity (Table 4). PBB markedly reduced the nephrotoxicity produced by 100 and 200 mg/kg PAP while BNF completely blocked nephrotoxicity even at the highest dose of PAP. None of the pretreatment regimens, individually or in combination with PAP, produced significant changes in SGPT (data not shown).

C. Strain Differences in APAP Nephrotoxicity and Metabolism

1. APAP-induced histopathological and functional alterations in kidneys of SD and F344 rats

F344 and SD rats were divided into 4 groups of 4 rats each. One group served as control (0 mg/kg); the other groups received 250,

Figure 11. Effect of PAP on SGPT activity in F344 rats. Animals received an s.c. dose of PAP and were killed 24 or 48 hr later. Data are represented as the mean $\pm$ S.E.M. of four rats. *Significantly different from control (0 mg/kg PAP), $p<0.05$.

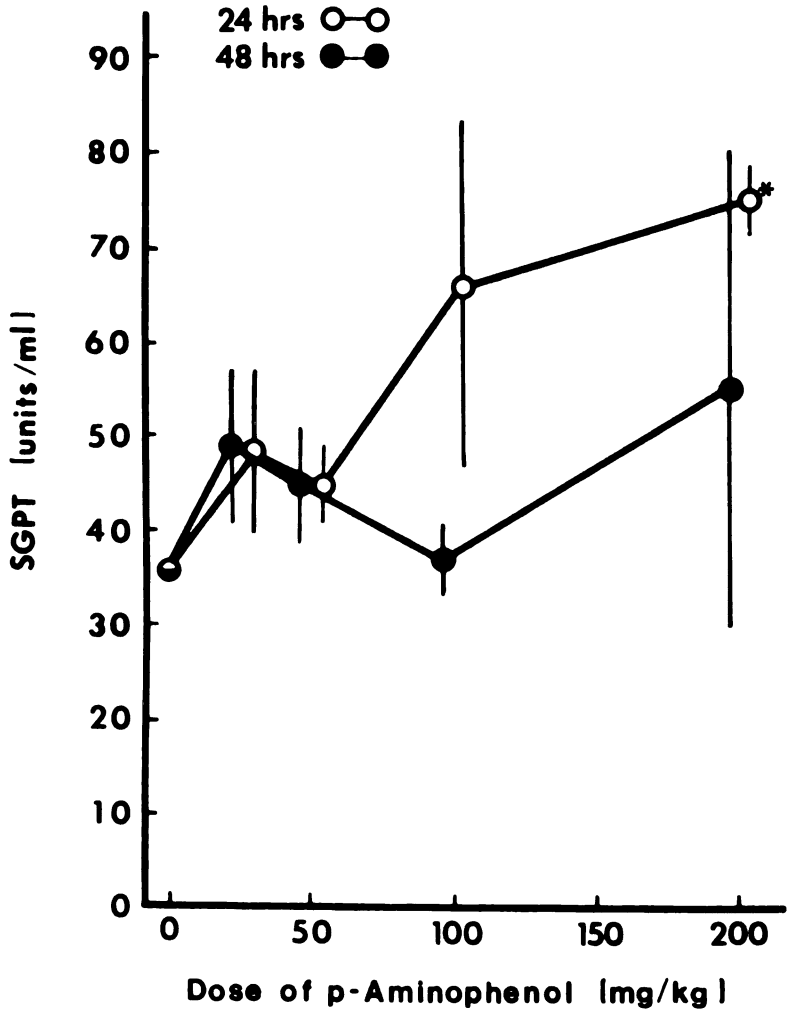
24 hrs
48 hrs
90
80
70
60
50
40
30
20
10
0
SGPT (units/ml)
0
50
100
150
200
Dose of p-Aminophenol (mg/kg)
*

Figure 11

TABLE 3

Toxicity of Aminophenols[a,c]

	Treatment			
	Saline	o-Aminophenol	m-Aminophenol	p-Aminophenol
KW/BW x 100	0.792±0.002	0.811±0.018	0.776±0.020	1.063±0.023[b]
SGPT (units/ml)	42±9	65±7	88±28[b]	70±9[b]
BUN (mg %)	33±3	26±2	27±3	218±15[b]
PAH S/M	25.9±1.7	24.3±0.6	27.2±0.7	14.2±1.2[b]

[a]Values are means ± SEM for four animals.

[b]Significantly different from saline control, $p<0.05$.

[c]Measured 24 hr after treatment (s.c.) with 1.37 mmol/kg aminophenol dissolved in 0.5 mM HCl in isotonic saline (20 mg/ml).

TABLE 4

Effect of Inducers of Renal Mixed Function Oxidases on PAP Nephrotoxicity[a,c]

Pretreatment	Dose of PAP (mg/kg)	BUN (% of Control)	PAH S/M (% of Control)
Peanut Oil	100	203±29	77±8
PBB	100	86± 3[b]	79±4[b]
BNF	100	97±11[b]	107±3[b]
Peanut Oil	200	809±57	47±3[a]
PBB	200	154± 9[b]	72±4[b]
BNF	200	72± 3[b]	101±3[b]

[a]Animals were treated daily with a gavage of commercial polybrominated biphenyls (PBB, Firemaster BP-6, 90 mg/kg for 2 days) or β-naphthoflavone (BNF, 100 mg/kg for 4 days) dissolved in corn oil or corn oil alone and were then administered PAP (0, 100 or 200 mg/kg, s.c.) 24 hr after the last dose of inducer. Animals were killed 24 hr after PAP administration.

[b]Significantly different from peanut oil pretreatment, $p<0.05$.

[c]Values are means ± SEM for four animals.

750 or 900 mg/kg of APAP. The kidneys of SD rats showed minimal changes after any of these doses of APAP (Figure 12; Table 5).

F344 rats exhibited renal necrosis involving 5%, 10-20% and 20-30% of cortical area after 250, 750, and 900 mg/kg doses of APAP, respectively (Figures 12 and 13; Table 5). Necrotic areas were predominately along the medullary rays indicating preferential damage to the straight segment of the proximal tubules. Necrosis was most severe (3+) in animals receiving the two highest doses of APAP (750 mg/kg and 900 mg/kg), protein precipitates and protein casts were observed in the distal tubules or collecting ducts (Table 5).

Measurements of renal function also indicated extensive APAP-induced renal damage in F344 rats but not SD rats. BUN was elevated in F344 rats after 750 mg/kg APAP (Figure 14). Absolute kidney weights and kidney weight to body weight ratios were also increased at the two highest doses of APAP (data not shown). The accumulation of PAH by renal cortical slices from F344 rats was not reduced until doses of 900 mg/kg APAP were used (Figure 15). Alterations in renal function in SD rats were not evident at any dose of APAP used.

2. Renal and hepatic mixed function oxidase activity

Cytochrome P-450 content and ethoxycoumarin-O-deethylase (ECOD) activity was similar in hepatic microsomes isolated from SD and F344 rats (Table 6). Renal P-450 content and ECOD activity were lower than the corresponding hepatic measurements in both strains. However, renal P-450 content and ECOD activity were greater in F344 rats than SD rats (Table 6). Microsomal recovery from liver or kidney was not different between the two strains.

Figure 12. Strain differences in APAP-induced renal necrosis. Animals were administered APAP (900 mg/kg, i.p.) and killed 24 hr later. (A) SD rat; negligible damage of renal tissues; PAS, x100. (B) SD rat; inconspicuous change; PAS, x250. (C) F344 rat; moderate to severe focal necrosis predominantly in straight segment of proximal tubules and some protein casts within distal tubules; PAS, x100. (D) F344 rat; fragmentation, pyknosis and karyorrhexis of straight segment of proximal tubules and intact convoluted tubules and collecting ducts; PAS, x250.

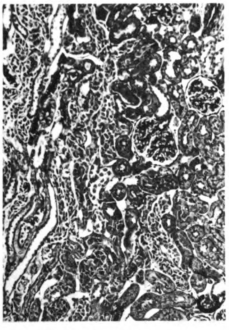

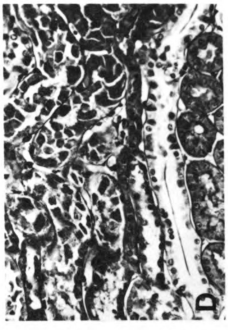

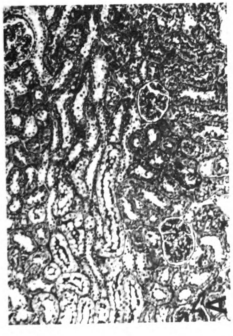

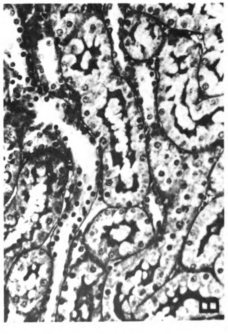

Figure 12

TABLE 5

Comparison of Renal Lesions Produced in Male F344 and SD Rats by APAP[a]

Strain	Dose of APAP (mg/kg)	No. of Rats	Necrosis (%)	Distribution	Protein Precipitate[b]	Protein Casts[b]	Droplets[b]
Fischer 344	0	4	0	0	0	0	1+
	250	4	0-5	P[c]	0-1+	0	1-2+
	750	4	10-20	P	1+	1+	1+
	900	4	20-30	P	0-2+	1-2+	2-3+
Sprague-Dawley	0	4	0	0	0	0	0-1+
	250	4	0	0	0	0	1+
	750	4	0	0	0	0	1+
	900	4	0	0	0-1+	0	1+

[a]Animals were treated with APAP (i.p.) and killed 24 hr later.

[b]Extent of histopathological changes was scored by criteria given under "Methods".

[c]Proximal tubule.

Figure 13. Effect of dose on APAP-induced renal cortical necrosis in F344 rats. Animals were killed 24 hr after APAP (i.p.) administration. All sections were stained with PAS and magnified 120x. (A) APAP (0 mg/kg); normal. (B) APAP (250 mg/kg); mild focal necrosis of the straight segment of proximal tubules. (C) APAP (750 mg/kg); moderate necrosis predominantly in straight segment of proximal tubules; mild protein precipitate and casts within the distal tubules. (D) APAP (900 mg/kg); moderate to severe focal necrosis predominantly in straight segment of proximal tubules; some protein casts within distal tubules.

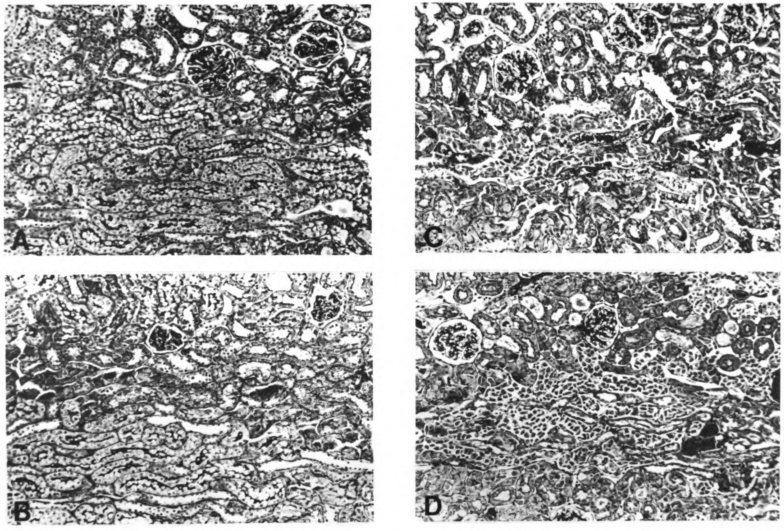

Figure 13

Figure 14. Effect of APAP on BUN in F344 and SD rats. Animals were administered APAP (i.p.) and killed 24 hr later. Data are represented as the mean ± S.E.M. of four rats. *Significantly different from respective control (0 mg/kg APAP), $p \leq 0.05$.

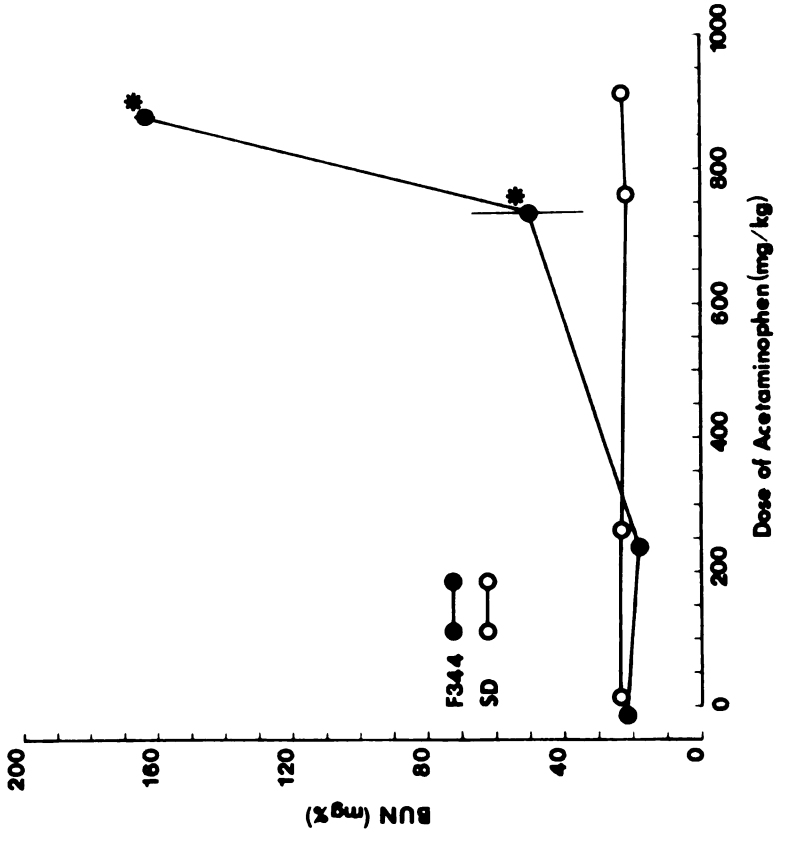
BUN (mg%)
200
160
120
80
40
0
F344
SD
0
200
400
600
800
1000
Dose of Acetaminophen (mg/kg)

Figure 14

Figure 15. Accumulation of PAH by renal cortical slices from F344 and SD rats 24 hr after APAP (i.p.) administration. Data are represented as the mean ± S.E.M. of four rats. *Significantly different from respective control (0 mg/kg APAP), $p<0.05$.

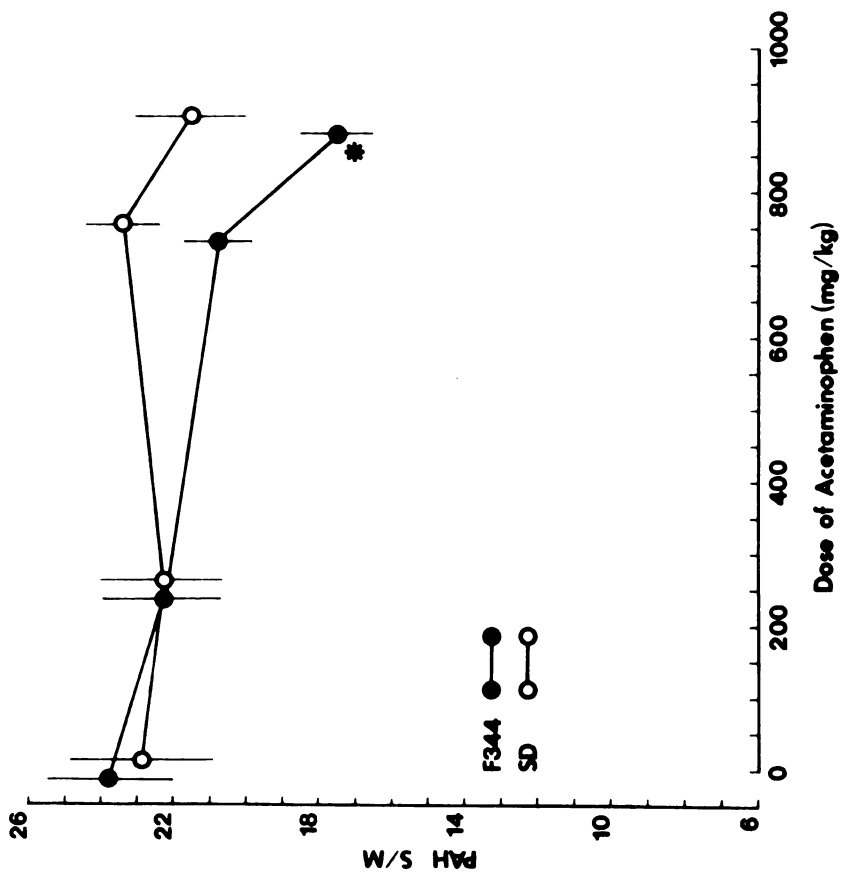
PAH S/M
26
22
18
14
10
6
0
200
400
600
800
1000
Dose of Acetaminophen (mg/kg)
F344
SD
*

Figure 15

TABLE 6

Strain Differences in Renal and Hepatic Cytochrome P-450 Content and Ethoxycoumarin Metabolism[a]

	Fischer 344		Sprague-Dawley	
	Kidney	Liver	Kidney	Liver
Cytochrome P-450 (nmol/mg protein)	0.15±0.02	1.02±0.09	0.07±0.01[b]	0.82±0.08
Ethoxycoumarin-O-deethylase (nmol/min/mg protein)	0.06±0.01	4.36±0.18	0.03±0.01[b]	4.04±0.38
Microsomal recovery (mg microsomal protein/ gm tissue wet wt)	3.28±0.37	6.48±0.50	2.99±0.32	6.05±0.17

[a]Values are the means ± SEM of 4 observations.

[b]Significantly different from corresponding tissue from F344 rats.

3. Covalent binding of [ring-^{14}C]-APAP in renal and hepatic microsomes

[Ring-^{14}C]-APAP was incubated with renal and hepatic microsomes from SD and F344 rats (Table 7). Linearity of covalent binding with protein concentration and time was assured in renal microsomal incubations. NADPH-dependent APAP binding in hepatic microsomes was approximately two times that in renal microsomes. Unlike MFO activity, strain-related differences were not evident in the renal NADPH-dependent activation of APAP. Incubation concentrations of APAP were almost ten times the reported K_m for APAP activation by F344 rat renal microsomes (McMurtry et al., 1978). Noncofactor-dependent nonspecific binding of [ring-^{14}C]-APAP was determined by the amount bound to boiled microsomes. Nonspecific binding of [^{14}C] occurred in both hepatic and renal microsomal incubations but was proportionally greater in renal microsomal incubations. However, in contrast to NADPH-dependent binding, the nonspecific binding occurred almost instantaneously and was not linear with time.

4. Urinary metabolites of APAP in SD and F344 rats

Metabolites of APAP recovered in the urine during a twenty-four hour period following APAP administration are summarized in Table 8. As might be expected, a lower recovery of the administered dose was evident in animals exhibiting significant nephrotoxicity (F344, 900 mg/kg APAP).

An increase in the proportion of APAP excreted unchanged was apparent in SD rats at the higher doses of APAP. F344 rats also exhibited this dose-related increase up to 750 mg/kg. At doses of 500 and 750 mg/kg APAP, the proportion of APAP excreted unchanged was

TABLE 7

Strain Differences in Covalent Binding of [Ring-^{14}C]-APAP in Renal and Hepatic Microsomes[a]

	Fischer 344		Sprague-Dawley	
	Kidney[d]	Liver[d]	Kidney[d]	Liver[d]
Microsomes Boiled[b,c]	0.062±0.007	0.080±0.010	0.056±0.010	0.098±0.006
Microsomes -NADPH[b]	0.093±0.012	0.118±0.048	0.081±0.009	0.073±0.011
Microsomes +NADPH[b]	0.310±0.026	0.601±0.130	0.306±0.045	0.560±0.037

[a]Values are the means ± SEM of 4 observations.

[b]Renal and hepatic microsomes (2.5 mg protein/ml) were incubated under air for 10 min at 37°C in the presence of 1 mM [ring-^{14}C]-APAP (500 dpm/nmol) and an NADPH regenerating system.

[c]Heated at 100°C for 10 min.

[d]Activity expressed as nmoles APAP bound/mg protein/10 min.

TABLE 8

Effect of Dose on Urinary Metabolites of APAP in F344 and SD Rats[a]

APAP Dose (mg/kg)	Strain	APAP	APAP-CONJ[b]	APAP-MAP[b]	PAP[b]	% of Administered Dose Recovered
		Percent of Recovered Dose[c]				
250	F344	10.15±1.32	81.90±2.07	6.53±0.73	1.45±0.18	90.2± 5.5
250	SD	10.03±2.09	83.88±2.34	4.19±0.10	1.85±0.17	85.3± 4.9
500	F344	15.70±0.76	72.88±1.03	9.73±0.42	1.73±0.12	75.0± 5.8
500	SD	11.35±1.96	81.57±3.15	5.40±0.86	1.68±0.46	86.8±10.8
750	F344	17.93±3.10	70.39±3.40	8.94±0.78	2.75±0.34	87.6± 4.9
750	SD	11.90±1.58	75.44±1.52	8.21±0.28	3.59±0.24	90.6± 2.5
900	F344	10.80±1.43	81.66±2.58	2.36±1.44	5.29±0.51	34.7± 7.7
900	SD	15.40±1.03	76.02±1.59	5.90±0.55	2.69±0.37	98.3± 3.5

[a]Values are the means ± SEM of four animals of urinary excretion over a 24 hr period following an i.p. dose of APAP.

[b]APAP-CONJ is the sum of APAP metabolized by conjugation only at the 4 position; APAP-MAP is the sum of all thioether metabolites including those that may also be conjugated at the 4 position, PAP is the sum of unconjugated PAP and PAP conjugated at the 4 position.

[c]The amount of a compound factored by the sum of the parent drug plus total metabolites, all on a molar basis.

greater for F344 than SD rats. At the highest dose of APAP, this trend was reversed. The proportion of APAP-CONJ (phenolic glucuronides and sulfates) was reduced (when compared to the amount of APAP-CONJ excreted at the lowest dose of APAP) for SD rats at doses of 750 and 900 mg/kg APAP. A similar dose-related effect occurred for F344 rats at 500 and 750 mg/kg. Difference between strains in the proportion of APAP-CONJ was only evident at a dose of 500 mg/kg APAP (Table 8).

Of the five thioether metabolites of APAP (APAP-MAP) for which analytical procedures were available (APAP-GSH, APAP-CYS, APAP-NAC, APAP-SCH_3, APAP-$SOCH_3$) only APAP-NAC, APAP-SCH_3 and APAP-$SOCH_3$ were detected in the urine. APAP-$SOCH_3$ was not detected in the urine of every animal; its presence was not related to dose or the strain of rat. APAP-SCH_3 accounted for 25-35% of all thioether metabolites excreted by F344 rats, 8-20% by SD rats. More than 90% of APAP-SCH_3 was conjugated at the four position in both strains. The proportion of all thioether metabolites was greater at the 750 mg/kg dose of APAP, than at 250 mg/kg APAP, for both strains. Strain differences in the proportion of APAP-MAP were evident at all but the 750 mg/kg dose of APAP (Table 8).

The proportion of PAP in urine increased in a dose-related manner for F344 rats. Of the PAP excreted, greater than 90% was conjugated. The proportion of PAP was greater for F344 rats than SD rats at the highest dose of APAP (Table 8).

5. In vitro deacetylation of APAP in renal and hepatic 10,000 x g supernatants

Renal and hepatic 10,000 x g supernatants deacetylated APAP to PAP (Figure 16). The deacetylation of APAP by renal homogenates was dependent upon the hydrogen ion concentration. Renal deacetylation rates increased 400 percent over the pH range of 7.00 to 8.13. In contrast, hepatic deacetylation rates increased less than 50 percent over a similar pH range. Renal and hepatic deacetylation rates were not different at pH values above 7.6. Strain differences between renal and hepatic deacetylation were not apparent at any hydrogen ion concentration (Figure 16).

6. Metabolism of APAP by the IPK

Metabolites recovered from the urine of isolated kidneys perfused with two different concentrations of APAP are summarized in Table 9. APAP-SO_3 was analyzed directly by HPLC because of the inability to quantitate it as APAP following enzymatic hydrolysis. APAP-GLUC, APAP-$SOCH_3$, and PAP conjugated at the 4 position were not quantified due to technical problems. APAP-CYS, APAP-SCH_3 and APAP-GSH were not detectable in the urine of the IPK. At both concentrations of APAP, APAP-SO_3 was the major metabolite excreted by IPKs from both strains of rat. However, IPKs from SD rats excreted greater quantities of APAP-SO_3 than did IPKs from F344 rats. No differences were noted between strains in the excretion of APAP-NAC or of free PAP. APAP metabolites were not detectable in the perfusates.

Figure 16. Deacetylation of APAP by renal and hepatic 10,000 x g supernatants from F344 and SD rats. Incubations were carried out for 30 min at 37°C under air. Approximately 15-20 mg of 10,000 x g supernatant protein was incubated in the presence of 10 mM APAP.

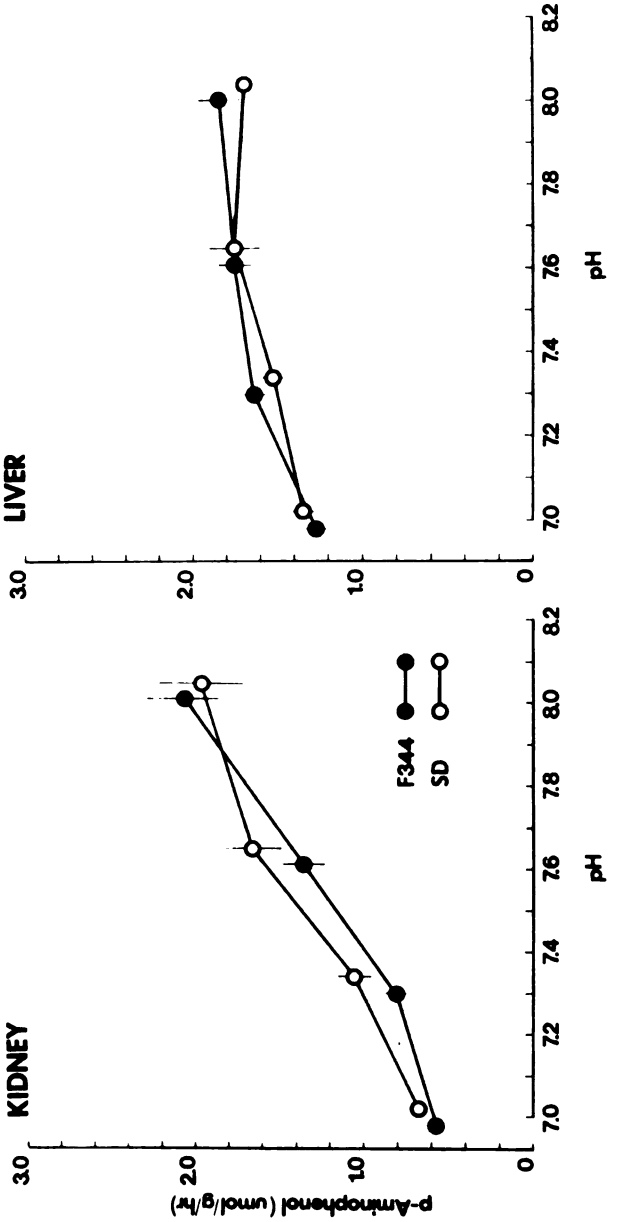
KIDNEY
LIVER
p-Aminophenol (umol/g/hr)
3.0
2.0
1.0
0
7.0
7.2
7.4
7.6
7.8
8.0
8.2
pH
F344
SD

Figure 16

TABLE 9

Strain Differences in
APAP Metabolism by the Isolated Perfused Kidney[a]

Metabolite Excreted	APAP Concentration in Perfusate (mM)	Strain of Rat	
		SD	F344
		nmoles metabolite excreted/ minute/gram wet kidney weight	
APAP-SO_3	5.0	1.84 ±0.20[c]	1.34 ±0.13
	10.0	1.98 ±0.15[c]	1.24 ±0.18
APAP-NAC	5.0	1.03 ±0.11	0.95 ±0.15
	10.0	1.09 ±0.21	1.05 ±0.11
PAP[b]	5.0	0.201±0.069	0.241±0.082
	10.0	0.345±0.077	0.313±0.058

[a]Values are means ± SEM for four isolated kidneys of each strain.

[b]Includes only free, unconjugated PAP.

[c]Significant difference between strains perfused with similar concentrations of APAP, $p<0.05$.

D. Strain Differences in PAP Nephrotoxicity and Metabolism

1. PAP-induced histopathological and functional alterations in kidneys of SD and F344 rats

F344 and SD rats were divided into 5 groups of 4 rats each. Animals in each group received 0, 50, 100, 200 or 400 mg/kg of PAP. The results of histopathological studies are summarized in Figures 17 and 18 and Table 10. Kidneys of SD rats exhibited necrosis involving 0-5%, 0-10% and 20-50% of the cortical area after 100, 200 and 400 mg/kg of PAP, respectively. Necrosis was not observed with the lowest dose (50 mg/kg) (Figure 18; Table 10). Kidneys of F344 rats exhibited necrosis involving 5-10%, 40-50% and 60-70% of cortical area after 100, 200 and 400 mg/kg doses of PAP, respectively (Table 10). There was a considerable difference in susceptibility to PAP between F344 and SD rats (Figure 17; Table 10). However, qualitative differences in renal damage between the two strains were not apparent upon light microscopic examination (Figure 17). The pathological lesions consisted chiefly of proximal tubular necrosis, protein precipitates and casts in proximal tubules, distal tubules, and collecting ducts, and numerous protein droplets in the tubular epithelial cells. Necrotic areas were predominantly along the medullary rays, indicating preferential damage in both strains to straight segments. With increasing dose, however, necrosis affected convoluted segments of the proximal tubules and possibly distal tubules. Glomerular abnormalities, interstitial inflammation, vascular lesions and papillary necrosis were not detected.

Significant changes in renal function twenty-four hours after administration of PAP were evident in both F344 and SD rats.

Figure 17. Strain differences in PAP-induced renal necrosis. Animals were administered PAP (400 mg/kg), s.c.) and killed 24 hr later. (A) SD rat; moderate focal necrosis predominantly of the straight segment of proximal and distal tubules, protein precipitates and casts within distal tubules and collecting ducts; PAS, x100. (B) SD rats; fragmentation, pyknosis and karyorrhexis of straight segment of proximal tubules; PAS, x250. (C) F344 rat; generally more severe than (A), necrotic areas localized not only to the straight segment but also extend into the convoluted proximal and distal tubules; PAS, x100. (D) Severe fragmentation, pyknosis and karyorrhexis of the straight segment of the proximal tubule; PAS, x100.

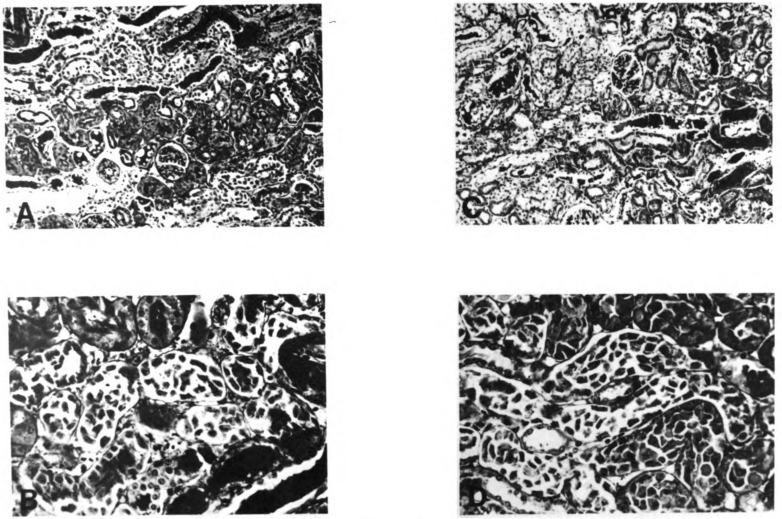

Figure 17

Figure 18. Effect of dose on PAP-induced renal necrosis in F344 rats. Animals were killed 24 hr after PAP (s.c.) administration. All sections were stained with PAS and magnified 120x. (A) PAP (0 mg/kg); normal. (B) PAP (100 mg/kg); mild focal necrosis of straight segment. (C) PAP (200 mg/kg); moderate focal necrosis predominantly in straight segment of proximal tubules, protein precipitate and casts within the distal tubules and collecting ducts. (D) PAP (400 mg/kg); severe focal necrosis of the straight and convoluted segment of proximal and distal tubules.

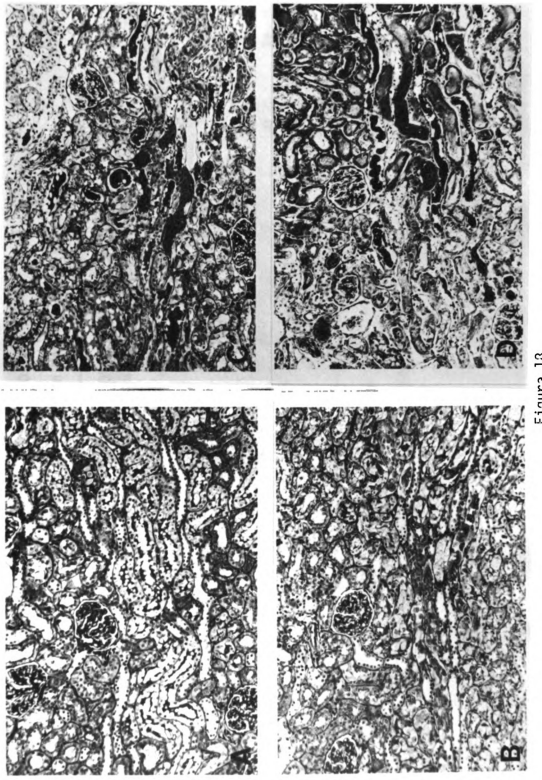

Figure 18

TABLE 10

Comparison of Renal Lesions Produced in Male F344 and SD Rats by PAP[a]

Strain	Dose of PAP (mg/kg)	No. of Rats	Necrosis (%)	Distribution[c]	Protein Precipitate[b]	Protein Casts[b]	Droplets[b]
Fischer 344	0	4	0	0	0-1+	0	1-2+
	50	4	0	0	0-1+	0	1-2+
	100	4	5-10	P	0	0	1-2+
	200	4	40-50	P&D	1+	3+	3+
	400	4	60-70	P&D	2+	3+	3+
Sprague-Dawley	0	4	0	0	0	0	1+
	50	4	0	0	0	0	1+
	100	4	0-5	P	0	0	1-2+
	200	4	0-10	P	0	0	2-3+
	400	4	20-50	P&D	2+	1-3+	2-3+

[a]Animals were treated with PAP (s.c.) and killed 24 hr later.

[b]Extent of histopathological changes was scored by criteria given under "Methods".

[c]P = Proximal tubule, D = distal tubule.

However, decreases in renal function were apparent in the F344 rat at much lower doses of PAP. BUN was elevated in F344 rats at doses of PAP as low as 200 mg/kg, whereas BUN was elevated in SD rats only at the highest (400 mg/kg) dose (Figure 19). Similarly, accumulation of PAH by renal cortical slices from F344 rats was reduced at a dose of 100 mg/kg PAP while PAH accumulation in slices from SD rats was reduced at only the highest dose (Figure 20). Significant strain differences in the susceptibility to PAP-induced nephrotoxicity were also evident in absolute kidney weights and kidney weight to body weight ratios (data not shown).

2. Urinary metabolites of PAP

Metabolites of PAP recovered in the urine during a twenty-four hour period following PAP administration are summarized in Table 11. As might be expected, lower recoveries of PAP and metabolites were evident in animals exhibiting significant nephrotoxicity. Furthermore, the strain differences in metabolite recovery at the highest doses of PAP matched other differences in nephrotoxicity.

A dose-related decrease in the proportion of PAP-CONJ (phenolic glucuronides and sulfates of PAP) was detected in both strains. The decrease was more pronounced in SD than in F344 rats, especially at the two highest doses of PAP. A dose-related increase in the proportion of APAP-CONJ reflected the decrease in PAP-CONJ. Furthermore, strain differences were apparent in the proportion of APAP-CONJ at the two highest doses of PAP. The proportion of PAP increased in a dose-related manner in F344 rats. However, the proportion of PAP in SD rats was elevated (in comparison to the lowest dose of PAP) only at the highest dose of PAP. The proportion of APAP also increased in a

Figure 19. Effect of PAP on BUN in F344 and SD rats. Animals were administered PAP (s.c.) and killed 24 hr later. Data are represented as the mean ± S.E.M. of four rats. *Significantly different from respective control (0 mg/kg PAP), $p<0.05$.

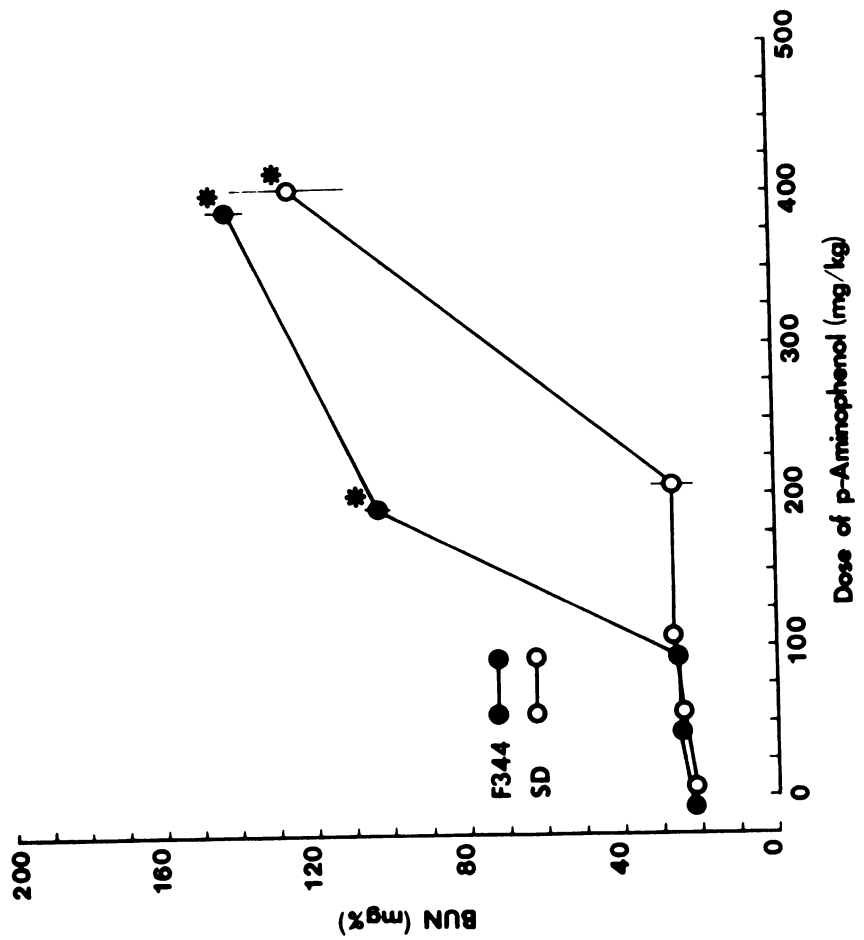
BUN (mg%)
200
160
120
80
40
0
F344
SD
0
100
200
300
400
500
Dose of p-Aminophenol (mg/kg)

Figure 19

Figure 20. Accumulation of PAH by renal cortical slices from F344 and SD rats 24 hr after PAP (s.c.) administration. Data are represented as the mean ± S.E.M. of four rats. *Significantly different from respective control (0 mg/kg PAP), $p<0.05$.

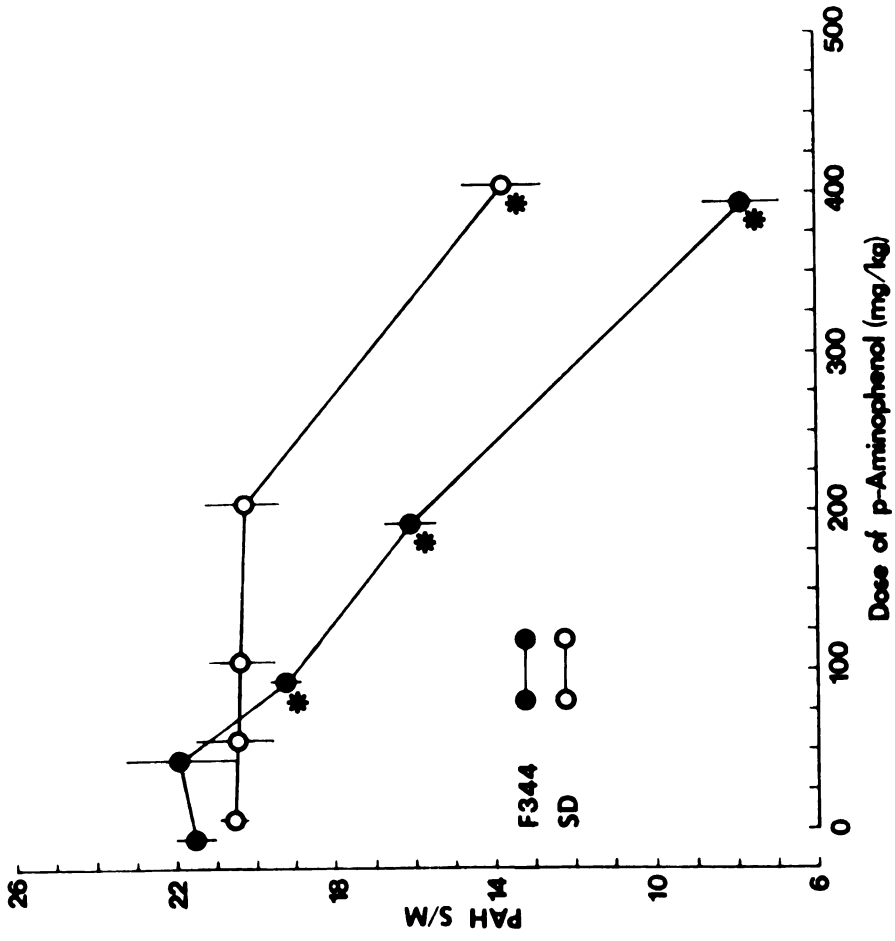
PAH S/M
26
22
18
14
10
6
0
100
200
300
400
500
Dose of p-Aminophenol (mg/kg)
F344
SD

Figure 20

TABLE 11

Effect of Dose on Urinary Metabolites of PAP in F344 and SD Rats[a]

PAP Dose (mg/kg)	Strain	APAP	APAP-CONJ[b]	PAP	PAP-CONJ[b]	APAP-MAP[b]	% of Administered Dose Recovered
		Percent Fractional Abundance[c]					
50	F344	2.17±0.52	28.91±1.20	1.60±0.47	65.49±1.61	0.74±0.14	45.8± 5.8
50	SD	2.41±0.43	27.91±3.43	3.55±0.47	65.24±3.44	0.85±0.11	74.7±10.6
100	F344	1.40±0.33	52.10±4.81	2.34±0.77	42.95±5.66	1.44±0.38	65.0± 4.1
100	SD	2.33±0.27	50.70±1.50	3.30±0.87	41.24±2.43	3.13±0.53	75.9± 7.6
200	F344	6.29±0.62	44.32±2.92	5.16±0.89	44.17±4.05	N.D.[d]	11.9± 2.6
200	SD	3.09±0.97	71.26±6.08	2.46±0.32	21.41±6.12	2.77±0.38	47.4± 3.2
400	F344	5.14±1.33	39.71±9.42	5.17±0.46	50.00±8.12	N.D.[d]	6.5± 0.7
400	SD	4.37±0.91	52.39±16.01	21.61±6.51	19.86±9.49	3.81±3.13	36.9± 5.8

[a]Values are the means ± SEM of four animals of urinary excretion over a 24 hr period following an s.c. dose of PAP.

[b]APAP-CONJ is the sum of APAP metabolized by conjugation only at the 4 position; APAP-MAP is the sum of all thioether metabolites including those that may also be conjugated at the 4 position, PAP is the sum of free PAP, and PAP-CONJ is the sum of PAP conjugated at the 4 position.

[c]The amount of a compound factored by the sum of the parent drug plus total metabolites, all on a molar basis.

[d]Not detectable.

dose-related manner. However, strain differences in the proportion of APAP were not apparent.

3. Renal and hepatic non-protein sulfhydryl concentrations

Non-protein sulfhydryl (NPSH) concentrations in the liver and renal cortex of both strains are summarized in Table 12. The hepatic NPSH concentration was approximately 2.5 times that found in the renal cortex. Strain differences in hepatic NPSH concentrations were not noted. However, renal NPSH concentrations were higher in renal cortical tissue from SD rats than from F344 rats.

4. Covalent binding of [ring-^{14}C]-PAP in vitro

The effect of PAP concentration on covalent binding was evaluated *in vitro* with renal microsomes from SD and F344 rats. Enzymatic binding of PAP to renal microsomes could be demonstrated without addition of cofactors. At PAP concentrations $\leq$5 mM, the covalent binding of PAP was greater in renal microsomes from F344 rats than in renal microsomes from SD rats (Figure 21). As the velocity versus substrate curves began to plateau at the highest concentration of PAP used, the strain differences in renal microsomal covalent binding were no longer apparent (Figure 21).

E. Renal Metabolic Activation of APAP In Vitro

1. Cytochrome P-450 dependent covalent binding of [ring-^{14}C]-APAP

Enzymatic binding of [ring-^{14}C]-APAP to hepatic and renal cortical microsomes was dependent upon the presence of an NADPH regenerating system and oxygen (Table 13). The enzymatic nature of this binding was demonstrated by the decreased binding following heating of

TABLE 12

Strain Differences in Non-Protein Sulfhydryl Content of Liver and Renal Cortex[a,b]

Strain	Non-Protein Sulfhydryl Conc (μmol/g tissue wet weight)	
	Renal Cortex	Liver
Fischer 344	2.66±0.13	7.20±0.46
Sprague-Dawley	3.14±0.09[c]	7.09±0.53

[a]Values are the means ± SEM of 5 animals.

[b]All animals were killed between 11 a.m. and 12 noon.

[c]Significantly different from corresponding tissue from F344 rats.

Figure 21. Effect of substrate concentration on [ring-^{14}C]-PAP binding to renal microsomal protein *in vitro*. Incubations were carried out for 30 min at 37°C under air. Reaction vessels contained renal microsomes (4.0 mg/ml), 2.0 ml of 0.1 M sodium phosphate buffer (pH 7.4) and various concentrations of [ring-^{14}C]-PAP (500 dpm/nmole). Data are represented as the mean ± S.E.M. of incubations from four rats. *Significant difference between strains at a respective PAP concentration, $p<0.05$.

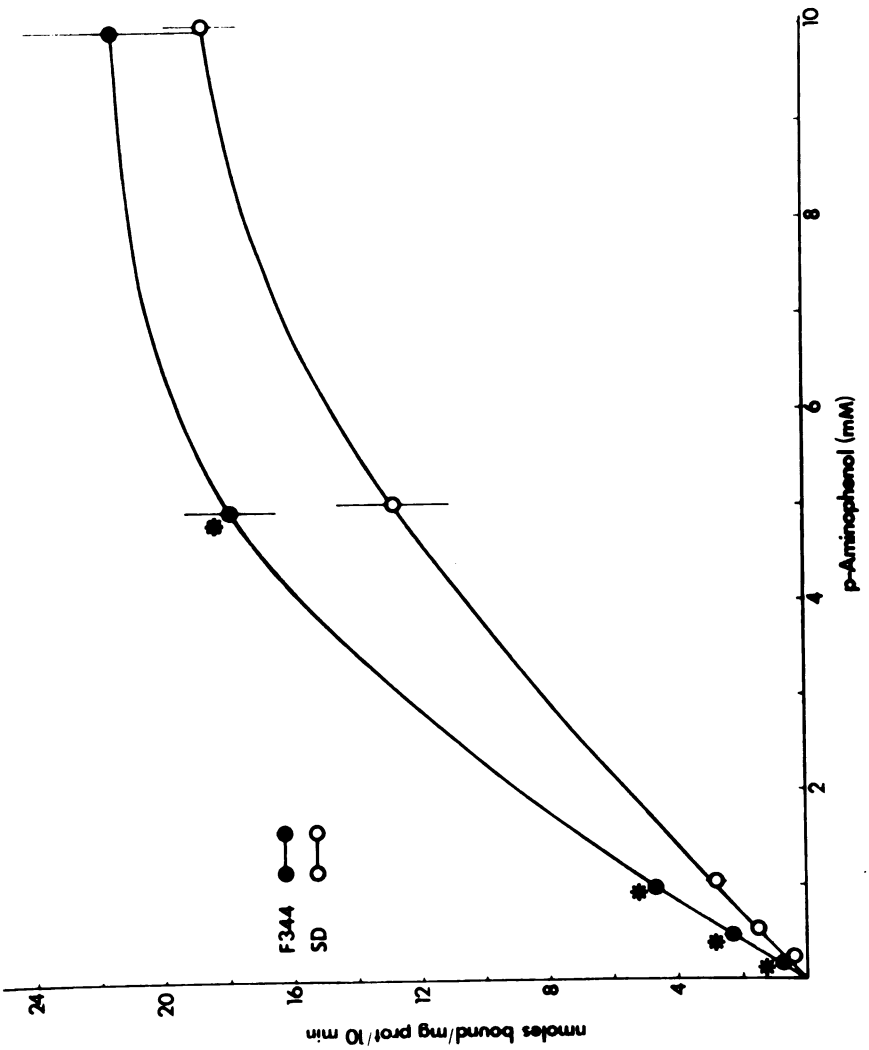
nmoles bound/mg prot/10 min
24
20
16
12
8
4
F344
SD
2
4
6
8
10
p-Aminophenol (mM)

Figure 21

TABLE 13

Covalent Binding of [Ring-^{14}C]-APAP in Renal and Hepatic Microsomes

	APAP Bound[c] (nmol/mg prot/10 min)	
	Kidney	Liver
Microsomes + NADPH[a]	0.236±0.039	0.493±0.192
Microsomes - NADPH[a]	0.064±0.019	0.052±0.007
Microsomes Boiled[a,b]	0.106±0.007	0.029±0.003

[a]Renal and hepatic microsomes (2.5 mg protein/ml) from male F344 rats were incubated under air for 10 min at 37°C in the presence of 2 mM [ring-^{14}C]-APAP (500 dpm/nmol) and an NADPH regenerating system.

[b]Heated at 100°C for 10 min.

[c]Values are means ± SEM of at least three different determinations per reaction mixture.

microsomes at 100°C for 10 min prior to incubation. Covalent binding of APAP was similar in boiled microsomes and viable microsomes without an NADPH regenerating system (Table 13). This nonenzymatic binding occurred instantaneously and was dependent upon the specific activity of APAP within the incubation vessel. This linear relationship between nonenzymatic binding and the specific activity of APAP suggests that the material that bound nonenzymatically was not APAP itself but some trace contaminant of the radioactive APAP. Enzymatic NADPH-dependent covalent binding of APAP was 2.5 times greater in liver than kidney (Table 13). The NADPH-dependent binding of [ring-^{14}C]-APAP was linear with renal microsomal protein up to an incubation concentration of 2.5 mg/ml (Figure 22). At a renal microsomal protein concentration of 2.5 mg/ml, binding of [ring-^{14}C]-APAP was linear for at least 15 minutes (Figure 22).

2. Covalent binding of [ring-^{14}C]-PAP in vitro

Enzymatic binding of [ring-^{14}C]-PAP to renal and hepatic cortical microsomes was dependent only upon the presence of oxygen (Table 14). The enzymatic nature of this binding was demonstrated by the decreased binding following heating of microsomes at 100°C for 10 min prior to incubation. A large percentage (>50%) of this nonenzymatic binding occurred instantaneously and was dependent upon the specific activity of PAP in the incubation vessel. This linear relationship between nonenzymatic binding and the specific activity of PAP suggests that the material that bound nonenzymatically was not PAP itself but some contaminant of the radioactive PAP. However, some of the nonenzymatic binding measured after 25 min of incubation occurred during

Figure 22. Effect of incubation duration (A) and protein concentration (B) on covalent binding of [ring-^{14}]-APAP to renal microsomes. Time course incubations (A) contained 2.5 mg/ml microsomal protein. Protein concentration incubations (B) were carried out for 10 min. All incubations were carried out at 37°C under air in the presence of 2 mM [ring-^{14}C]-APAP. Total covalent binding was determined with viable microsomes fortified with an NADPH regenerating system. Non-enzymatic binding was determined with heat-denatured (100°C for 10 min) microsomes. Enzymatic NADPH-dependent binding was calculated from the difference between total and non-enzymatic binding. Data represented are means $\pm$ S.E.M. of at least three different determinations per reaction mixture.

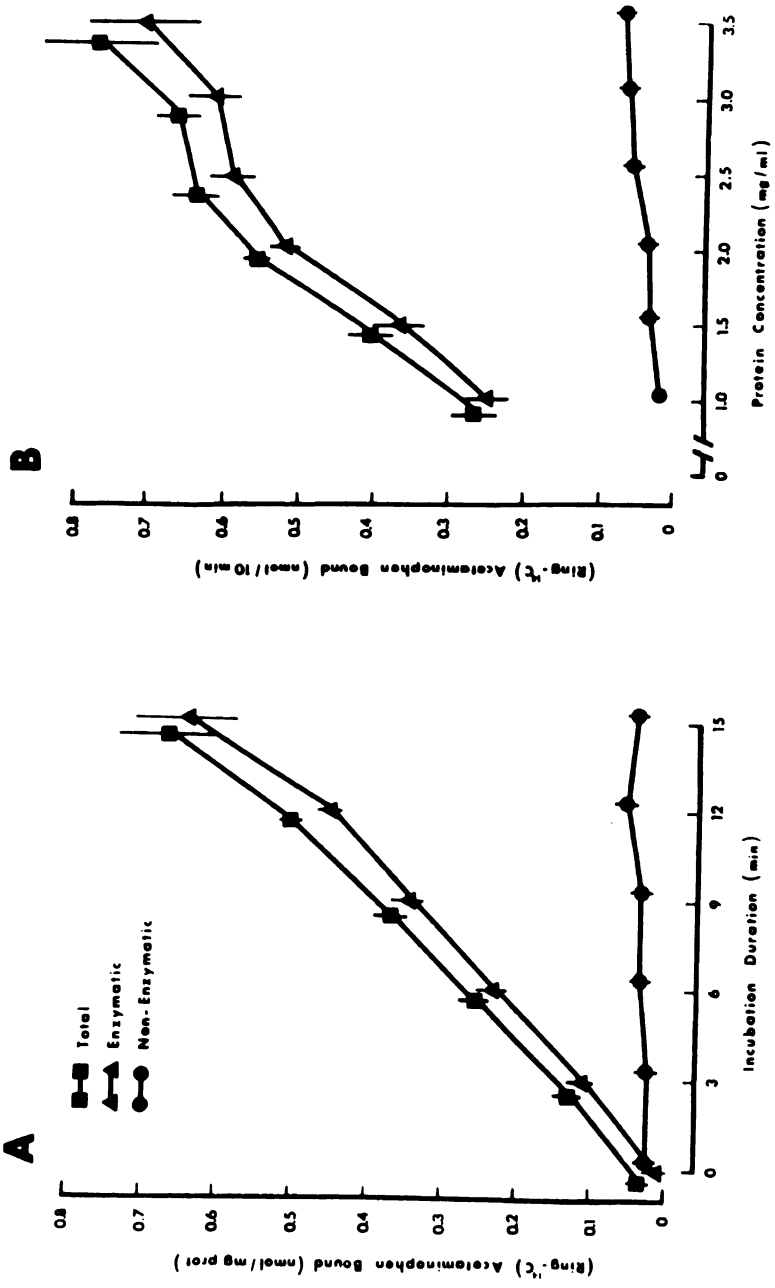
A
B
Total
Enzymatic
Non-Enzymatic
(Ring-^{14}C) Acetaminophen Bound (nmol/mg prot)
(Ring-^{14}C) Acetaminophen Bound (nmol/10 min)
Incubation Duration (min)
Protein Concentration (mg/ml)
0
0.1
0.2
0.3
0.4
0.5
0.6
0.7
0.8
3
6
9
12
15
1.0
1.5
2.0
2.5
3.0
3.5

Figure 22

TABLE 14

Covalent Binding of [Ring-^{14}C]-PAP in Renal and Hepatic Microsomes

	PAP Bound[c] (nmol/mg prot/10 min)	
	Kidney	Liver
Microsomes + NADPH[a]	1.037±0.163	0.792±0.090
Microsomes - NADPH[a]	4.603±0.357	1.110±0.108
Microsomes Boiled[a,b]	0.474±0.002	0.482±0.016

[a]Renal and hepatic microsomes (4 mg protein/ml) from male F344 rats were incubated under air for 10 min at 37°C in the presence of 1 mM [ring-^{14}C]-PAP (500 dpm/nmol) and an NADPH regenerating system.

[b]Heated at 100°C for 10 min.

[c]Values are means ± SEM of at least three different determinations per reaction mixture.

the incubation (Figure 23). Addition of an NADPH regenerating system markedly reduced PAP covalent binding in both hepatic and renal microsomes (Table 14). Enzymatic binding of [ring-^{14}C]-PAP was linear with renal microsomal protein up to an incubation concentration of at least 10 mg/ml (Figure 23). At a renal microsomal protein concentration of 4 mg/ml, binding of [ring-^{14}C]-PAP was linear for at least 25 min (Figure 23).

3. Deacetylation of APAP in renal and hepatic subcellular fractions

APAP was deacetylated to PAP by microsomes and cytosol from liver and kidney (Table 15). Hepatic microsomes exhibited greater deacetylase activity than renal microsomes. However, both renal and hepatic cytosol deacetylated APAP at similar rates. Microsomal protein accounts for less than 3% of the protein (>97% is cytosolic protein) in a 10,000 x g supernatant. Therefore, the expected deacetylation rates for renal and hepatic 10,000 x g supernatants were similar. However, the observed deacetylation rate in renal 10,000 x g supernatant was only 69% of the expected rate, whereas the expected and observed deacetylation rates in hepatic 10,000 x g supernatants were comparable (Table 15).

4. Covalent binding of [ring-^{14}C]-APAP to renal and hepatic subcellular fractions

Under incubation conditions (protein and duration) that were optimized to demonstrate deacetylase-dependent covalent binding, enzymatic binding of [ring-^{14}C]-APAP to protein was evident in renal microsomes. This enzymatic binding was inhibited by the addition of an NADPH regenerating system (Table 16). Enzymatic binding of

Figure 23. Effect of incubation duration (A) and protein concentration (B) on covalent binding of [ring-^{14}C]-PAP to renal microsomes. Time course incubations (A) contained 4.0 mg/ml microsomal protein. Protein concentration incubations (B) were carried out for 10 min. All incubations were carried out at 37°C under air in the presence of 1 mM [ring-^{14}C]-PAP. Total covalent binding was determined with viable microsomes. Non-enzymatic binding was determined with heat-denatured (100°C for 10 min) microsomes. Enzymatic binding was calculated from the difference between total and non-enzymatic binding. Data represented are means $\pm$ S.E.M. of at least three different determinations per reaction mixture.

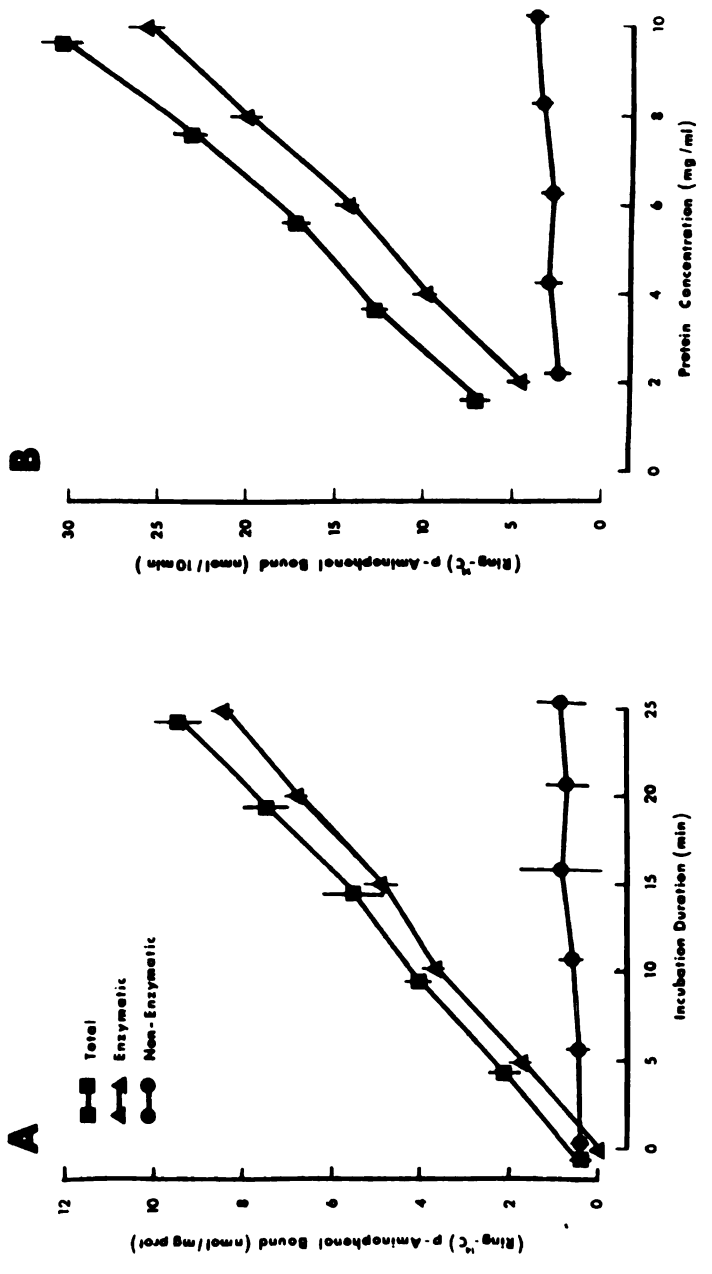
A
Total
Enzymatic
Non-Enzymatic
(Ring-^{14}C) p-Aminophenol Bound (nmol/mg prot)
Incubation Duration (min)
B
(Ring-^{14}C) p-Aminophenol Bound (nmol/10min)
Protein Concentration (mg/ml)

Figure 23

TABLE 15

Subcellular Distribution of APAP Deacetylation in Liver and Renal Cortex

Subcellular Fraction	PAP Formation[d] (nmol/mg protein/60 min)	
	Renal Cortex	Liver
Cytosol[a,b]	13.8±0.6	14.1±1.0
Microsome[a,b]	1.7±0.1	6.2±0.1
Post-mitochondrial Supernatant[a,b]		
Expected[c]	13.5±0.6	13.9±1.0
Observed	9.2±0.6	13.9±0.6
$\frac{\text{Observed}}{\text{Expected}}$	0.69±0.02	1.03±0.12

[a]Subcellular fractions (12 mg/ml) from male F344 rats were incubated under air for 60 min at 37°C in the presence of 10 mM APAP.

[b]Cytosol is 100,000 x g supernatant, microsome is 100,000 x g pellet and post-mitochondrial supernatant 10,000 x g supernatant.

[c]Expected deacetylation rates were calculated from component (microsomal or cytosolic) deacetylation expressed as a function of the fraction of post-mitochondrial protein. Renal microsomal protein accounted for 2.6±0.3 percent of renal post-mitochondrial protein, hepatic microsomal protein accounted for 2.5±0.2 percent of hepatic post-mitochondrial protein.

[d]Values are means ± SEM of at least four incubations.

TABLE 16

Covalent Binding of [Ring-^{14}C]-APAP to Renal Subcellular Fractions *In Vitro*

Reaction Mixture	APAP Bound[c] (nmol/mg prot/120 min)		
	Microsome	Cytosol	Microsome + Cytosol
Complete[a]	0.262±0.005	0.050±0.017	1.075±0.115
Without NADPH[a]	0.555±0.021	0.077±0.006	2.446±0.116
Heat-Denatured[a,b]	0.240±0.001	0.091±0.006	0.062±0.006

[a]Renal subcellular fractions (12 mg prot/ml) from male F344 rats were incubated under air for 120 min in the presence of 2 mM [ring-^{14}C]-APAP (500 dpm/nmol) and an NADPH regenerating system.

[b]Heated at 100°C for 10 min.

[c]Values are means ± SEM of at least three different determinations per reaction mixture.

[ring-^{14}C]-APAP was not detectable in renal cytosolic fractions (Table 16). However, combination of cytosol and microsomes, in the proportion normally found in post-mitochondrial (10,000 x g) supernatants, resulted in significantly greater covalent binding of APAP compared to cytosolic or microsomal fractions alone (Table 16). This binding was much greater than would be expected from the simple addition of cytosol and microsomes. Enzymatic covalent binding of APAP to cytosolic and microsomal combinations was inhibited by the addition of NADPH (Table 16). Approximately one-third of the nonenzymatic binding occurred instantaneously while the remaining portion increased with time during the incubation (Figure 24). Binding of [ring-^{14}C]-APAP to renal 10,000 x g supernatants increased over time in a non-linear fashion (Figure 24). The binding of [ring-^{14}C]-APAP to renal 10,000 x g supernatants was linear up to incubation protein concentrations of 20 mg/ml (Figure 24). Enzymatic covalent binding of [ring-^{14}C]-APAP to hepatic subcellular fractions could not be established in microsomes or cytosol or upon the combination of both (Table 17).

In an attempt to characterize the binding of [ring-^{14}C]-APAP to renal 10,000 x g supernatants, several inhibitors of APAP and PAP metabolism were used. Among these were the acyl amidase inhibitor bis-(p-nitrophenyl)phosphate (BNPP), PAP and the endogenous nucleophile glutathione (GSH). Equal molar amounts of all three compounds reduced the binding of [ring-^{14}C]-APAP to renal 10,000 x g supernatants (Table 18). Slight strain differences were noted in the binding of [ring-^{14}C]-APAP to renal 10,000 x g supernatants; supernatants from

Figure 24. Effect of incubation duration (A) and protein concentration (B) on covalent binding of [ring-^{14}C]-APAP to renal 10,000 x g supernatants. Time course incubations (A) contained 12 mg/ml protein. Protein dependency incubations (B) were carried out for 120 min. All incubations were carried out at 37°C under air in the presence of 2 mM [ring-^{14}C]-APAP. Total covalent binding was determined with viable 10,000 x g supernatants. Non-enzymatic binding was determined with heat-denatured (100°C for 10 min) 10,000 x g supernatants. Enzymatic binding was calculated from the difference between total and non-enzymatic binding. Data represented are means $\pm$ S.E.M. of at least three different determinations per reaction mixture.

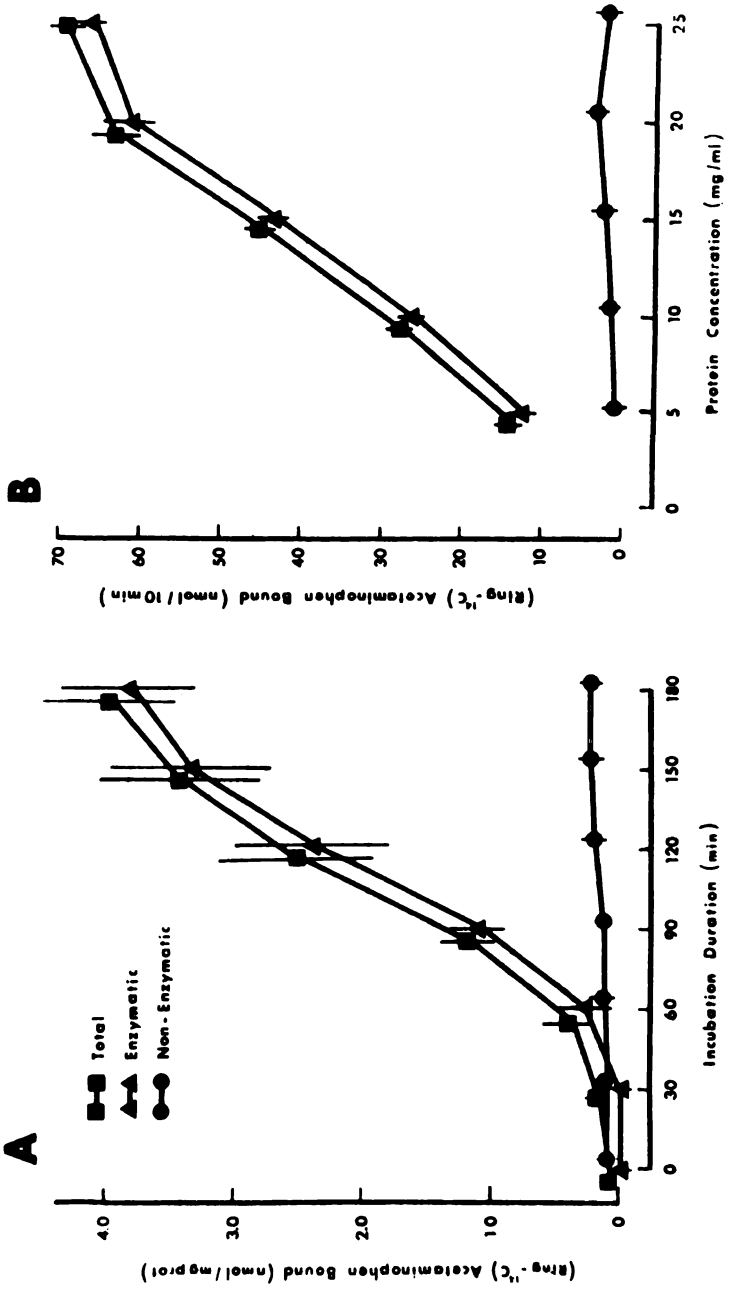
A
Total
Enzymatic
Non-Enzymatic
(Ring-^{14}C) Acetaminophen Bound (nmol/mg prot)
Incubation Duration (min)
B
(Ring-^{14}C) Acetaminophen Bound (nmol/10 min)
Protein Concentration (mg/ml)

Figure 24

TABLE 17

Covalent Binding of [Ring-^{14}C]-APAP to Hepatic Subcellular Fractions *In Vitro*

Reaction Mixture	APAP Bound[c] (nmol/mg prot/120 min)		
	Microsome	Cytosol	Microsome + Cytosol
Complete[a]	0.390±0.023	0.042±0.010	0.133±0.006
Without NADPH[a]	0.328±0.009	0.051±0.005	0.121±0.010
Heat-Denatured[a,b]	0.310±0.078	0.094±0.013	0.146±0.043

[a]Hepatic subcellular fractions (12 mg prot/ml) from male F344 rats were incubated under air for 120 min in the presence of 2 mM [ring-^{14}C]-APAP (500 dpm/nmol) and an NADPH regenerating system.

[b]Heated at 100°C for 10 min.

[c]Values are means ± SEM of at least three different determinations per reaction mixture.

TABLE 18

Covalent Binding of [Ring-^{14}C]-APAP to Renal 10,000 x g Supernatants *In Vitro*

Reaction Mixture	APAP Bound[b,c] (% of Control)
Control[a]	
+ Bis-(p-nitrophenyl)phosphate (1 mM)[a]	82±1
+ p-Aminophenol (1 mM)[a]	51±2
+ Glutathione (1 mM)[a]	47±6

[a]10,000 x g Supernatants (12 mg/ml) from male F344 rats were incubated under air at 37°C for 120 min in the presence of 2 mM [ring-^{14}C]-APAP (500 dpm/nmol).

[b]Values are corrected for non-specific binding to heat-denatured supernatants.

[c]Values are means ± SEM of at least three determinations per reaction mixture.

F344 rats exhibited greater enzymatic binding than supernatants from SD rats (Table 19).

5. Covalent binding of [acetyl-^{14}C]- and [ring-^{14}C]-APAP

NADPH-dependent binding of APAP to renal and hepatic microsomes, using protein concentrations and incubation times optimized to demonstrate P-450 dependent binding, was slightly greater when [ring-^{14}C]-APAP was used as a substrate than when [acetyl-^{14}C]-APAP was used (Table 20). Non-specific binding of both [acetyl-^{14}C]-APAP and [ring-^{14}C]-APAP was similar in both renal and hepatic microsomal incubations (Table 20).

Enzymatic covalent binding of APAP to renal 10,000 x g supernatants, using protein concentrations and incubation times optimized to demonstrate deacetylase-dependent binding, was detectable only when [ring-^{14}C]-APAP was used as a substrate (Table 21). Enzymatic covalent binding of [acetyl-^{14}C]-APAP to renal 10,000 x g supernatants was not apparent under any incubation conditions (Table 21). Enzymatic binding of APAP to hepatic 10,000 x g supernatants was not detectable when either [acetyl-^{14}C]-APAP or [ring-^{14}C]-APAP was used as a substrate (Table 21).

F. Effect of BNPP on APAP and PAP Nephrotoxicity and Metabolism

1. In vitro deacetylation and covalent binding of APAP

Renal cortical 10,000 x g supernatants deacetylated APAP to PAP at rates similar to those previously reported for mice (Carpenter and Mudge, 1981). Addition of BNPP to renal incubations containing APAP resulted in a concentration-dependent decrease in APAP

TABLE 19

Strain Differences in the Covalent Binding of [Ring-^{14}C]-APAP to Renal and Hepatic 10,000 x g Supernatants

Reaction Mixture	APAP Bound[c] (nmol/mg prot/120 min)	
	SD	F344
Renal Complete[a]	0.910±0.050	1.197±0.147
Renal Heat Denatured[a,b]	0.079±0.004	0.059±0.004
Hepatic Complete[a]	0.077±0.005	0.098±0.013
Hepatic Heat Denatured[a,b]	0.142±0.008	0.105±0.013

[a]Renal and hepatic 10,000 x g supernatants (approximately 12 mg prot/ml) were incubated under air for 120 min at 37°C in the presence of 2 mM [ring-^{14}C]-APAP (500 dpm/nmol).

[b]Heated at 100°C for 10 min.

[c]Values are means ± SEM of at least four determinations per reaction mixture.

TABLE 20

Covalent Binding of Specifically Labelled [^{14}C]-APAP to Renal and Hepatic Microsomes *In Vitro*

Reaction Mixture	APAP Bound[c] (nmol/mg prot/10 min)	
	(Acetyl-^{14}C)-APAP	(Ring-^{14}C)-APAP
Renal Complete[a]	0.229±0.014	0.257±0.027
Renal Without NADPH[a]	0.034±0.002	0.041±0.007
Renal Heat Denatured[a,b]	0.036±0.006	0.037±0.004
Hepatic Complete[a]	0.885±0.125	1.095±0.145
Hepatic Without NADPH[a]	0.048±0.007	0.082±0.014
Hepatic Heat Denatured[a,b]	0.041±0.007	0.059±0.007

[a]Renal and hepatic microsomes (2.5 mg prot/ml) from male F344 rats were incubated under air at 37°C for 10 min at 37°C in the presence of 2 mM [^{14}C]-APAP (500 dpm/nmol) and an NADPH regenerating system.

[b]Heated at 100°C for 10 min.

[c]Values are means ± SEM of at least three determinations per reaction mixture.

TABLE 21

Covalent Binding of Specifically Labelled [^{14}C]-APAP to Renal and Hepatic 10,000 x g Supernatants *In Vitro*

Reaction Mixture	APAP Bound[c] (nmol/mg prot/120 min)	
	(Acetyl-^{14}C)-APAP	(Ring-^{14}C)-APAP
Renal Complete[a]	0.042±0.004	0.105±0.002
Renal Without NADPH[a]	0.055±0.002	1.594±0.025
Renal Heat Denatured[a,b]	0.071±0.002	0.151±0.025
Hepatic Complete[a]	0.066±0.003	0.161±0.002
Hepatic Without NADPH[a]	0.045±0.002	0.111±0.002
Hepatic Heat Denatured[a,b]	0.123±0.025	0.108±0.009

[a]10,000 x g Supernatants (12 mg prot/ml) from male F344 rats were incubated under air for 120 min at 37°C in the presence of 2 mM [^{14}C]-APAP (500 dpm/nmol) and an NADPH regenerating system.

[b]Heated at 100°C for 10 min.

[c]Values are means ± SEM of at least three determinations per reaction mixture.

deacetylation (Figure 25). Deacetylation was inhibited as much as 60 percent with 8 mM BNPP.

Incubation of [ring-^{14}C]-APAP with renal 10,000 x g supernatants resulted in significant binding of label to renal proteins. Addition of BNPP to incubations resulted in a concentration-dependent reduction in covalent binding; 8 mM BNPP inhibited arylation of renal proteins by 70 percent (Figure 26).

2. APAP- and PAP-induced nephrotoxicity

Administration of high doses of APAP to naive F344 rats resulted in dose-dependent increases in kidney weight/body weight (KW/BW) ratios and blood urea nitrogen (BUN), indicative of extensive renal damage (Table 22). Pretreatment of rats with BNPP alone did not affect renal function. The increase in BUN produced by 750 mg/kg APAP was not altered by BNPP pretreatment (Table 22). However, BNPP reduced the increase in BUN and KW/BW ratios following 900 mg/kg APAP (Table 22). BNPP pretreated rats that received 900 mg/kg APAP exhibited BUN concentrations and KW/BW ratios similar to rats that received 750 mg/kg APAP (Table 22).

PAP produced changes in renal function at doses much lower than required for APAP (Table 22). Both BUN and KW/BW ratios were elevated after doses of 150 and 300 mg/kg PAP in naive and BNPP pretreated rats. BNPP did not have a consistent effect on PAP-induced changes in renal function. BUN of rats pretreated with BNPP prior to receiving 150 mg/kg PAP was higher than in naive animals receiving a similar dose of PAP; KW/BW was not influenced by BNPP (Table 22).

Figure 25. Effect of BNPP on APAP deacetylation by renal cortical 10,000 x g supernatants from F344 rats. Incubations were carried out for 30 min at 37°C under air. Approximately 15-20 mg of 10,000 x g supernatant protein was incubated in the presence of 10 mM APAP and various concentrations (0-8 mM) BNPP. Data are represented as the mean ± S.E.M. of incubations from 4 rats. Enzyme activity was expressed as μmoles of PAP generated per gram, wet weight, of cortical tissue per hour.

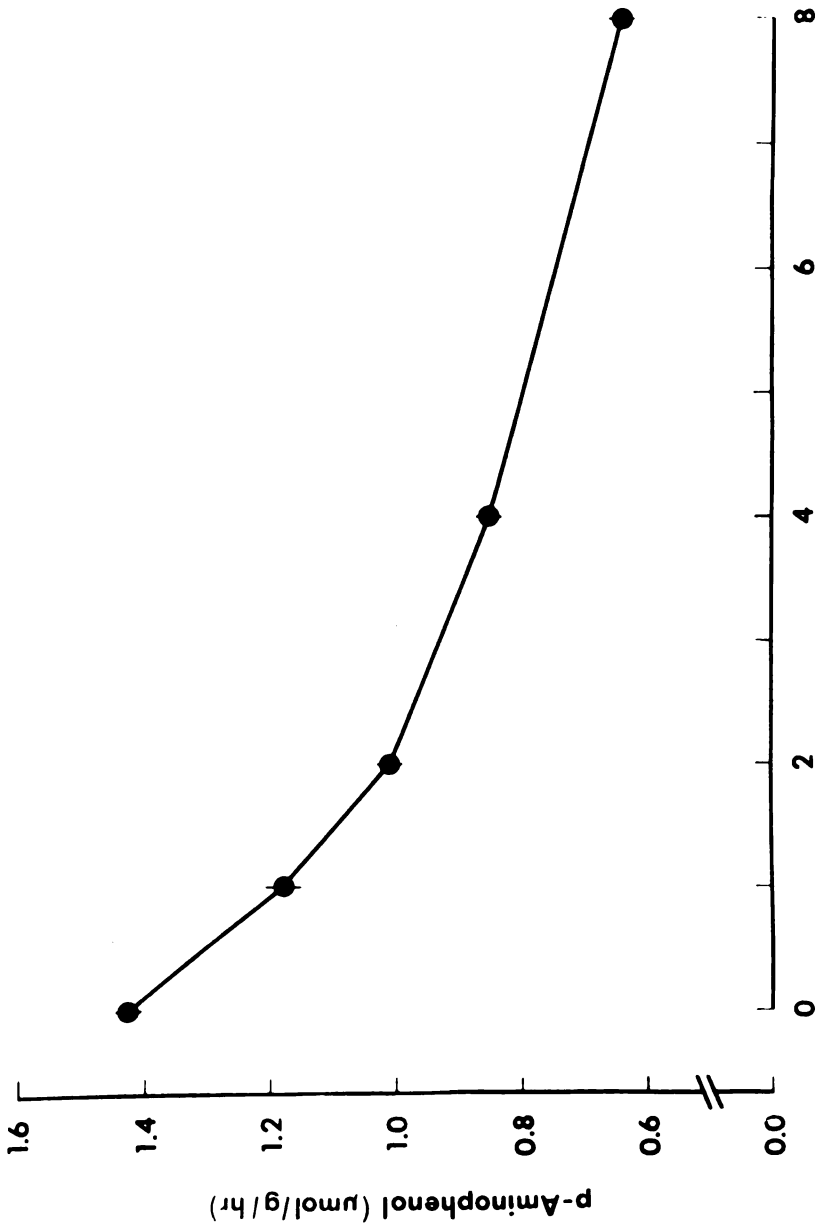
p-Aminophenol (μmol/g/hr)
1.6
1.4
1.2
1.0
0.8
0.6
0.0
0
2
4
6
8
BNPP in Incubation (mM)

Figure 25

Figure 26. Effect of BNPP on covalent binding of [ring-^{14}C]-APAP to renal cortical 10,000 x g supernatants from F344 rats. Incubations were carried out for 120 min at 37°C under air. Approximately 10 mg of 10,000 x g supernatant protein was incubated in the presence of 2 mM [ring-^{14}C]-APAP and various concentrations (0-8 mM) BNPP. Data are represented as the mean $\pm$ S.E.M. of incubations from 3 rats. Enzyme activity was expressed as nmoles [^{14}C] bound per mg protein per 120 min incubation. Non-enzymatic binding (arylation of heat-denatured supernatant) was subtracted from binding to viable tissue to determine enzymatic binding.

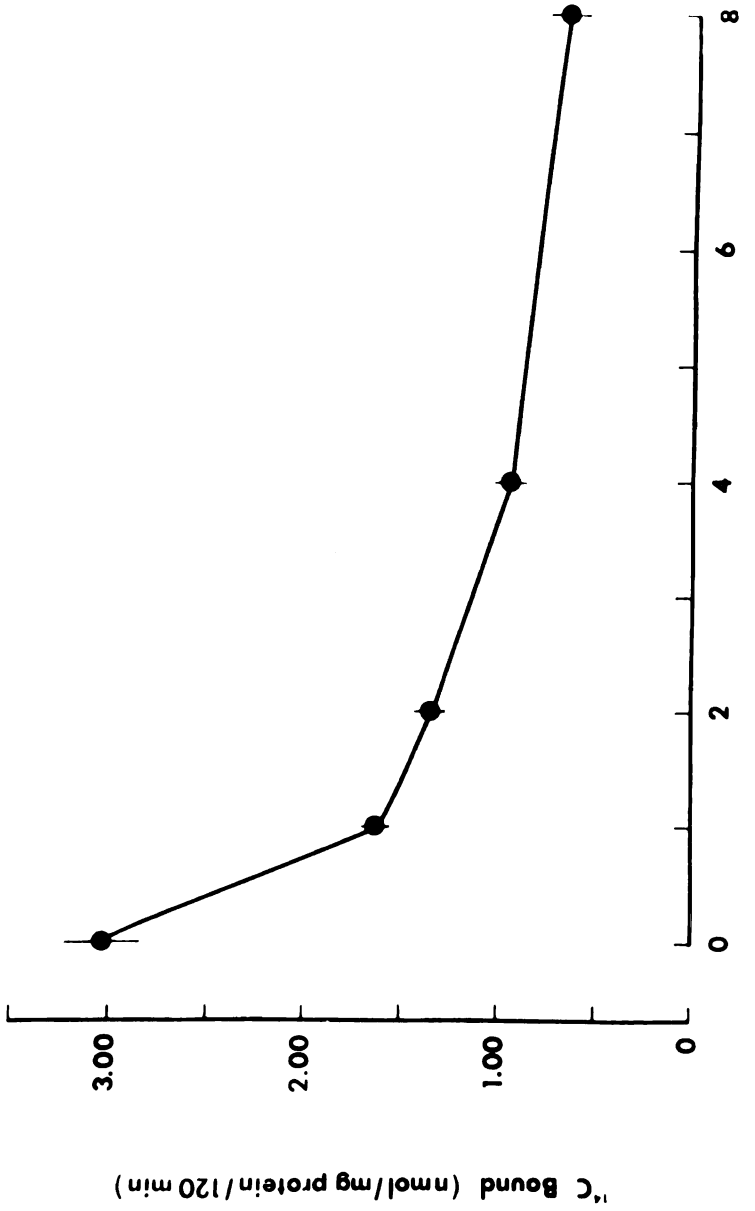
^{14}C Bound (nmol/mg protein/120 min)
3.00
2.00
1.00
0
0
2
4
6
8
BNPP in Incubation (mM)

Figure 26

TABLE 22

Effect of BNPP on APAP and PAP Nephrotoxicity in F344 Rats[a,b]

			Dose of APAP (mg/kg)		Dose of PAP (mg/kg)	
		Water	750	900	150	300
	Pretreatment					
Kidney Weight/ Body Weight (g/kg)	Water	0.78±0.01	0.84±0.03	0.93±0.01[c]	1.00±0.03	0.92±0.02
	BNPP	0.77±0.04	0.84±0.03	0.83±0.01[c]	1.00±0.02	0.86±0.02
BUN (mg %)	Water	18±1	48±13	168±17[c]	97±23[c]	185±7
	BNPP	17±2	49±16	53±16[c]	150±18[c]	193±7
PAH S/M	Water	36.4±1.9	31.4±1.6	27.7±1.2	29.1±1.7	13.0±1.0
	BNPP	33.4±2.3	29.1±2.5	28.3±1.8	26.8±2.5	8.7±1.7
TEA S/M	Water	29.7±2.6	27.5±1.8	26.1±1.6	28.5±1.8	14.7±1.1
	BNPP	27.1±1.8	24.7±2.7	26.2±2.9	25.6±1.4	11.0±2.5

[a]Animals were pretreated with BNPP (100 mg/kg) or water thirty minutes prior to APAP or PAP administration.

[b]Values are the means ± SEM for at least 5 animals.

[c]Significantly different from the water group receiving an equivalent dose of APAP or PAP ($p<0.05$).

3. Disposition of APAP and metabolites

Plasma concentrations of APAP were highest 2 hr following a nephrotoxic (900 mg/kg) dose of APAP, falling to approximately 60 percent of this value 5 hr following injection (Figure 27). BNPP pretreatment did not have a consistent effect on the plasma concentration of APAP. Only at the 3 hr time point were plasma concentrations of APAP higher in the BNPP pretreated animals (Figure 27). Plasma concentrations of APAP-CONJ (phenolic glucuronides and sulfates) increased at every time point following injection, reaching their highest concentration 5 hr after APAP administration (Figure 27). Of the five thioether metabolites of APAP (APAP-MAP) for which analytical procedures were available (APAP-GSH, APAP-CYS, APAP-NAC, APAP-SCH_3, and APAP-$SOCH_3$) only APAP-NAC could be detected in the plasma. However, the plasma concentrations of APAP-NAC were highly variable; an effect of BNPP pretreatment was not evident (Figure 27).

Renal cortical concentrations of APAP and metabolites reflected plasma concentrations (Figure 28). Renal cortical concentrations of APAP were approximately 20-30 percent greater than plasma concentrations. BNPP pretreatment did not have a consistent effect on renal cortical APAP concentration (Figure 28). However, BNPP pretreatment resulted in greater cortical concentrations of APAP-CONJ at later time points (2-5 hr). Renal cortical concentrations of APAP-CONJ were 5-10 times plasma concentrations. The time-dependent increase in the cortical concentrations of APAP-CONJ roughly paralleled plasma concentrations (Figure 28). Thioether metabolites of APAP detected in renal cortex included APAP-NAC and APAP-CYS. Renal

Figure 27. Effect of BNPP on plasma concentrations of APAP and its metabolites. Animals were pretreated with either water or BNPP (100 mg/kg, i.p.) dissolved in water 30 min prior to administration of APAP (900 mg/kg, i.p.). Metabolites of APAP detected in plasma included the phenolic sulfates and glucuronides (APAP-CONJ) and the mercapturic acid (APAP-NAC). Data are represented as the mean $\pm$ S.E.M. of at least 5 rats.

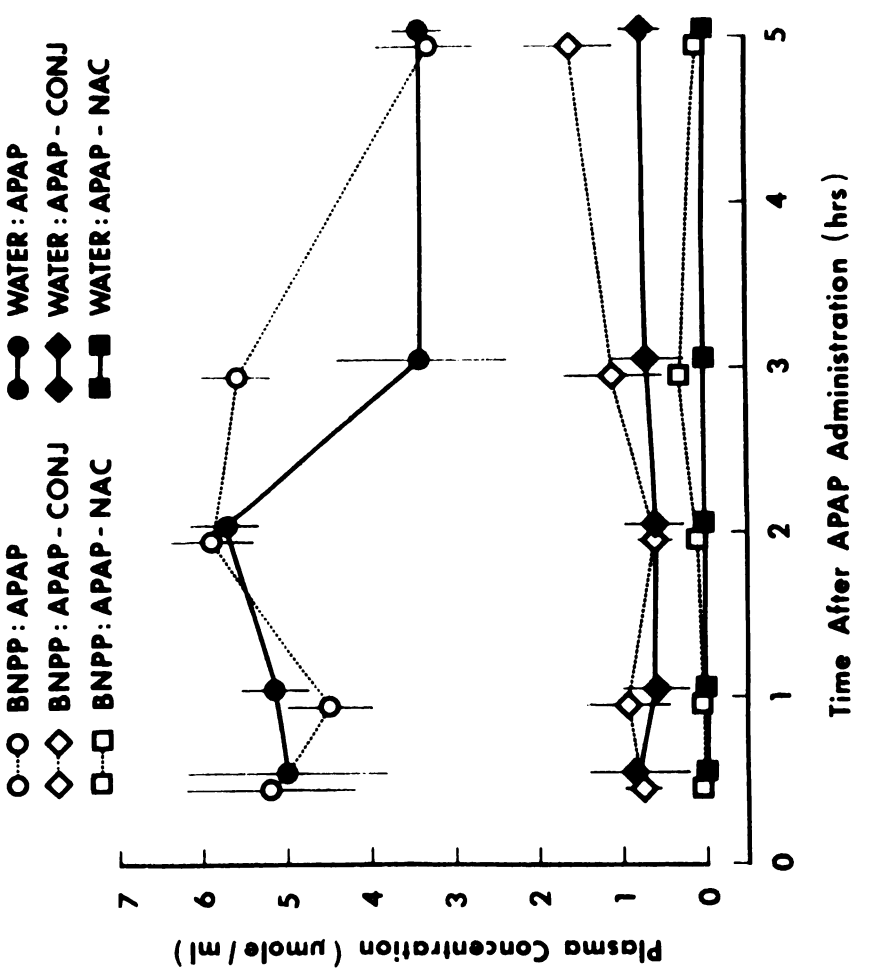
BNPP : APAP
BNPP : APAP - CONJ
BNPP : APAP - NAC
WATER : APAP
WATER : APAP - CONJ
WATER : APAP - NAC
Plasma Concentration (µmole / ml)
Time After APAP Administration (hrs)
0
1
2
3
4
5
7
6
5
4
3
2
1
0

Figure 27

Figure 28. Effect of BNPP on renal cortical concentrations of APAP and metabolites. Animals were pretreated with either water or BNPP (100 mg/kg, i.p.) dissolved in water 30 min prior to administration of APAP (900 mg/kg, i.p.). Metabolites of APAP detected in renal cortex included the phenolic sulfates and glucuronides (APAP-CONJ), the cysteine conjugate (APAP-CYS) and the mercapturic acid (APAP-NAC). Data are represented as the mean $\pm$ SEM of at least 5 rats.

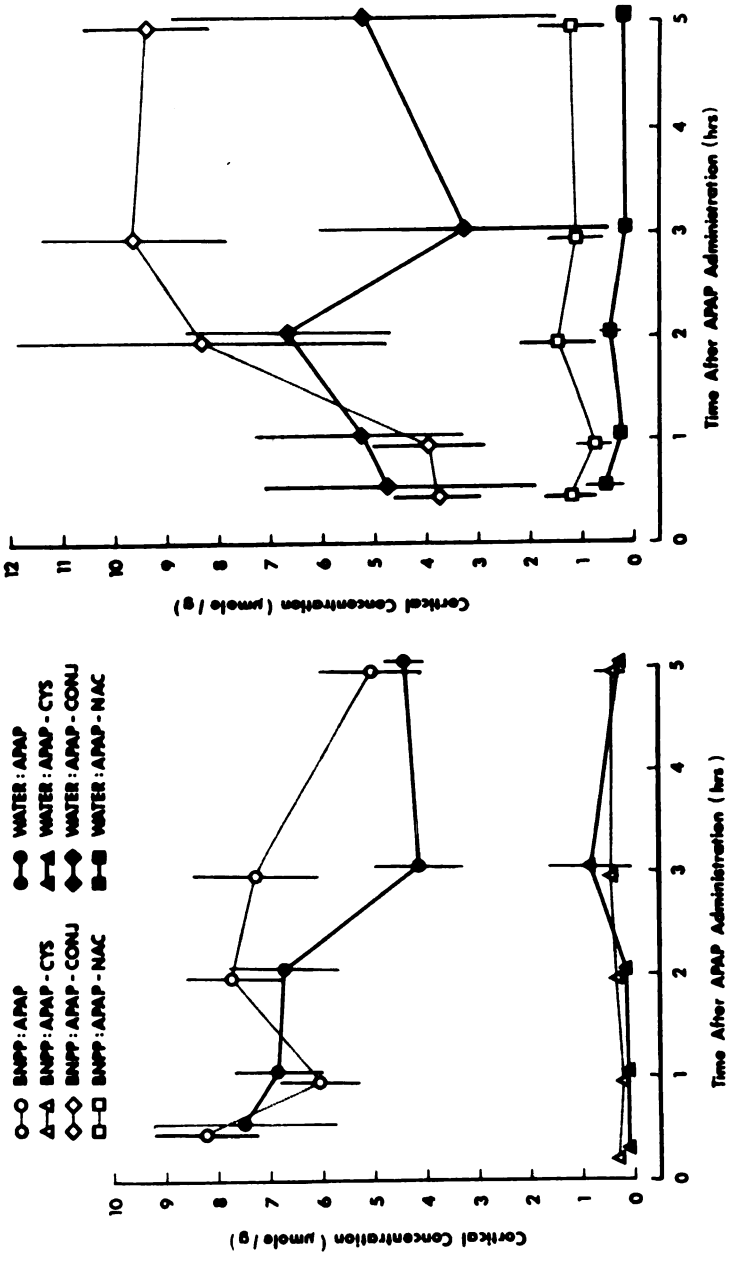
BNPP : APAP
BNPP : APAP - CYS
BNPP : APAP - CONJ
BNPP : APAP - NAC
WATER : APAP
WATER : APAP - CYS
WATER : APAP - CONJ
WATER : APAP - NAC
Cortical Concentration (μmole / g)
Time After APAP Administration (hrs)

Figure 28

cortical concentrations of APAP-NAC were consistently 10-20 times greater than plasma concentrations. Like the effect on APAP-CONJ, BNPP pretreatment resulted in greater renal cortical concentrations of APAP-NAC. BNPP pretreatment did not affect the cortical concentration of APAP-CYS (Figure 28).

Hepatic concentrations of APAP were very similar to those found in the renal cortex (Figure 29). BNPP pretreatment did not result in a consistent effect on hepatic concentrations of APAP. However, BNPP pretreated animals had a tendency for higher hepatic concentrations of APAP-CONJ especially at the latter time points (Figure 29). Thioether metabolites of APAP detected in hepatic tissue included APAP-NAC and APAP-GSH. BNPP pretreatment did not affect the hepatic concentration of either of these metabolites (Figure 29).

4. Urinary metabolites of APAP and PAP

Metabolites of APAP recovered in the urine during a 24 hr period following APAP administration are summarized in Figure 30. 70.0±4.5 and 30.0±7.9 percent of the administered dose was recovered in the urine of animals that received 750 and 900 mg/kg APAP, respectively. In contrast, 60.6±8.4 and 65.4±9.1 percent of the administered dose was recovered in the urine of BNPP pretreated animals that received 750 and 900 mg/kg APAP, respectively.

APAP-CONJ (phenolic glucuronides and sulfates) accounted for 70-80 percent of the recovered dose (%RD) at both doses of APAP; APAP accounted for 15-20 %RD. BNPP pretreatment did not affect the percentages of APAP or APAP-CONJ. Of the five thioether metabolites of APAP (APAP-MAP) only APAP-NAC and APAP-SCH_3 were detected in the urine at

Figure 29. Effect of BNPP on hepatic concentrations of APAP and metabolites. Animals were pretreated with either water or BNPP (100 mg/kg, i.p.) dissolved in water 30 min prior to administration of APAP (900 mg/kg, i.p.). Metabolites of APAP detected in liver included the phenolic sulfates and glucuronides (APAP-CONJ), the glutathione conjugate (APAP-GSH) and the mercapturic acid (APAP-NAC). Data are represented as the mean $\pm$ S.E.M. of at least 5 rats.

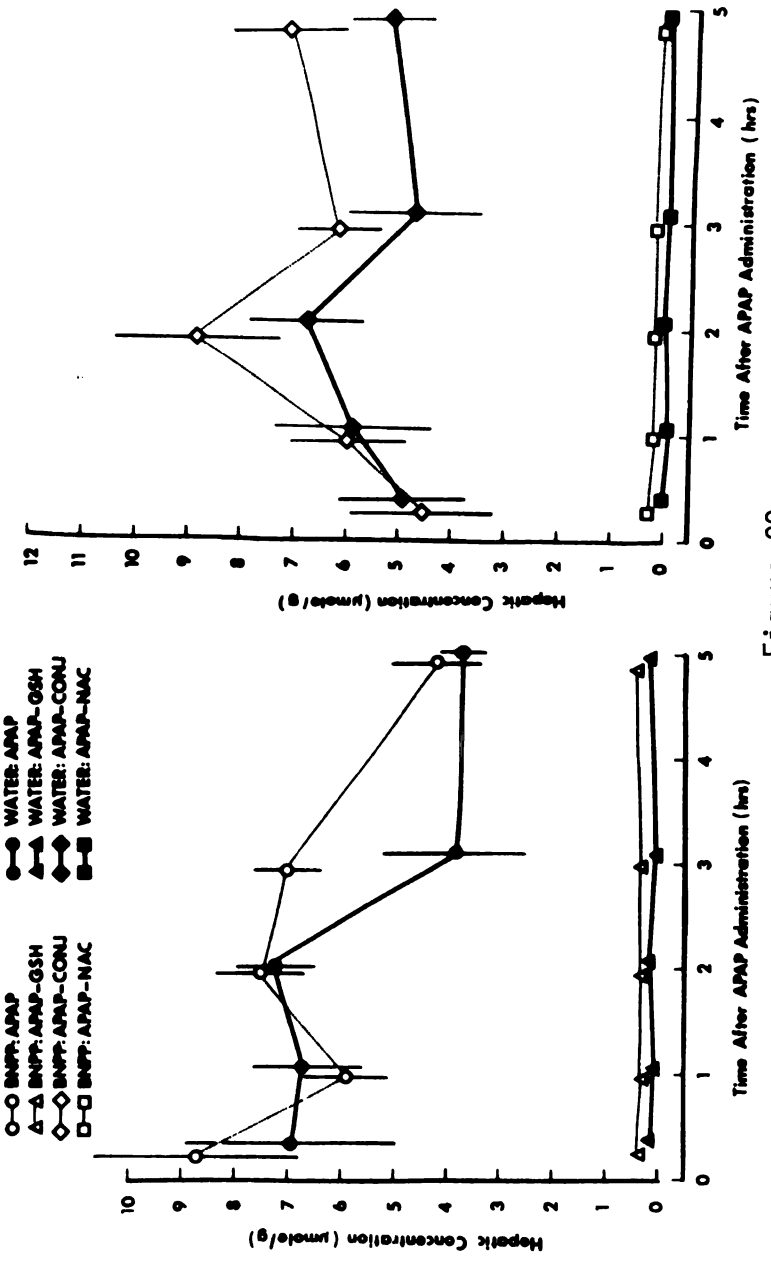
BNPP: APAP
BNPP: APAP-GSH
BNPP: APAP-CONJ
BNPP: APAP-NAC
WATER: APAP
WATER: APAP-GSH
WATER: APAP-CONJ
WATER: APAP-NAC
Hepatic Concentration (μmole/g)
Time After APAP Administration (hrs)

Figure 29

Figure 30. Effect of BNPP on urinary metabolites of APAP. Animals were pretreated with either water (-) or BNPP (+) dissolved in water (100 mg/kg, i.p.) 30 min prior to administration of APAP (750 or 900 mg/kg, i.p.). Urine was collected for 24 hr following APAP administration. APAP-CONJ is the sum of APAP conjugated at the 4 position; APAP-MAP is the sum of all thioether metabolites including those that may be conjugated at the 4 position; PAP is the sum of free PAP and PAP conjugated at the 4 position. Metabolites are expressed as a percent of the recovered dose. Data represented are the mean $\pm$ S.E.M. of at least 5 rats. *Significantly different percentage of metabolite excreted in comparison to animals pretreated with water receiving an equivalent dose of APAP.

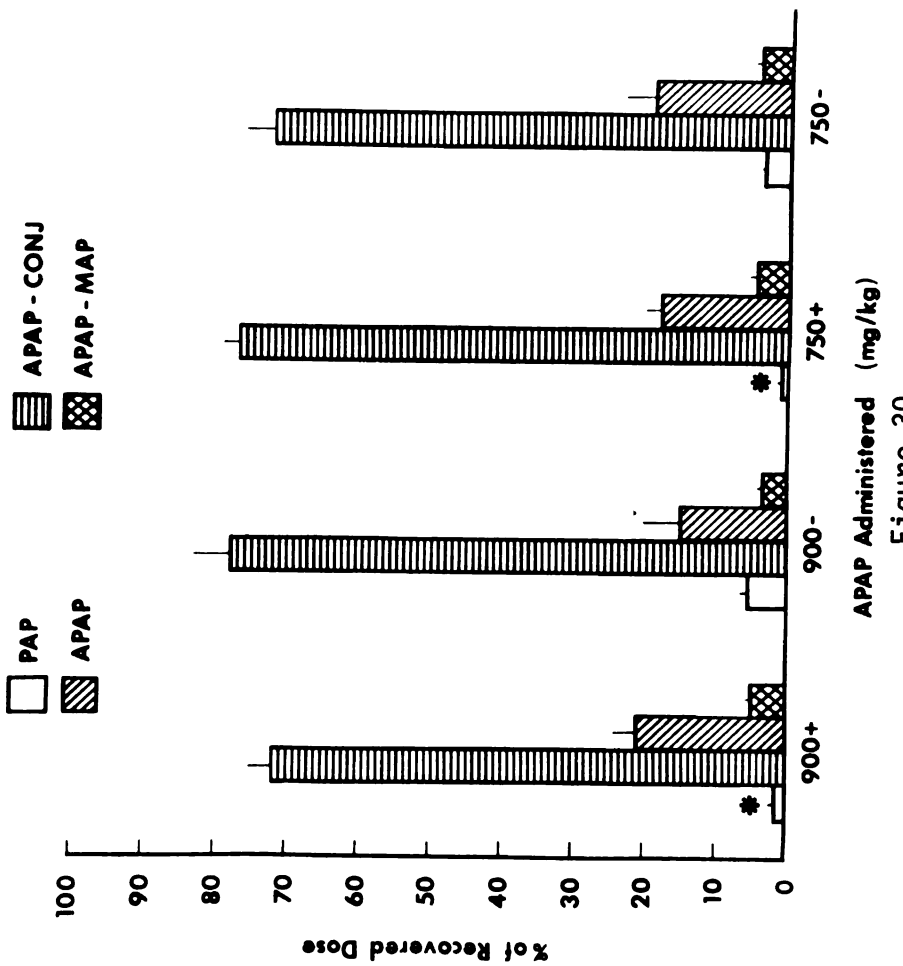
PAP
APAP
APAP-CONJ
APAP-MAP
% of Recovered Dose
100
90
80
70
60
50
40
30
20
10
0
900+
900-
750+
750-
APAP Administered (mg/kg)

Figure 30

the doses of APAP used in these studies. APAP-SCH_3, 90% of which was conjugated at the 4 position, accounted for 10-25 percent of APAP-MAP. APAP-MAP accounted for 3-4 %RD; BNPP pretreatment did not alter this value.

PAP accounted for 3.29±0.22 and 5.13±0.78 %RD in naive animals that received 750 and 900 mg/kg APAP, respectively. In contrast, PAP accounted for only 1.17±0.39 and 1.36±0.48 %RD in BNPP pretreated animals that received 750 and 900 mg/kg APAP, respectively. Of the PAP excreted, greater than 90 percent was conjugated regardless of the pretreatment regimen. PAP was also detected in the urine of animals treated only with BNPP (Figure 31). After a dose of 100 mg/kg BNPP, 20.57±5.66 μmole/kg of PAP was excreted. Therefore, approximately 60 and 43 percent of PAP excreted by BNPP pretreated animals that received 750 and 900 mg/kg APAP, respectively, could have originated from BNPP (Figure 31).

Metabolites of PAP recovered in the urine during a 24 hr period following PAP administration are summarized in Figure 32. 62.0±7.3 and 13.0±1.0 percent of the administered dose was recovered in the urine of naive animals that received 150 and 300 mg/kg PAP, respectively. Similarly, 45.6±12.3 and 5.4±1.7 percent of the administered dose was recovered in the urine of BNPP pretreated animals that received 150 and 300 mg/kg PAP, respectively.

Metabolites of PAP detected in the urine included PAP-CONJ, APAP, APAP-CONJ and APAP-NAC. The presence of APAP-NAC was highly variable and accounted for less than 1.0 %RD. PAP-CONJ accounted for approximately 60 %RD following 150 mg/kg PAP and increased to approximately 75 %RD following 300 mg/kg PAP. Free PAP accounted for 1-2 %RD

Figure 31. Effect of BNPP on the absolute excretion of PAP. Animals were pretreated with either water (-) or BNPP (+) dissolved in water (100 mg/kg, i.p.) 30 min prior to administration of APAP (0, 750 or 900 mg/kg, i.p.). Urine was collected for 24 hr following APAP administration. PAP is the sum of free PAP and PAP conjugated at the 4 position. Data represented are the mean $\pm$ S.E.M. of at least 5 rats. *Significantly less PAP excreted in comparison to animals pretreated with water receiving an equivalent dose of APAP ($p<0.05$).

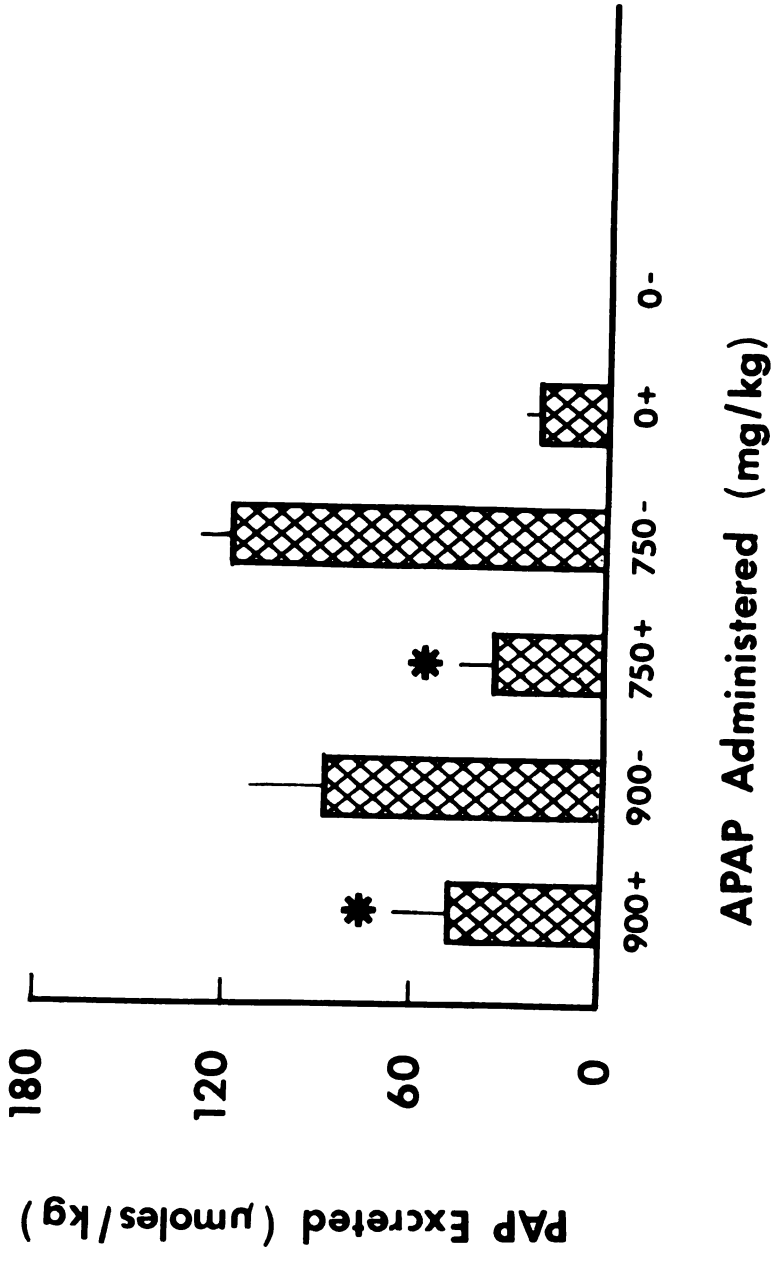
PAP Excreted (μmoles/kg)
180
120
60
0
900+
900-
750+
750-
0+
0-
APAP Administered (mg/kg)

Figure 31

Figure 32. Effect of BNPP on urinary metabolites of PAP. Animals were pretreated with either water (-) or BNPP (+) dissolved in water (100 mg/kg, i.p.) 30 min prior to administration of PAP (150 or 300 mg/kg, i.p.). Urine was collected for 24 hr following PAP administration. APAP-CONJ is the sum of APAP conjugated at the 4 position; PAP-CONJ is the sum of PAP conjugated at the 4 position. Metabolites are expressed as a percent of the recovered dose. Data represented are the mean ± S.E.M. of at least 5 rats. *Significantly different percentage of metabolite excreted in comparison to animals pretreated with water receiving an equivalent dose of PAP ($p<0.05$).

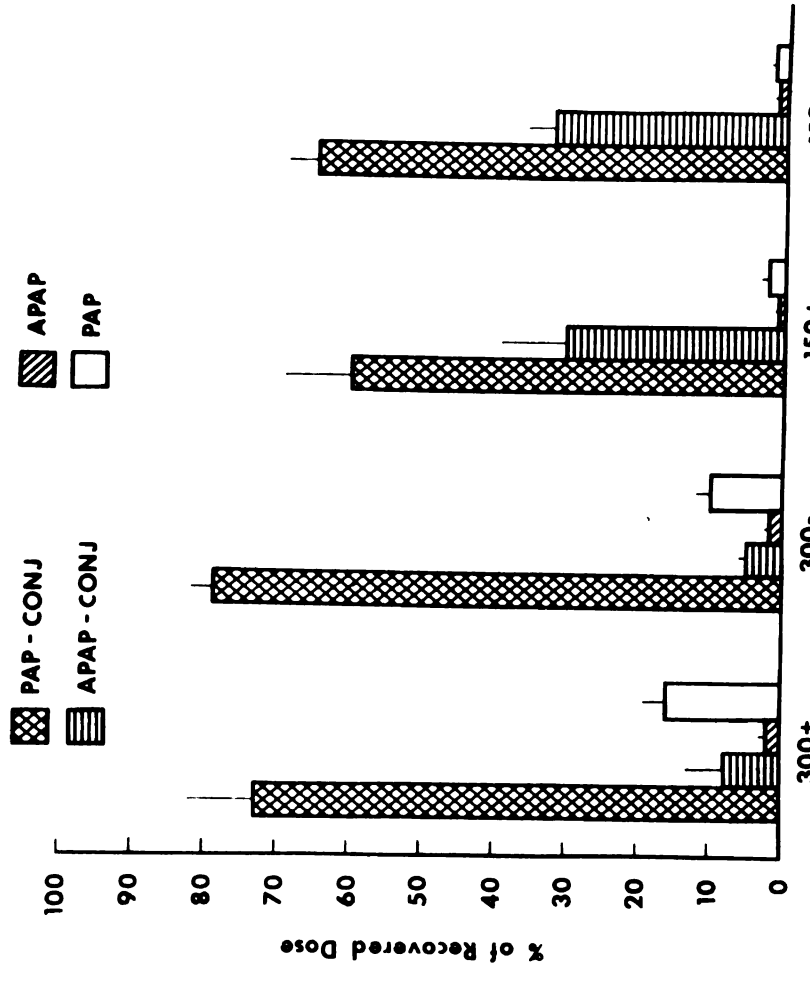
PAP - CONJ
APAP - CONJ
APAP
PAP
% of Recovered Dose
100
90
80
70
60
50
40
30
20
10
0
300+
300-
150+
150-
PAP Administered (mg/kg)

Figure 32

dose following 150 mg/kg PAP, 10-16 %RD following 300 mg/kg. Free APAP excretion was relatively constant, accounting for 1-2 %RD at both doses of PAP used. However, APAP-CONJ excretion decreased as the PAP dose was raised. Differences between naive and BNPP pretreated animals in PAP and metabolites were not evident.

G. Covalent binding of APAP and PAP In Vivo

Administration of [ring-^{14}C]-APAP (900 mg/kg; 50 dpm/nmol) to male F344 rats resulted in significant arylation of renal cortical and hepatic protein which increased with time up to a maximal level six hours following APAP administration (Figure 33). Both six and nine hours following APAP administration, arylation of renal cortical protein was slightly greater than arylation of hepatic protein. In contrast, binding of APAP to muscle protein was less than 0.07 nmole/mg protein and did not increase with time (Figure 33). Since binding six hr following APAP administration was not different from that at nine hr, all subsequent arylation experiments were carried out 6 hr following APAP administration.

In an attempt to reduce acetate incorporation into protein following administration of [acetyl-^{14}C]-APAP, half of the animals were pretreated with cycloheximide (HEX) (1 mg/kg) one hr prior and 3 hr after [^{14}C]-APAP administration. This HEX dosage regimen reduced acetate incorporation into renal protein by 70% following an i.p. dose of [^{14}C]-sodium acetate (0.6 mmol/kg). However, acetate incorporation into hepatic protein was not altered by HEX pretreatment. In F344 rats, HEX pretreatment resulted in greater radioactivity in renal

Figure 33. Time course of [ring-^{14}C]-APAP covalent binding to renal cortical, hepatic and muscle protein. [Ring-^{14}C]-APAP (approximately 50 dpm/nmole) was administered as a single (900 mg/kg) i.p. dose. Data are expressed as nmole [ring-^{14}C]-APAP bound per mg extracted protein. Data represented are the mean $\pm$ S.E.M. of at least 6 rats at each time point.

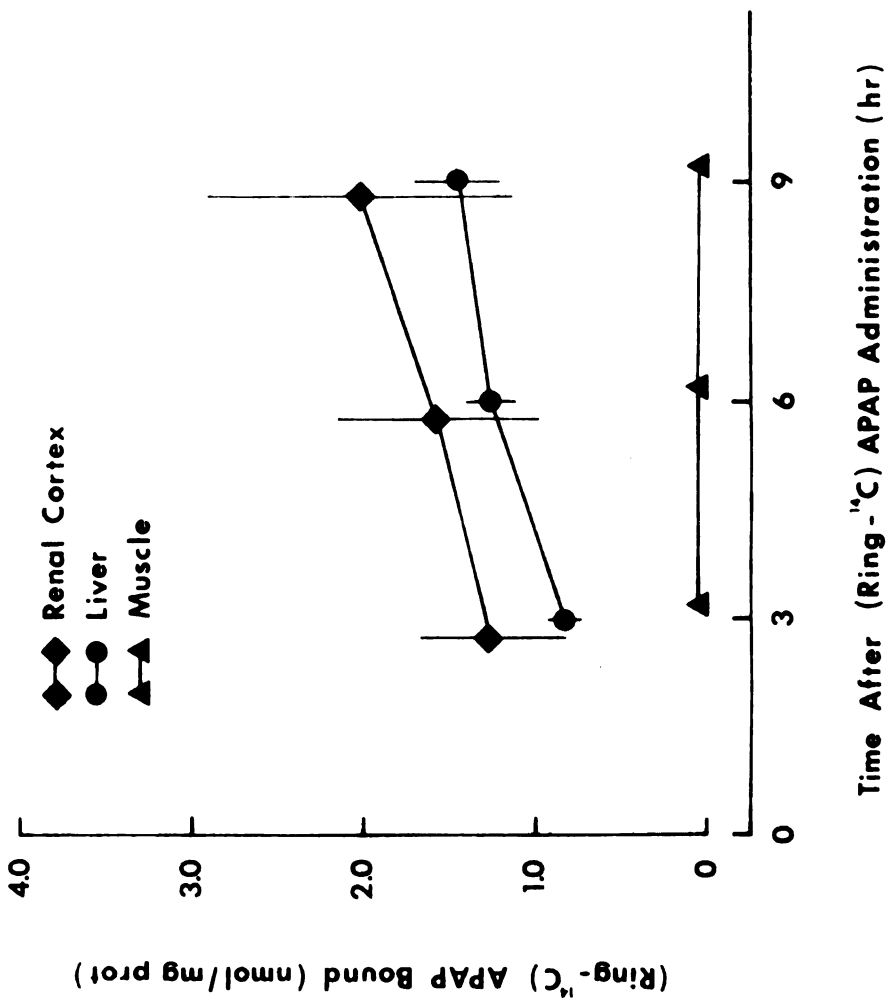
Renal Cortex
Liver
Muscle
4.0
3.0
2.0
1.0
0
0
3
6
9
(Ring-^{14}C) APAP Bound (nmol/mg prot)
Time After (Ring-^{14}C) APAP Administration (hr)

Figure 33

cortex, in comparison to vehicle pretreated F344 rats, regardless of the type of radiolabeled APAP administered (Table 23). Furthermore, more ^{14}C was associated with renal cortical tissue in F344 rats than SD regardless of the pretreatment regimen used (Table 23). In contrast, differences in the hepatic ^{14}C concentration were not noted between strains (Table 24).

In contrast to the effect on ^{14}C distribution, HEX pretreatment did not alter arylation of renal cortical protein in SD or F344 rats following administration of [ring^{14}C]-APAP (Table 25). However, HEX pretreatment markedly reduced arylation in both strains following the administration of [acetyl-^{14}C]-APAP. More importantly, however, [ring-^{14}C]-APAP arylated renal protein to a greater extent than [acetyl-^{14}C]-APAP; this is especially evident in the HEX pretreated F344 rats (Table 25). Furthermore, the difference in the arylation of renal cortical protein following [acetyl-^{14}C]- or [ring-^{14}C]-APAP noted in F344 rats was not evident in HEX pretreated SD rats (Table 25). In contrast, arylation of hepatic macromolecules was similar regardless of the position of the ^{14}C on the APAP molecule (Table 26). However, strain differences in hepatic covalent binding of APAP were evident (Table 26).

Following administration of [ring-^{14}C]-PAP, arylation of renal cortical protein was more extensive in F344 than SD rats, possibly reflecting the marked strain differences in the distribution of radioactivity into the renal cortex (Table 27). Furthermore, HEX pretreatment of F344 rats resulted in greater cortical concentrations and covalent binding of PAP in comparison to vehicle pretreated F344

TABLE 23

Concentrations of Specifically Labelled [^{14}C]-APAP in Renal Cortical Tissue *In Vivo*[a]

Strain		^{14}C Concentration[b] (μmol/g tissue, wet weight)	
		[Acetyl-^{14}C]-APAP	[Ring-^{14}C]-APAP
	Pretreatment		
F344	HEX	8.02±1.56	7.71±2.12
	WATER	3.76±0.71	4.68±0.53
SD	HEX	2.81±0.39	3.22±0.47
	WATER	2.31±0.30	1.90±0.12

[a]Animals received HEX (1 mg/kg) or water (i.p.) one hr prior to and 3 hr after administration (i.p.) of either [acetyl-^{14}C]- or [ring-^{14}C]-APAP (900 mg/kg, 50 dpm/nmol). Six hr following APAP administration animals were killed and ^{14}C concentration determined.

[b]Values are the mean ± SEM of six animals.

TABLE 24

Concentrations of Specifically Labelled [^{14}C]-APAP in Hepatic Tissue *In Vivo*[a]

Strain	Pretreatment	^{14}C Concentration[b] (μmol/g tissue, wet weight)	
		[Acetyl-^{14}C]-APAP	[Ring-^{14}C]-APAP
F344	HEX	6.30±0.68	6.24±0.80
	WATER	5.08±0.43	4.35±0.43
SD	HEX	5.20±0.82	5.40±0.69
	WATER	4.56±0.62	3.81±0.37

[a]Animals received HEX (1 mg/kg) or water (i.p.) one hr prior to and 3 hr after administration (i.p.) of either [acetyl-^{14}C]- or [ring-^{14}C]-APAP (900 mg/kg, 50 dpm/nmol). Six hr following APAP administration animals were killed and ^{14}C concentration determined.

[b]Values are the mean ± SEM of six animals.

TABLE 25

Covalent Binding of Specifically Labelled [^{14}C]-APAP to Renal Cortical Protein In Vivo[a]

Strain	Pretreatment	APAP Bound[b] (nmol/mg prot)	
		[Acetyl-^{14}C]-APAP	[Ring-^{14}C]-APAP
F344	HEX	0.38±0.03	1.36±0.41
	WATER	0.80±0.04	1.28±0.20
SD	HEX	0.26±0.04	0.24±0.04
	WATER	0.69±0.08	0.21±0.01

[a]Animals received HEX (1 mg/kg) or water (i.p.) one hr prior to and 3 hr after administration (i.p.) of either [acetyl-^{14}C]- or [ring-^{14}C]-APAP (900 mg/kg, 50 dpm/nmol). Six hr following APAP administration animals were killed and covalent binding determined.

[b]Values are the mean ± SEM of six animals.

TABLE 26

Covalent Binding of Specifically Labelled [^{14}C]-APAP to Hepatic Protein *In Vivo*[a]

Strain		APAP Bound[b] (nmol/mg prot)	
		[Acetyl-^{14}C]-APAP	[Ring-^{14}C]-APAP
	Pretreatment		
F344	HEX	0.98±0.13	0.73±0.06
	WATER	1.04±0.08	1.02±0.13
SD	HEX	0.54±0.06	0.40±0.04
	WATER	0.64±0.09	0.56±0.05

[a]Animals received HEX (1 mg/kg) or water (i.p.) one hr prior to and 3 hr after administration (i.p.) of either [acetyl-^{14}C]- or [ring-^{14}C]-APAP (900 mg/kg, 50 dpm/nmol). Six hr following APAP administration animals were killed and covalent binding determined.

[b]Values are the mean ± SEM of six animals.

TABLE 27

Distribution and Covalent Binding in Renal Cortical Tissue of [Ring-^{14}C]-PAP *In Vivo*[a]

Strain		[Ring-^{14}C]-PAP	
		Total[b] (μmol/g tissue, wet weight)	Bound[b] (nmol/mg prot)
	Pretreatment		
F344	HEX	5.20±0.22	19.19±3.35
	WATER	3.53±0.30	10.65±1.34
SD	WATER	1.44±0.06	4.15±0.49

[a]Animals received HEX (1 mg/kg) or water (i.p.) one hr prior to and 3 hr after administration (i.p.) of [ring-^{14}C]-PAP (200 mg/kg, 40 dpm/nmol). Six hr following PAP administration animals were killed and covalent binding and ^{14}C concentration determined.

[b]Values are the mean ± SEM of five animals.

rats (Table 27). Strain differences in arylation and distribution into hepatic tissue of PAP were also noted (Table 28). However, HEX pretreatment of F344 rats did not alter hepatic concentrations or covalent binding of PAP (Table 28).

TABLE 28

Distribution and Covalent Binding in Hepatic Tissue of [Ring-^{14}C]-PAP *In Vivo*[a]

Strain	Pretreatment	[Ring-^{14}C]-PAP Total[b] (μmol/g tissue, wet weight)	[Ring-^{14}C]-PAP Bound[b] (nmol/mg prot)
F344	HEX	1.07±0.12	1.69±0.11
	WATER	0.98±0.11	1.50±0.21
SD	WATER	0.57±0.04	0.89±0.08

[a]Animals received HEX (1 mg/kg) or water (i.p.) one hr prior to and 3 hr after administration (i.p.) of [ring-^{14}C]-PAP (200 mg/kg, 40 dpm/nmol). Six hr following PAP administration animals were killed and covalent binding and ^{14}C concentration determined.

[b]Values are the mean ± SEM of five animals.

DISCUSSION

Sublethal doses of APAP result in extensive histopathological changes in the renal cortex of the male F344 rat. Necrosis initially was restricted to the pars recta of the proximal tubule. Physiological correlates of APAP-induced proximal tubular necrosis included a slight decrease in PAH, but not TEA, accumulation by renal cortical slices and a marked elevation of kidney weight and kidney weight/body weight ratios. However, significant functional alterations were only noted as doses substantially higher than those at which histological changes were evident. In contrast, a decrease in renal GSH and arylation of renal macromolecules were noted at time points and doses substantially less than those at which histological changes were evident (McMurtry et al., 1978). Furthermore, a significant portion of the bound radioactivity in the renal cortex after administration of ^{3}H-APAP was associated with necrotic areas of the proximal tubule (Mitchell et al., 1977). These observations, although not conclusive, are consistent with the formation of a reactive intermediate from APAP which upon arylation of macromolecules results in the observed renal functional and histopathological responses. At least two different mechanisms for the generation of reactive intermediates from APAP within the renal cortex can be envisioned. McMurtry and coworkers

(1978) suggested that the generation of a reactive electrophile within the proximal tubular cell is a cytochrome P-450-dependent process. In contrast, the formation of reactive intermediates from APAP within the kidney could be dependent upon deacetylation prior to the renal metabolism of the deacetylated product, PAP, to an electrophilic intermediate.

The excretion of APAP-NAC by IPKs perfused with APAP may reflect the generation of reactive intermediates by a P-450-dependent mechanism. It is recognized, however, that APAP-NAC could be formed within the kidney by at least two non-P-450 mechanisms of metabolic activation (Figure 34). APAP-NAC could result from PES activation of APAP. Because of the medullary localization of the PES system and the improbability that reactive intermediates formed from PES activation of APAP could travel from medulla to cortex, this system of activation probably does not play a significant role in APAP-induced cortical necrosis. In addition, the contribution of PES activation of APAP to the excretion of APAP-NAC in the IPK is probably very small as there is significant excretion of APAP-NAC at perfusate concentrations of APAP (2.5-10.00 mM) that would be expected to completely inhibit PES. Mohandas and coworkers (1981b) have previously demonstrated the dose-dependent inhibition/stimulation of the PES system by APAP; concentrations greater than 2 mM in a microsomal incubation almost completely inhibited PES activity.

Another non-P-450 mechanism of APAP-NAC formation may be via the deacetylase-dependent mechanism of activation. If a reactive intermediate formed from PAP could combine with GSH it would be rapidly

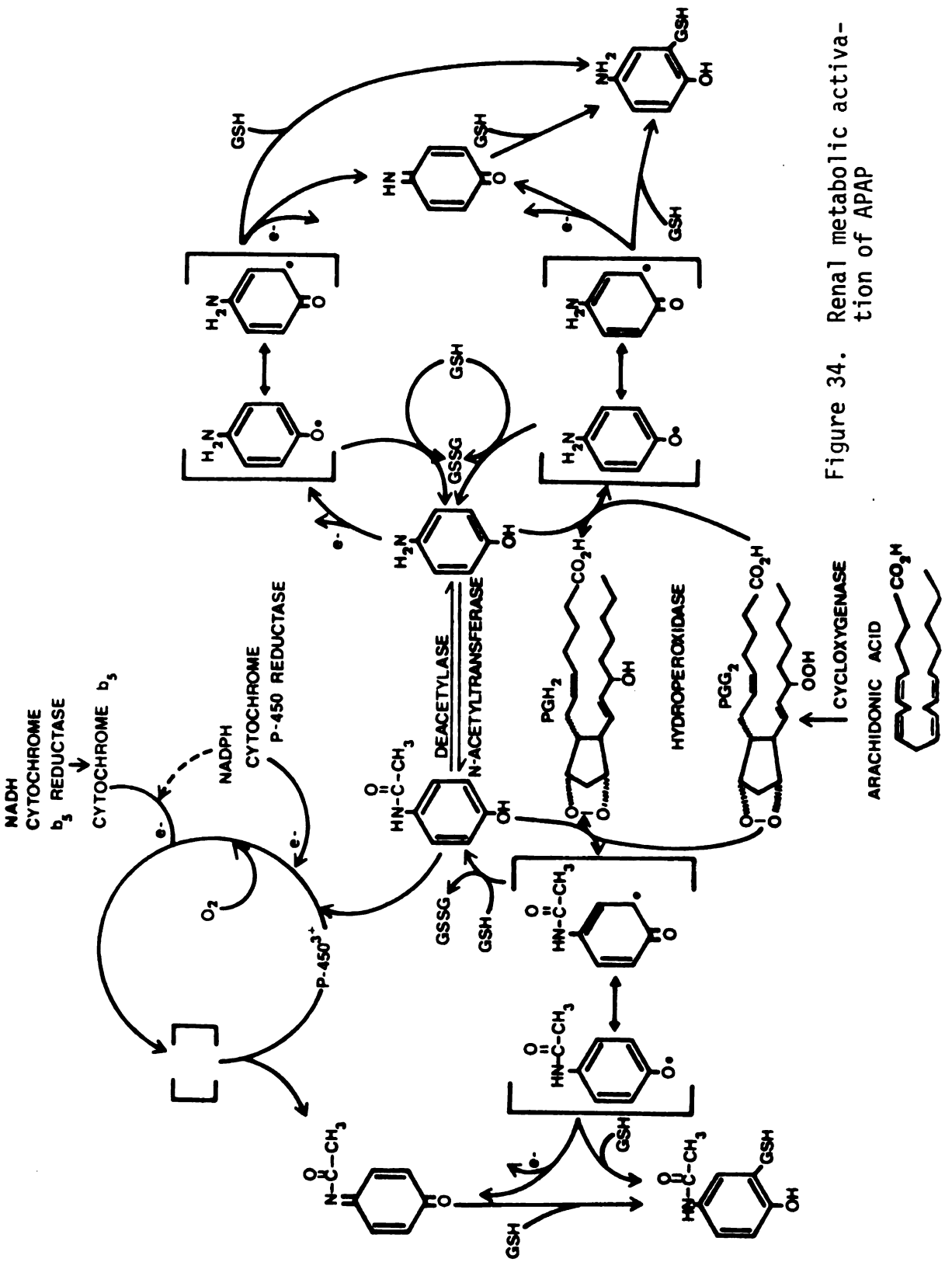

Figure 34. Renal metabolic activation of APAP

degraded within the IPK to PAP-NAC. PAP-NAC could then be reacetylated back to APAP-NAC. However, several lines of evidence fail to support this possibility. First, although synthesized standards were not available, PAP-NAC, chromatographically, would not be expected to be dramatically different from APAP-NAC. However, all HPLC peaks within the chromatographic region of APAP-NAC corresponded to peaks in urine of IPKs perfused without APAP. Second, addition of ^{35}S-GSH to renal incubations in vitro reduced arylation of protein by PAP but did not result in the appearance of peaks chromatographically different than from ^{35}S-GSH or ^{35}S-GSSG. While these experiments are preliminary in nature, they indicate that a GSH conjugate of PAP may not be formed.

Therefore, it appears that most of the APAP-NAC excreted by the IPK could have resulted from a P-450-dependent mechanism of activation. This observation was corroborated by the demonstration of NADPH-dependent covalent binding of APAP to renal microsomes in vitro. Furthermore, the formation of APAP-NAC by the IPK was consistent with reports of other investigators who quantified APAP-NAC production in isolated cells and isolated kidneys (Jones et al., 1979; Ross et al., 1980; Emslie et al., 1981a,b). The formation of APAP-NAC may account for a small part of the APAP-induced depletion of GSH in all three sections of the kidney.

Several investigators have reported that compounds that induce and inhibit hepatic drug-metabolizing enzymes influence APAP-induced depletion of hepatic GSH concentration (Mitchell et al., 1973b; Mudge et al., 1978). This was presumably due to alterations in the

generation of the reactive intermediate which can conjugate with and deplete hepatic GSH. Our studies may indicate that some GSH-depleting metabolites were formed via cytochrome P-450-dependent pathways. In the present study, PIP BUT, an inhibitor of mixed-function oxidases (Mitchell et al., 1973a), reduced APAP-induced GSH depletion in cortex and medulla while PBB, a potent inducer of renal mixed-function oxidases (Kluwe and Hook, 1981), enhanced APAP-induced GSH depletion in cortex and medulla. In addition, the enhanced GSH depletion produced by PBB was accompanied by accelerated excretion of APAP-NAC, the major sulfide-containing APAP metabolite excreted by the IPK (Ross et al., 1980; Emslie et al., 1981a,b). This was presumably the result of an enhanced formation of a reactive intermediate of APAP which could conjugate with and deplete GSH. Treatment with 3MC, another potent inducer of renal mixed-function oxidases, also enhanced the formation of sulfide-containing metabolites by isolated renal cells (Jones et al., 1979).

Experimental protocols utilizing inducers of mixed-function oxidases should, however, be interpreted with caution as alternative pathways of metabolism may also be induced. Indeed, PBB by inducing GSH transferases may facilitate the conjugation of GSH with reactive intermediates of APAP resulting in enhanced excretion of APAP-NAC and depletion of medullary and cortical GSH. Conversely, PIP BUT, by interfering with GSH transferases, may result in less depletion of medullary and cortical GSH. While GSH can combine non-enzymatically with many electrophilic xenobiotics, the rate of conjugation of the electrophilic intermediate formed by P-450 metabolism with GSH is

markedly enhanced by the presence of cytosolic GSH transferases (Rollins and Buckpitt, 1979). Recently, Emslie and coworkers (1981b) demonstrated that 3MC pretreatment resulted in a marked increase in the excretion of APAP-NAC in IPKs perfused with APAP. However, the covalent binding of APAP to the IPK was not enhanced. These findings were attributed to induction of GSH transferases by 3MC (Emslie et al., 1981b). Induction of renal GSH transferases and not P-450 by such compounds as PBB and 3MC may explain the apparent discrepancy between APAP activation and nephrotoxicity. Pretreatment with both compounds increased APAP-NAC excretion in isolated renal cells (3MC) and IPKs (3MC + PBB) (Jones et al., 1979; Emslie et al., 1981b). However, neither pretreatment regimen enhanced APAP-induced nephrotoxicity in vivo in the F344 rat (McMurtry et al., 1978; J.F. Newton and J.B. Hook, unpublished). Furthermore, 3MC pretreatment did not increase NADPH-dependent covalent binding in renal microsomes from F344 rats (McMurtry et al., 1978). These observations suggest that the effects of PBB and PIP BUT on APAP-induced GSH depletion and APAP-NAC excretion in the IPK may not merely be due to modulation of P-450-dependent APAP activation.

Two lines of evidence suggest that the GSH-depleting metabolite produced in the papilla may not be formed via cytochrome P-450. The papilla of the rat kidney (inner medulla and papilla) does not contain detectable amounts of cytochrome P-450 (K.S. Hilliker, W.M. Kluwe and J.B. Hook, unpublished observations). In addition, the consistent lack of effect of modulators of cytochrome P-450 activity on GSH depletion in the papilla in the present study also suggests that the

GSH-depleting metabolite is not formed via a cytochrome P-450-mediated process in the papilla. Recently, Moldeus and Rahimtula (1980) demonstrated that an intermediate of APAP capable of conjugating with GSH was formed via a prostaglandin synthetase-dependent reaction. The renal inner medulla contains considerable prostaglandin synthetase activity (Zenser et al., 1979). Therefore, in our experiments, APAP may have been activated by prostaglandin synthetase in the papilla of the IPK. Recently, Boyd and Eling (1981) demonstrated arachidonic acid-dependent metabolism of APAP to an arylating metabolite by rabbit renal medulla. Alternatively, it has been demonstrated that APAP can be deacetylated to PAP in cortex and medulla (Carpenter and Mudge, 1981). The activation of PAP to a reactive intermediate capable of depleting GSH appears to occur via a cytochrome P-450-independent reaction (Calder et al., 1979). Therefore, in our experiments APAP may have reduced the GSH concentration in the papilla of the IPK subsequent to deacetylation and metabolic activation. In fact, both mechanisms of activation may be involved in the generation of a reactive intermediate capable of reducing papillary GSH. Recently, Andersson and coworkers (1982) demonstrated that PAP could be metabolized to a reactive intermediate by a PES-dependent mechanism.

The reduction in GSH concentrations by APAP in the IPK is consistent with the effect produced in vivo. McMurtry et al. (1978) demonstrated that APAP could reduce the "whole kidney" GSH concentration, whereas Mudge et al. (1978) separated APAP-induced GSH depletion into cortical and papillary components. In addition, McMurtry et al. (1978) demonstrated a correlation between GSH depletion and renal

cortical necrosis. Our studies with the IPK suggest the APAP metabolite responsible for GSH depletion and possibly cortical necrosis could be formed directly within the kidney. However, the depletion of GSH concentrations in the IPK cannot be accounted for entirely by the production of APAP-NAC. In fact, the formation of APAP-NAC can only account for a small fraction (<1%) of the reduction in GSH concentrations. Glutathione (APAP-GSH) or cysteine (APAP-CYS) conjugates were not present in the urine or perfusate, probably due to the rapid degradation of these conjugates by the kidney. It is not likely that APAP-GSH or some degradation product of it could have been sequestered within renal tissue. Recently, it was demonstrated that the IPK rapidly metabolizes the APAP-GSH to APAP-NAC and APAP-CYS, which are recovered quantitatively from perfusate and urine (J.F. Newton, D. Hoefle and J.B. Hook, unpublished observations). Perhaps some of the nucleophilic centers attacked by the reactive intermediate of APAP may be located on enzymes responsible for either glutathione synthesis or energy metabolism which supports glutathione synthesis, resulting in the marked reduction of GSH concentrations . Indeed, the findings of Tange et al. (1977) which demonstrate that APAP alters energy metabolism in isolated renal cortical tubules is consistent with this hypothesis. Furthermore, arylating agents such as phosgene have been demonstrated to reduce GSH content in isolated hepatocytes by the selective inhibition of the rate-limiting enzyme in GSH synthesis, γ-glutamyl-cysteine synthetase (Ekstrom et al., 1982).

Alternatively, the nonstoichiometric relationship between the reduction in GSH concentrations in the IPK and APAP-NAC excretion may

be explained by an alternative mechanism of APAP activation in which APAP-NAC is not an end-product. Such discrepancies between P-450 metabolism and the formation of electrophilic intermediates, as indicated by arylation of renal macromolecules or depletion of renal GSH, have also been noted in vivo. After a nephrotoxic dose of APAP, binding to liver and kidney (^{3}H per mg protein) was roughly equal in the two organs, even though P-450, on a nanomole per milligram basis, was 10 times greater in liver than in kidney (McMurtry et al., 1978). This observation, along with those made in the IPK, lend credence to the possibility that, in the renal cortex, APAP is activated by other pathways in addition to P-450.

Another mechanism for generation of a reactive intermediate within renal tissue could involve deacetylation with subsequent metabolic activation of the deacetylated product, PAP. Although PAP has been established as a urinary metabolite of APAP in the hamster, this observation did not define PAP as the nephrotoxic metabolite in the F344 rat since there are considerable species variations in the amount and types of APAP metabolites found in urine (Gemborys and Mudge, 1981). The data in Table 1 clearly document PAP formation from APAP in the F344 rat. Identification of unconjugated PAP in the urine of the IPK substantiated the intrinsic ability of the intact kidney to deacetylate APAP to PAP. Such studies indicate that the kidney can account for some, if not all, of urinary PAP in intact animals. PAP formation may also occur in the liver and intestinal microflora (Smith and Griffiths, 1974). However, the fraction of PAP formed extrarenally that reaches the kidney unconjugated is unknown.

Se

by APAP

been re

tion (

Tange

renal

al., 1

bioche

energy

to be

to the

nephro

rat a

gical

able

PAP i

APAP

the r

tive

deli

PAH

ion

alte

of h

PAH

Several of the biochemical and histopathological effects produced by APAP in the kidney of the F344 rat (McMurtry et al., 1978) have been reported to occur in other strains of rats after PAP administration (Green et al., 1969; Calder et al., 1971; Cottrell et al., 1976; Tange et al., 1977; Crowe et al., 1979). Both PAP and APAP reduce renal GSH concentrations and arylate renal macromolecules (Crowe et al., 1979; McMurtry et al., 1978). However, some of the initial biochemical changes produced by the two chemicals, especially in energy metabolism, e.g., reduced renal gluconeogenesis, do not appear to be similar (Tange et al., 1977). These differences may be related to the use of animal models that are not equally sensitive to the nephrotoxic effects of APAP. The functional renal lesions in the F344 rat are similar after APAP and PAP administration. The histopathological renal lesions produced by PAP in the F344 rat are indistinguishable from the renal lesions following APAP administration. However, PAP is approximately 5-10 times more potent as a nephrotoxicant than APAP in the F344 rat. Substantiation of qualitative similarities in the renal lesions produced by APAP and PAP in an animal model sensitive to APAP-induced nephrotoxicity is an important step in the delineation of the mechanism of APAP-induced nephrotoxicity.

There appear to be subtle differences in the effects of PAP on PAH and TEA accumulation. The differential effect of PAP on organic ion accumulation may be the biochemical correlate to morphological alterations at a specific site along the nephron similar to the effect of hexachlorobutadiene. Hexachlorobutadiene also selectively reduces PAH accumulation at doses which have no effect on TEA accumulation

(Lock and Ishmael, 1979). The reduction in PAH accumulation has been correlated with a selective destruction of the straight segment of the proximal tubule, the area where PAH transport is maximal.

Of the possible isomeric forms of monoaminophenols, only PAP was nephrotoxic. Therefore, the *para* arrangement on the benzene ring of the hydroxyl and amino groups is required for nephrotoxicity. Whether the difference in nephrotoxicity between isomeric forms is related to oxidation-reduction potentials (Calder *et al.*, 1975) or isomeric differences in conjugation kinetics is yet to be investigated. Both PAP and o-aminophenol produce developmental anomalies in the Syrian golden hamster (Rutkowski and Ferm, 1982).

Although some PAP binds covalently to renal protein nonenzymatically, a significant amount binds enzymatically (Calder *et al.*, 1979). The mechanism of PAP oxidation does not appear to be P-450-dependent. Inhibitors of P-450 had no apparent effect on PAP covalent binding *in vitro* while NADPH reduced covalent binding (Crowe *et al.*, 1979). The present study used inducers with dosage regimens known to stimulate renal MFOs. The subsequent reduction in nephrotoxicity may indicate that PAP is not activated via a P-450 mechanism. However, care must be used in interpreting such results since inducers may enhance alternative pathways of metabolism, especially those involved in conjugation of PAP (Gillette and Mitchell, 1975).

The question arises as to whether the amount of PAP formed from APAP can account quantitatively for the renal damage which results from the administration of APAP. Any calculation becomes complicated in view of the facts that: (1) administered PAP may be N-acetylated

to APAP as well as conjugated at the phenolic group to the sulfate or glucuronide; (2) PAP derived from the deacetylation of APAP might be conjugated in similar reactions; and (3) while recovery of reactive metabolites such as PAP in the voided urine may identify an overall metabolic pathway, since the metabolite in question is thought to bind irreversibly to renal macromolecules (and possibly other tissues), it is apparent that the amount excreted cannot be a quantitatively accurate index of the amount generated. Isolation of PAP in the urine of IPKs perfused with APAP documents that PAP can be formed within the kidney, possibly producing higher concentrations intracellularly than indicated by concentrations in the urine. In the present studies in the male Fischer 344 rat, at the 750 mg/kg dose of APAP a total of approximately 17 mg/kg of PAP was recovered in the urine in 24 hr. At an approximately equinephrotoxic dose of PAP of 218 mg/kg Calder et al. (1971) recovered 44 mg/kg of PAP in the urine at 48 hr in female hooded rats. Furthermore, male F344 rats that received approximately equal nephrotoxic doses of PAP of 100 mg/kg (s.c.) and 150 mg/kg (i.p.) excreted approximately 30 mg/kg and 60 mg/kg of PAP, respectively, over a 24 hr period. Despite obvious experimental differences, the results are in sufficient agreement to lend plasuibility to the proposed hypothesis that the amount of PAP found in the urine could account for APAP-induced cortical necrosis in the F344 rat. Because of the complex metabolic interactions which are involved, it is doubtful if further simple studies of urinary excretion would provide more meaningful data.

The identification of PAP as a urinary metabolite of APAP is an important step in delineating its possible role in APAP-induced cortical necrosis in the F344 rat. In addition, quantitation of functional and histopathological changes produced by PAP at doses much lower than that required for APAP is also consistent with the hypothesis that APAP-induced cortical necrosis is mediated by PAP in the F344 rat.

Since APAP can be deacetylated *in vivo* and *in vitro* and PAP could be metabolically activated *in vitro* it seemed feasible that APAP could be activated under appropriate conditions, by renal subcellular fractions *in vitro* by this two-step mechanism. Thus, experiments were designed to identify and characterize the renal subcellular localization of APAP deacetylation and PAP oxidation in the F344 rat. Using these data, attempts were made to demonstrate and substantiate a deacetylase-dependent mechanism of APAP activation *in vitro*.

In vitro, two separate mechanisms of APAP activation in renal cortical tissue were demonstrated which may play a role in APAP-induced renal cortical necrosis. One mechanism, due to its microsomal location and requirement for NADPH and oxygen, appears to be mediated by cytochrome P-450. This mechanism of APAP activation *in vitro* was demonstrated previously in renal cortical tissue from New Zealand rabbits and F344 rats (Mohandas *et al.*, 1981a; McMurtry *et al.*, 1978). Another mechanism appears to involve deacetylation prior to metabolism of the deacetylated product, PAP, to an arylating intermediate. Evidence in support of this suggestion includes: 1) maximal covalent binding of APAP when renal cytosol (subcellular localization of

maximal APAP deacetylation) and microsomes (subcellular localization of PAP oxidation) were combined, 2) inhibition of APAP binding to renal 10,000 x g supernatants by NADPH which also inhibits microsomal binding of PAP (Calder et al., 1979), and 3) inhibition of binding by the deacetylase inhibitor, BNPP. Binding of [ring-^{14}C]-APAP but not [acetyl-^{14}C]-APAP provided conclusive evidence that APAP was binding to renal macromolecules subsequent to deacetylation and metabolic activation of PAP. Nelson and coworkers (1981) recently demonstrated that NADPH-dependent microsomal binding of [acetyl-^{14}C]-APAP in vitro was less than binding of [ring-^{14}C]-APAP, presumably due to the complete oxidation of APAP resulting in release of acetamide. However, it is unlikely that this mechanism can explain lack of binding of [acetyl-^{14}C]-APAP to renal 10,000 x g supernatants. The inhibitory effect of NADPH and BNPP on [ring-^{14}C]-APAP binding to renal 10,000 x g supernatants suggests that acetyl evolution is due to deacetylation, not release of acetamide resulting from full oxidation of APAP. APAP deacetylation and PAP activation in renal 10,000 x g supernatants and microsomes, respectively, from F344 rats has been demonstrated. However, this is the first demonstration of APAP activation by a deacetylase-dependent mechanism.

The deacetylase-dependent mechanism of APAP activation appears to be primarily a renal event. This is surprising since both renal and hepatic cytosol deacetylated APAP at almost identical rates. However, the inability to demonstrate a deacetylase-dependent mechanism of APAP activation in hepatic subcellular fractions may be related to the low rate of PAP activation in hepatic microsomes. Alternatively, this may

be due to greater amounts of endogenous GSH in hepatic than in renal post-mitochondrial incubations. The possibility that small amounts of endogenous GSH may interfere with binding is suggested by the sigmoidal time course of APAP binding to renal post-mitochondrial supernatants. However, endogenous GSH was not detectable in hepatic or renal microsomal fractions, yet NADPH independent enzymatic binding of APAP could only be demonstrated in renal microsomes. Furthermore, deacetylation of APAP in renal 10,000 x g supernatants was less than predicted, possibly reflecting further metabolism of PAP, while hepatic deacetylation in hepatic 10,000 x g was identical to predicted values.

The toxicological relevance of each mechanism of APAP activation to APAP-induced cortical necrosis is difficult to establish from *in vitro* studies. Relative rates of APAP activation *in vitro* by each mechanism are difficult to extrapolate to conditions *in vivo*. However, the possibility that both mechanisms may contribute to the arylation of renal macromolecules *in vivo* may explain the non-linear dose-dependent covalent binding of APAP in kidney but not liver, where only P-450-dependent APAP activation could be demonstrated (McMurtry *et al.*, 1978). Furthermore, the two different mechanisms of metabolic activation may result in reactive intermediates that are different with respect to sites of arylation and the subsequent biochemical and physiological response. In support of this proposal, Andersson and coworkers (1982) demonstrated differences in the nature of the reactive products formed from prostaglandin synthetase-catalyzed activation of APAP and PAP. Even though arylating intermediates were formed

from the oxidation of both compounds only those intermediates formed from PAP were capable of damaging human skin fibroblast DNA (Andersson et al., 1982).

Therefore, it was concluded that APAP activation in renal cortical tissue could proceed by at least two discrete mechanisms in vitro and, by implication, in vivo. However, the toxicological significance of each mechanism of activation to APAP-induced renal cortical necrosis could not be established from the studies. Three types of experimental approaches were therefore undertaken in an attempt to quantify the contribution of the deacetylase-dependent mechanism of APAP activation to APAP-induced cortical necrosis. These included: 1) determination of differences in APAP activation in SD and F344 rats; 2) quantification of the effect of the deacetylase inhibitor, BNPP, on APAP and PAP nephrotoxicity and metabolism; 3) quantification of renal and hepatic arylation after a nephrotoxic dose of either [acetyl-^{14}C]-APAP or [ring-^{14}C]-APAP.

Strain-related differences may be a useful tool in determining the mechanism(s) of APAP-induced nephrotoxicity. In the present study, the direct comparison of the two strains, employing histopathologic and functional evaluations, substantiated and expanded the previously reported strain-dependent differences in APAP-induced nephrotoxicity. Species-related differences in APAP hepatotoxicity appear to be related to the ability of the liver to activate APAP by a cytochrome P-450 mechanism (Davis et al., 1974). Comparative studies of F344 and SD rats have identified some strain differences in certain drug metabolizing enzymes. Dent and coworkers (1980) demonstrated

that microsomal epoxide hydrolase activity was lower in F344 than in SD rats and that the pattern of microsomal metabolism of benzo(a)-pyrene differed in the two strains. Furthermore, dexamethasone-stimulated phenol sulfotransferase activity in kidney is higher in SD rats than in F344 rats (Maus et al., 1982). In contrast, renal glucuronyl transferase activity is higher in F344 than in SD rats (unpublished observation). Mitchell and coworkers have suggested that renal P-450 concentrations may be greater in F344 than in SD rats and that this is the mechanism of strain differences in APAP-induced nephrotoxicity (Mitchell et al., 1977). The present study confirmed the suggested strain differences in renal P-450 content and in the metabolism of a model substrate, ethoxycoumarin.

Surprisingly, strain-related differences were not evident in renal or hepatic P-450 activation of APAP. Rat kidney appears to contain several forms of P-450 (Rush et al., 1983); therefore, it is possible that APAP may be activated by a relatively minor form of renal P-450, the presence or absence of which may not be detected by total P-450 measurements. The assay conditions used in this study, however, provide data only on apparent maximum velocities for the activation of APAP by renal microsomes. They do not provide information on the relative microsomal affinity for APAP in the two strains. However, renal cortical concentrations of APAP during the period for which covalent binding of APAP in vivo to renal and hepatic macromolecules is maximal, are 2-4x higher than those used in vitro in the present studies.

The mechanism of APAP-induced nephrotoxicity may be related to deacetylation of APAP to PAP which could produce renal pathological changes subsequent to its own activation. Strain differences in hepatocyte deacetylation of the arylamine, acetylaminofluorene, have been observed in mice (Hultin and Weber, 1982). In contrast, there were not strain differences in the deacetylation of APAP by either hepatic or renal 10,000 x g supernatants or by isolated perfused kidneys. In vivo, F344 rats appeared to eliminate more PAP in the urine after a nephrotoxic dose (900 mg/kg) of APAP. However, caution must be used in interpreting such results in view of the reduced recovery of the administered dose of APAP in those animals suffering from acute oliguric renal failure. The apparent increase in the proportion of PAP in urine from F344 rats may represent the increased elimination of PAP in comparison to other metabolites at early time points before the onset of renal failure. Such a phenomenon would not occur during a 24 hr collection in SD rats that exhibit normal renal function. While PAP formation appears to be relatively similar in the two strains, there may be strain differences in PAP-induced nephrotoxicity. Strain differences due to the differential activation of the metabolite have been reported in the tumorigenic effect of the N-hydroxylated metabolite of acetylaminofluorene (King et al., 1976; Melijke-Giganti and Rydell, 1978).

Strain differences have also been reported for the phase II metabolism of certain xenobiotics (Gutmann et al., 1972; King et al., 1976; Melijka-Giganti and Rydell, 1978). Therefore, strain differences in APAP-induced nephrotoxicity may be related to 1) differences

in the delivery of APAP to the kidney due to competing extrarenal phase II reactions or 2) to the availability of APAP for activation within the kidney due to competing intrarenal phase II reactions. Jollow and coworkers have demonstrated that differences in phase II reactions, specifically glucuronidation, can markedly alter APAP-induced hepatotoxicity (Price and Jollow, 1982; Jollow et al., 1974). If it is assumed that the amount of APAP excreted can be used as an index of the amount of APAP reaching the kidney, it appears that more APAP reaches the kidneys of F344 rats than of SD rats at subnephrotoxic doses (500 and 750 mg/kg) of APAP. However, even at those doses some histopathological changes are evident in the proximal tubules of F344 rats. APAP is extensively resorbed (70-80%) from tubular urine (Duggin and Mudge, 1975; Ross, 1981). Therefore, the apparent greater excretion of APAP in F344 rats may merely represent abnormalities in proximal tubular reabsorption undetectable by total recovery of the administered dose.

Data from arylation experiments indicate that less total radioactivity was associated with the SD than the F344 kidney at the time of maximal arylation, which may be indicative of less APAP present within the SD kidney. It is recognized, however, that much of the radioactivity within the kidney may not be in the form of the parent drug; distribution experiments in the F344 rat indicated almost half of the radioactivity in the renal cortex 5 hr after APAP administration was in the form of APAP metabolites. However, even if renal cortical concentration of APAP in the SD rat are half those in the F344, this may not play a prominent role in the ultimate quantity of

APAP metabolically activated if the mechanisms of APAP activation are at maximum velocity at the cortical concentration of APAP found in the SD rat. If the systems of metabolic activation are not at maximum velocity, the differences in cortical concentrations of APAP are undoubtedly a contributing factor in strain differences in APAP-induced nephrotoxicity.

Renal phase II metabolism may reduce the amount of APAP available for activation within the kidney. Renal cells and IPKs metabolize APAP to its phenolic glucuronide and sulfate conjugates (Jones et al., 1978; Emslie et al., 1981a,b). Strain differences in the dexamethasone-stimulated sulfation of 3-methoxy-4-hydroxyphenylglycol have been noted in F344 and SD renal cytosol in vitro (Maus et al., 1982). Furthermore, SD IPKs excreted more APAP-SO_3 than corresponding F344 IPKs. Whether differences in phase II metabolism within the kidney result in different intrarenal activation rates of APAP and subsequent differences in the susceptibility to APAP-induced nephrotoxicity is yet to be determined. However, modulation of phase II metabolism in isolated hepatocytes by specific inhibitors of phase II metabolism does not affect P-450-dependent APAP activation (Moldeus et al., 1979). Therefore, it is unlikely that intrarenal phase II metabolism could reduce the flux of APAP through deacetylation or P-450 metabolism probably because intrarenal phase II metabolism could not effectively reduce the renal concentration of APAP. On the other hand, intrarenal phase II metabolism may reduce the activation of PAP formed after a nephrotoxic dose of APAP because concentrations of PAP would be expected to be relatively low. Therefore, renal phase II metabolism

may effectively reduce the concentration of PAP such that activation is now reduced. This may be the case in the SD rat that has greater sulfation and glucuronidation activity.

Dramatic strain differences in rats exist in the susceptibility to APAP-induced nephrotoxicity. These differences do not appear to be the result of differences in direct P-450 renal activation or deacetylation of APAP to the nephrotoxic metabolite, PAP. Therefore, experiments were designed to determine if strain-related differences exist in PAP-induced nephrotoxicity and metabolism.

The renal histopathologic and functional lesions produced by PAP were qualitatively similar in F344 and SD rats although quantitatively less in the SD rat. Such data support the interpretation that strain-related differences in APAP-induced nephrotoxicity are related to APAP deacetylation with subsequent activation of the metabolite, PAP. Three mechanisms may be responsible for such differences in the susceptibility to PAP: (1) differences in the intrarenal availability of PAP because of differences in clearance of PAP from the blood or competitive alternative intrarenal pathways of metabolism, (2) differences in renal activation of PAP, and (3) differences in the detoxification of a reactive intermediate of PAP prior to arylation of important cellular constitutents.

Urinary excretion of the metabolites of PAP differs between the two strains. Substantially greater amounts of acetylated metabolites were evident in the urine of SD rats following higher doses of PAP, perhaps reflecting a greater capacity of the SD rat to reduce, via acetylation, the amount of PAP available for activation within the

kidney. Such strain differences in the metabolism of PAP may be responsible for lower total radioactivity, possibly indicative of parent drug, in kidneys of SD rats than in kidneys of F344 rats following a nephrotoxic dose of [ring-^{14}C]-PAP.

In vitro, PAP binds covalently to renal and hepatic microsomes by an enzymatic process that has not been fully characterized (Calder *et al.*, 1979). *In vitro* activation of PAP is five to ten times greater in kidney than in liver. At concentrations $\leq$5 mM PAP, the activation of PAP was much greater in renal microsomes from F344 rats than from SD rats. The renal PAP concentration following both PAP and APAP administration would be expected to be many times lower than 5 mM. Therefore, if rates of covalent binding *in vitro* can be applied to the situation *in vivo* and if there is a linear relationship between covalent binding and nephrotoxicity, the differences in binding may explain the strain differences in PAP nephrotoxicity. However, these *in vitro* studies of PAP activation must be interpreted with caution, as the mechanism of PAP activation within renal microsomes has not been fully characterized. Indeed, the microsomal activation of PAP may not be an accurate representation of the biochemical mechanism of PAP-induced nephrotoxicity. The reason for the discrepancy between strain differences in PAP activation by renal microsomes and APAP activation by renal 10,000 x g supernatants is unclear. Since APAP deacetylation in renal 10,000 x g supernatants was nearly identical in the two strains and PAP activation in renal microsomes from the F344 rats is nearly two-fold greater than that from SD rats, one would expect a much greater difference between SD and F344 renal 10,000 x g

supernatants in APAP activation by the deacetylase-dependent mechanism. Perhaps there are more reducing equivalents in the 10,000 x g supernatants of F344 rats than SD rats available for reduction of reactive intermediates generated from PAP.

Differences in the detoxification of a reactive intermediate produced from PAP may also be responsible for strain differences in PAP-induced nephrotoxicity. PAP reduces renal cortical NPSH concentrations *in vivo* (Crowe *et al.*, 1979). GSH reduces the PAP arylation of renal and hepatic macromolecules *in vitro* (Calder *et al.*, 1979). Therefore, GSH may protect against PAP-induced nephrotoxicity. Small differences (<20%) exist between SD and F344 renal cortical NPSH concentrations. Whether such small differences in NPSH concentrations play a role in strain differences in susceptibility to toxicants is unknown. Preliminary results, employing small doses of the glutathione synthetase inhibitor, buthionine sulfoximine, indicate that even when renal NPSH concentrations in the SD rat are reduced to concentrations similar to or less than those in F344 rats, PAP is still significantly more nephrotoxic in F344 rats than SD rats.

Therefore, it appears that strain differences in PAP-induced nephrotoxicity may result from 1) a decreased concentration of PAP in the kidney of the SD rat possibly due to delayed absorption or greater clearance and (2) higher rates of PAP activation in the F344 rat kidney. Both of these mechanisms may also contribute to strain differences in APAP-induced nephrotoxicity since PAP generation from APAP appears similar in both strains. In addition, other factors may also contribute to strain differences in APAP-induced nephrotoxicity.

These include 1) a decreased concentration of APAP in the kidney of the SD rat possibly due to delayed absorption or greater clearance and 2) differences in intrarenal phase II metabolism such that less PAP, formed from APAP, is available for activation in the SD rat.

Certain carboxylesterase/amidase inhibitors such as diethyl-p-nitrophenyl phosphate (paraoxon) and BNPP have been employed in attempts to determine the role of deacetylation in the generation of reactive cytotoxic and genotoxic intermediates from structurally related aromatic amines (Schut et al., 1978; Timbrell et al., 1980; Wirth et al., 1980). Unfortunately, use of such deacetylase inhibitors in vivo has met with limited success due to systemic toxicity of these compounds. However, BNPP was used in vivo to prevent phenacetin-induced methemobloginemia, an effect attributed to the inhibition of phenacetin deacetylation (Heymann et al., 1969). In addition, BNPP was used to prevent the metabolic hydrolysis and hepatotoxicity of the antidepressant drug, iproniazid (Nelson et al., 1978).

Experiments utilizing BNPP were designed to determine the relevance of deacetylation to APAP-induced cortical necrosis in the F344 rat. Inhibition of cortical homogenate covalent binding of APAP by BNPP and the reduction by BNPP of APAP but not PAP nephrotoxicity in vivo suggests that the deacetylase-dependent mechanism of activation has toxicological relevance to APAP-induced cortical necrosis.

In previous studies, BNPP was effective in preventing hepatotoxicity of acetylisoniazid, a metabolite of the antitubercular agent isoniazid, but had no effect on the hepatotoxicity of the metabolite acetylhydrazine (Mitchell et al., 1976). These experiments were

critical in the elucidation of the mechanism of isoniazid-induced hepatotoxicity, that hydrolysis of an amide linkage was required to produce the proximate hepatotoxicant acetylhydrazine. An integral component of these investigations was the demonstration of BNPP-induced alterations in isoniazid metabolism in vivo.

In the present study, BNPP appeared to inhibit the deacetylation of APAP in vivo as indicated by the reduced amount of PAP in a 24 hr collection of urine. The BNPP-induced reduction in the excretion of PAP and its phenolic conjugates was apparently due to decreased formation of these metabolites, not reduction in the urinary elimination of PAP and its phenolic conjugates from the body, as BNPP did not alter the excretion of these metabolites following PAP administration. The effect of BNPP on deacetylation of APAP appeared to be relatively specific; BNPP did not affect the net metabolism of APAP by any other mechanism. BNPP pretreatment did not result in lower plasma, renal cortical or hepatic concentrations of APAP, suggesting the decreased formation of PAP in vivo resulting from BNPP pretreatment was not the result of reduced substrate concentrations. APAP concentrations at these early time points are particularly important because arylation of renal macromolecules, believed to be the initial biochemical event in APAP nephrotoxicity, was maximal 4-6 hr following APAP administration (Mudge et al., 1978; McMurtry et al., 1978). While BNPP pretreatment did not reduce renal cortical concentrations of APAP, it did result in much greater renal cortical concentrations of APAP-CONJ and APAP-NAC at the later time points studied. The major component of APAP-CONJ, which at this dose of APAP is the phenolic glucuronide

(Jollow et al., 1974), and APAP-NAC are both organic acids that are actively secreted by the kidney (Duggin and Mudge, 1975). Therefore, the lower renal cortical concentrations of APAP-CONJ and APAP-NAC in naive animals may reflect an early manifestation of nephrotoxicity. In support of this conclusion is a recent investigation in our laboratory which demonstrated that functional nephrotoxicity of chloroform, as indicated by the accumulation of organic anions in vitro, was detectable within 2 hr following chloroform administration (Hook et al., 1983).

It is apparent from the present investigation that PAP does play an important role in APAP-induced nephrotoxicity. However, the question arises as to whether the deacetylase-dependent mechanism of APAP activation is the sole mechanism which is relevant to APAP-induced nephrotoxicity. Certainly, the existence of a P-450-dependent mechanism of APAP activation has been demonstrated in several laboratories with in vitro microsomal preparations, isolated cells and perfused kidneys (McMurtry et al., 1978; Jones et al., 1979; Emslie et al., 1981a,b). However, data concerning the relevance of this mechanism of activation to APAP-induced nephrotoxicity in the non-induced animal is lacking. Cobaltous chloride, a P-450 inhibitor, reduced APAP-induced nephrotoxicity (McMurtry et al., 1978) which was interpreted to result from cobaltous chloride's inhibitory effect on renal P-450. However, further validation of this interpretation is required following the recent demonstration that cobaltous chloride markedly reduced the delivery to the kidney in vivo of the structurally similar aromatic amine, PAP (Calder et al., 1978). Perhaps the inability of

BNPP to protect against nephrotoxicity following a dose of 750 mg/kg APAP could reflect the extent of nephrotoxicity resulting from a P-450 mechanism of metabolic activation. The deacetylase-dependent mechanism of metabolic activation may only contribute to APAP-induced nephrotoxicity after higher doses of APAP. Alternatively, the nephrotoxicity evident at 750 mg/kg APAP may result from PAP generation by an amidase/carboxylesterase that is not sensitive to BNPP. In support of this proposal, Heymann and coworkers (1969) have demonstrated that phenacetin deacetylation is only partially inhibitable by BNPP while completely inhibitable by other deacetylase inhibitors. This suggests that certain amidases/carboxylesterases responsible for deacetylation of certain aromatic amines such as phenacetin and possibly APAP are insensitive to the inhibitory effects of BNPP.

Specifically labelled (^{14}C)-APAP was used to quantify the generation of reactive intermediates by each mechanism of activation <u>in vivo</u>. Basically, a comparison of the extent of binding of [acetyl-^{14}C]- or [ring-^{14}C]-APAP will reveal whether the molecule bound to tissue protein is APAP or PAP. If, in paired experiments, the ratio of acetyl to ring (^{14}C) bound is less than one, this would be indicative that some of the compound bound is PAP. A value approaching zero would indicate almost total PAP binding. A protein synthesis inhibitor, cycloheximide, was incorporated into the experimental design in an attempt to eliminate erroneous results from possible acetate (arising from deacetylation) incorporation into protein following administration of [acetyl-^{14}C]-APAP.

In the F344 rat, the deacetylase-dependent mechanism of APAP activation could account for between 38 and 82 percent of APAP arylation in renal cortical tissue. Closer approximation of the extent of arylation may be difficult due to the increased cortical concentrations of APAP resulting from HEX pretreatment. However, even at the higher cortical concentrations of APAP resulting from HEX pretreatment, arylation of cortical protein by [ring-^{14}C]-APAP was not increased in the F344 rat possibly suggesting that pathways of metabolic activation were saturated even at lower cortical concentrations of APAP. If this assumption is correct with respect to the deacetylase-dependent mechanism of APAP activation, then it appears that deacetylation, and not PAP activation, is the rate-limiting step in deacetylase-dependent APAP activation *in vivo* since HEX pretreatment resulted in an increased cortical concentration and arylation following [ring-^{14}C]-PAP but not [ring-^{14}C]-APAP. If HEX pretreatment completely inhibited acetate incorporation and pathways of metabolic activation were saturated, then the deacetylase-dependent mechanism of APAP activation accounted for 82% of renal cortical arylation in the F344 rat, 0% in the SD rat; incomplete inhibition of acetate incorporation would result in larger percentages of deacetylase-dependent arylation in both strains. A deacetylase-dependent mechanism of APAP activation was not detectable in liver as [acetyl-^{14}C]- and [ring-^{14}C]-APAP hepatic binding was similar in both strains of rat. This observation correlated with those determined in *in vitro* systems.

It is recognized that covalent binding measurements are only an indication of the generation of reactive intermediates *in vivo*. It

is not assumed that the reactive intermediates generated by the different mechanisms (deacetylase vs. P-450) of metabolic activation have similar "toxicological potential". In fact, as first suggested by Andersson and coworkers (1982), they are probably different with respect to specific subcellular sites of arylation and the resulting biochemical and physiological sequelae. However, a correlative relationship does exist, in general, between covalent binding and nephrotoxicity. F344 rats, which are sensitive to APAP-induced nephrotoxicity, have far greater renal cortical arylation following a nephrotoxic dose of APAP than SD rats. Furthermore, this difference in arylation between strains appears to be predominantly that which is deacetylation-dependent as the cortical binding of [acetyl-^{14}C]-APAP (indicative of non-deacetylase-dependent activation) was similar in HEX pretreated SD and F344 rats. The lack of deacetylation-dependent arylation in the SD rat may be due to the apparently low cortical concentrations of APAP. In support of the proposal is the marked increase (almost 10x) in net APAP deacetylation rates in IPKs from F344 rat when perfusate concentrations of APAP were increased only two-fold (2.5-5.0 mM).

Therefore, it is apparent that the deacetylase-dependent mechanism of APAP activation can account for a significant fraction of renal APAP arylation in vivo. Furthermore, this deacetylase-dependent arylation appears to have substantial toxicological relevance as it was correlated with APAP nephrotoxicity where P-450-dependent arylation was not.

CONCLUSIONS

There are at least two mechanisms of APAP activation within the renal cortex. One system is dependent upon cytochrome P-450 and another is dependent upon deacetylation with the subsequent metabolic activation of the deacetylated product PAP. The deacetylase-dependent mechanism of APAP activation can produce substantially greater amounts of reactive arylating intermediates within the renal cortex of the F344 rat. The formation of reactive intermediates from APAP by a deacetylase-dependent mechanism appears to play a significant role in APAP-induced cortical necrosis in the F344 rat. Two lines of evidence support this conclusion. First, arylation of renal macromolecules in vivo by the deacetylase-dependent mechanism was not apparent in SD rats; SD rats are not susceptible to APAP-induced nephrotoxicity. Second, BNPP, a deacetylase inhibitor, markedly reduced APAP-induced renal cortical necrosis in F344 rats, an event that correlated with the decreased urinary elimination of PAP. These observations suggest that formation of reactive intermediates from APAP within the renal cortex of the F344 rat by a deacetylase-dependent mechanism is a requisite step in APAP-induced renal cortical necrosis.

BIBLIOGRAPHY

Abe

Ang

Arr

At

Ar

B

E

E

E

E

BIBLIOGRAPHY

Abel, J.A. (1971). Analgesic nephropathy, a review of the literature, 1967-1970. Clin. Pharmacol. Ther. 12: 583-598.

Angervall, L. and Bengtsson, U. (1968). Impairment of renal concentrating capacity in albino rats induced by phenacetin and acetylsalicylic acid. Acta Pharmacol. 26: 105-112.

Arnold, L., Collins, C. and Starmer, G. (1973). The short-term effects of analgesics on the kidney with special reference to acetylsalicylic acid. Pathology 5: 123-134.

Atio, A. (1978). A simple and sensitive assay of 7-ethoxycoumarin deethylation. Anal. Biochem. 85: 488-491.

Andersson, B., Norderskjold, M., Rahimtula, A. and Moldeus, P. (1982). Prostaglandin synthetase-catalyzed activation of phenacetin metabolites to genotoxic products. Mol. Pharmacol. 22: 479-485.

Bengtsson, V. (1962). A comparative study of chronic non-obstructive pyelonephritis and renal papillary necrosis. Acta Med. Scand. 165: 321.

Bengtsson, V. (1975). Phenacetin containing analgesics and renal disease. Lancet 1: 1195.

Bonkowsky, H.L., Mudge, G.H. and McMurtry R.J. (1978). Chronic hepatic inflammation and fibrosis due to low doses of paracetamol. Lancet 1: 1016-1018.

Borei, H.G. and Bjorklund, U. (1953). Oxidation through the cytochrome system of substituted phenylenediamines. Biochem. J. 54: 357-361.

Boyd, J.A. and Eling, T.E. (1981). Prostaglandin endoperoxide synthetase-dependent cooxidation of acetaminophen to intermediates which covalently bind in vitro to rabbit renal medullary microsomes. J. Pharmacol. Exp. Ther. 219: 659-664.

Boyer, T.D. and Rouff, S.L. (1971). Acetaminophen-induced hepatic necrosis and renal failure. J. Am. Med. Assoc. 218: 440-441.

Breen, K., Wandscheer, J.-C., Peignoux, M. and Pessayre, D. (1982). In situ formation of the acetaminophen metabolite covalently bound in kidney and lung. Supportive evidence provided by total hepatectomy. Biochem. Pharmacol. 31: 115-116.

Brodie, B.B. and Axelrod, J. (1949). The fate of acetophenetidin (phenacetin) in man and methods for the estimation of acetophenetidin and its metabolites in biological material. J. Pharmacol. Exp. Ther. 95: 58.

Burry, H.C. and Dieppe, P.A. (1976). Apparent reduction of endogenous creatinine clearance by salicylate treatment. Brit. Med. J. 2: 16-17.

Calder, I.C., Funder, C.C., Green, C.R., Ham, R.N. and Tange, J.D. (1971). Comparative nephrotoxicity of aspirin and phenacetin derivatives. Brit. Med. J. 4: 518-521.

Calder, I.C., Williams, P.J., Woods, R.A., Funder, C.C., Green, C.R., Ham, K.N. and Tange, J.D. (1975). Nephrotoxicity and molecular structure. Xenobiotica 5: 303-307.

Calder, I.C., Yong, A.C., Woods, R.A., Crowe, C.A., Ham, K.N. and Tange, J.D. (1979). The nephrotoxicity of p-aminophenol. II. The effect of metabolic inhibitors and inducers. Chem.-Biol. Interactions 27: 245-254.

Carpenter, H.M. and Mudge, G.H. (1981). Acetaminophen nephrotoxicity: Studies on renal acetylation and deacetylation. J. Pharmacol. Exp. Ther. 218: 161-167.

Christ, E.J. and Van Dorp, D.A. (1972). Comparative aspects of prostaglandin biosynthesis in animal tissues. Biochim. Biophys. Acta 270: 537.

Clark, R., Borirakchanyavat, V., Davidson, A.R., Thompson, R.P.H., Widdop, B., Goulding, R. and Williams, R. (1973). Hepatic damage and death from overdose of paracetaminol. Lancet 1: 66-70.

Cobden, I., Record, C.O., Ward, M.K. and Ken, D.N.S. (1982). Paracetamol-induced acute renal failure in the absence of fulminant liver damage. Brit. Med. J. 284: 21-22.

Cottrell, R.C., Agrelo, C.E., Gangolli, S.D. and Grasso, P. (1976). Histochemical and biochemical studies of chemically induced acute kidney damage in the rat. Fd. Cosmet. Toxicol. 14: 593-598.

Cross, R.J. and Taggart, J.V. (1950). Renal tubular transport: Accumulation of p-aminohippurate by rabbit kidney slices. Am. J. Physiol. 161: 181-190.

Crowe, C.A., Calder, I.C., Madsen, N.P., Funder, C.C., Green, C.R., Ham, K.N. and Tange, J.D. (1977). An experimental model of analgesic-induced renal damage - some effects of p-aminophenol on rat kidney mitochondria. Xenobiotica 7: 345-356.

Crowe, C.A., Yong, A.C., Calder, I.C., Ham, K.N. and Tange, J.D. (1979). The nephrotoxicity of p-aminophenol. I. The effect on microsomal cytochromes, glutathione, and covalent binding in kidney and liver. Chem.-Biol. Interactions 27: 235-243.

Curry, R.W., Robbinson, J.D. and Sughrue, M.J. (1981). Acute renal failure after acetaminophen ingestion. J. Am. Med. Assoc. 247: 1012-1014.

Czapels, E.E. (1976). Aspirin, acetaminophen and bleeding. J. Am. Med. Assoc. 235: 636.

Davis, D.C., Potter, W.Z., Jollow, D.J. and Mitchell, J.R. (1974). Species differences in hepatic glutathione depletion, covalent binding and hepatic necrosis after acetaminophen. Life Sci. 14: 2099-2109.

Dent, J.G., Graichen, M.E., Schnell, S. and Lasker, J. (1980). Constitutive and induced hepatic microsomal cytochrome P-450 monooxygenase activities in male Fischer-344 and CD rats. A comparative study. Toxicol. Appl. Pharmacol. 52: 45-53.

Dubach, U.C., Rosner, B. and Muller, A. (1975). A relation between regular intake of phenacetin-containing analgesics and laboratory evidence for uro-renal disorders in a working female population of Switzerland. Lancet 1: 539.

Duggin, G.G. (1980). Mechanisms in the development of analgesic nephropathy. Kidney Int. 18: 553-561.

Duggin, G.G. and Mohandas, J. (1982). Biochemical mechanisms of acetaminophen (paracetamol) induced hepatic and renal toxicity. In Advances in Pharmacology and Therapeutics II (H. Yoshida, Y. Hagihara and S. Ebashi), Vol. 5, pp. 77-86, Pergamon Press, New York.

Duggin, G.G. and Mudge, G.H. (1975). Renal tubular transport of paracetamol and its conjugates in the dog. Brit. J. Pharmacol. 54: 359-366.

Ekstrom, T., Hogberg, J. and Jernstrom, B. (1982). Inhibition of hepatic γ-glutamyl-cysteine synthetase by chloroform. Biochem. Pharmacol. 31: 3510-3513.

Ellman, G.L. (1959). Tissue sulfhydryl groups. Arch. Biochem. Biophys. 82: 70-77.

Emslie, K.R., Smail, M.C., Calder, I.C., Hart, S.J. and Tange, J.D. (1981a). Paracetamol and the isolated perfused kidney: Metabolism and functional effects. Xenobiotica 11: 43-50.

Emslie, K.R., Calder, I.C., Hart, S.J. and Tange, J.D. (1981b). Induction of paracetamol metabolism in the isolated perfused kidney. Xenobiotica 11: 579-587.

Flower, R.J., Moncada, S. and Vane, J.R. (1980). Analgesic-antipyretics and anti-inflammatory agents; drugs employed in the treatment of gout. In The Pharmacological Basis of Therapeutics (A.G. Gilman, L.S. Goodman, and A. Gilman, eds.), 6th eds., pp. 682-728, Macmillan Publishing Co., New York.

Franklin, M.R., Bridges, J.W. and Williams, R.T. (1969). The enzymic deacetylation of p-acetmidobenzoic acid. Biochem. J. 114: 6P.

Frieden, E. and Hsieh, H.S. (1976). Ceruloplasmin: The copper transport protein with essential oxidase activity. Adv. Enzymol. 44: 187-236.

Frings, C.S. and Saloom, J.M. (1979). Colorimetric method for the quantitative determination of acetaminophen in serum. Clin. Toxicol. 15: 67-73.

Gabriel, R., Caldwell, J. and Hartley, R.B. (1982). Acute tubular necrosis, caused by therapeutic doses of paracetamol. Clin. Nephrol. 18: 269-271.

Gault, M.H., Blennerhassett, J. and Muehrcke, R.C. (1971). Analgesic nephropathy: A clinicopathologic study using electron microscopy. Am. J. Med. 51: 740-756.

Gemborys, M.W. and Mudge, G.H. (1981). Formation and disposition of the minor metabolites of acetaminophen in the hamster. Drug Metab. Disp. 9: 340-351.

Gemborys, M.W., Mudge, G.H. and Gribble, G.W. (1980). Mechanism of decomposition of N-hydroxyacetaminophen, a postulated toxic metabolite of acetaminophen. J. Med. Chem. 23: 204.

Gillette, J.R. and Mitchell, J.R. (1975). Drug actions and interactions. In Handbook of Experimental Pharmacology, Vol. 28, Part 3, Springer-Verlag, New York.

Green, C.R., Ham, K.N. and Tange, J.D. (1969). Kidney lesions induced in rats by p-aminophenol. Brit. Med. J. 1: 162-166.

Grimlund, K. (1963). Renal papillary necrosis at a Swedish factory. Acta Med. Scand. 174(5405): 1.

Gutmann, H.R., Malejka-Giganti, D., Barry, E.J. and Rydell, R.E. (1972). On the correlation between the hepatocarcinogenicity of the carciongen, N-2-fluorenylacetamide, and its metabolic activation by the rat. Cancer Res. 32: 1554-1561.

Hamberg, M. and Samuelsson, B. (1974). Prostaglandin endoperoxides: Novel transformation of arachidonic acid in human platelets. Proc. Natl. Acad. Sci. USA 71: 3400.

Hart, S.J., Calder, I.C. and Tange, J.D. (1982). The metabolism and toxicity of paracetamol in Sprague-Dawley and Wistar rats. Eur. J. Drug Metab. Pharmacol. 7: 203-222.

Hennis, H.L., Allen, R.C., Hennigar, G.R. and Simmons, M.A. (1981). A sensitive method for determining the nephrotoxic effects of the analgesic acetaminophen upon esterases using isoelectric focusing. Electrophoresis 2: 187-190.

Heymann, E., Krisch, K., Buch, H. and Buzello, W. (1969). Inhibition of phenacetin- and acetanilide-induced methemoglobinemia in the rat by the carboxylesterase inhibitor bis-(p-nitrophenyl)phosphate. Biochem. Pharmacol. 18: 801-811.

Hinson, J.A., Pohl, L.R. and Gillette, J.R. (1974). N-Hydroyacetaminophen: A microsomal metabolite of N-hydroxyphenacetin but apparently not of acetaminophen. Life Sci. 24: 2133-2138.

Hinson, J.A. (1980). Biochemical toxicology of acetaminophen. In Reviews of Biochemical Toxicology (E. Hodgson, J.R. Bend, R.M. Philpot, eds.), Vol. 2, pp. 103-130, Elsevier/North-Holland, New York.

Hook, J.B., Smith, J.H., Maita, K. and Sleight, S.D. (1983). Time course of chloroform toxicity in male and female ICR mice. Toxicologist 3: 99.

Hrycay, E.G. and O'Brien, P.J. (1972). Cytochrome P-450 as a microsomal peroxidase in steroid hydroperoxide reduction. Arch. Biochem. Biophys. 153: 480-482.

Hultin, T.A. and Weber, W. (1982). Pharmacokinetic differences of 2-aminofluorene (AF) in isolated hepatocytes from inbred mice. Fed. Proc. 41: 1639.

Ilett, K.F., Reid, W.D., Sipes, I.G. and Krishna, G. (1973). Chloroform toxicity in mice: Correlation of renal and hepatic necrosis with covalent binding of metabolites to tissue macromolecules. Exp. Mol. Pathol. 19: 125-129.

Jeffery, W.H. and Lafferty, W.E. (1981). Acute renal failure after acetaminophen overdose: Report of two cases. Am. J. Hosp. Pharm. 38: 1355-1358.

Jollow, D.J., Mitchell, J.R., Potter, W.Z., Davis, D.C., Gillette, J.R. and Brodie, B.B. (1973). Acetaminophen-induced hepatic necrosis. II. Role of covalent binding in vivo. J. Pharmacol. Exp. Ther. 187: 195-202.

Jollow, D.J., Thorgeirsson, S.S., Potter, W.Z., Hashimoto, M. and Mitchell, J.R. (1974). Acetaminophen-induced hepatic necrosis. VI. Metabolic disposition of toxic and non-toxic doses of acetaminophen. Pharmacology 12: 251-271.

Jones, D.P., Sunby, G.B., Ormstad, K. and Orrenius, S. (1979). Use of isolated kidney cells for study of drug metabolism. Biochem. Pharmacol. 28: 929-935.

Kaplan, A. (1965). Urinary nitrogen and urinary ammonia. In Standard Methods in Clinical Chemistry (Meites, S., ed.), Vol. 5, pp. 245-256, Academic Press, New York.

Kincaid-Smith, P. (1978). Analgesic nephropathy. Kidney Int. 13: 1-14.

King, C.M., Traub, N.R. and Lortz, Z.M. (1976). Arylhydroxamic acid acyltransferase (AT) of the mammary gland of the rat. Proc. Amer. Assoc. Cancer Res. 17: 51.

Kleinman, J.G., Breitenfield, R.V. and Roth, D.A. (1980). Acute renal failure associated with acetaminophen ingestion: Report of a case and review of the literature. Clin. Nephrol. 14: 201-205.

Kluwe, W.M. and Hook, J.B. (1981). Comparative induction of xenobiotic metabolism in rodent kidneys, testis and liver by commercial mixtures of polybrominated biphenyls and polychlorinated biphenyls, phenobarbital and 3-methylcholanthrene: Absolute and temporal effects. Toxicology 20: 259-273.

Larsen, K. and Moller, C.E. (1959). A renal lesion caused by the abuse of phenacetin. Acta Med. Scand. 164: 53-86.

Lindeneg, O., Fischer, S., Pederson, J. and Nissen, N.I. (1959). Necrosis of the renal papillae and prolonged abuse of phenacetin. Acta Med. Scand. 165: 321-332.

Lock, E.A. and Ishmael, J. (1979). The acute toxic effects of hexachloro-1:3-butadiene on the rat kidney. Arch. Toxicol. 43: 47-57.

Lowry, O.H., Rosebrough, N.J., Farr, A.C. and Randall, R.J. (1951). Protein measurement with Folin phenol reagent. J. Biol. Chem. 193: 265-275.

Malejka-Giganti, D. and Rydell, R.E. (1978). Lack of susceptibility of F-344 rats to mammary tumor induction by topically applied fluorenylacetohydroxamic acids and their acetates. J. Natl. Cancer Inst. 60: 433-435.

Marcus, A. (1978). The role of lipids in platelet function: With particular reference to the arachidonic acid pathway. J. Lipid Res. 19: 793.

Marnett, L., Wlodawer, P. and Samuelsson, B. (1975). Co-oxidation of organic substrates by the prostaglandin synthetase of sheep vesicular gland. J. Biol. Chem. 250: 8510.

Marnett, L.J. (1981). Polycyclic aromatic hydrocarbon oxidation during prostaglandin biosynthesis. Life Sci. 29: 531.

Maus, T.P., Pearson, R.K., Anderson, R.J., Woodson, L.C., Reiter, C. and Weinshilboum, R.M. (1982). Rat phenol sulfotransferase. Assay procedure, developmental changes, and glucocorticoid regulation. Biochem. Pharmacol. 31: 849-856.

McJunkin, B., Barwick, K.W., Little, W.C. (1976). Fatal massive hepatic necrosis following acetaminophen overdose. J. Am. Med. Assoc. 236: 1874-1875.

McMurtry, R.J., Snodgrass, W.R. and Mitchell, J.R. (1978). Renal necrosis, glutathione depletion and covalent binding after acetaminophen. Toxicol. Appl. Pharmacol. 46: 87-100.

Meredith, T.J., Vale, J.A. and Goulding, R. (1981). The epidemiology of acute acetaminophen poisoning in England and Wales. Arch. Intern. Med. 141: 397-400.

Miner, D.J. and Kissinger, P.T. (1979). Evidence for the involvement of N-acetyl-p-quinoneimine in acetaminophen metabolism. Biochem. Pharmacol. 28: 3285-3290.

Mitchell, J.R., Jollow, D.J., Potter, W.Z., Davis, D.C., Gillette, J.R. and Brodie, B.B. (1973a). Acetaminophen-induced hepatic necrosis. I. Role of drug metabolism. J. Pharmacol. Exp. Ther. 187: 185-199.

Mitchell, J.R., Jollow, D.J., Potter, W.Z., Gillette, J.R. and Brodie, B.B. (1973b). Acetaminophen-induced hepatic necrosis. IV. Protective role of glutathione. J. Pharmacol. Exp. Ther. 187: 211-217.

Mitchell, J.R., McMurtry, R.J., Statham, C.N. and Nelson, S.D. (1977). Molecular basis for several drug-induced nephropathies. Amer. J. Med. 62: 518-526.

Mitchell, J.R., Zimmerman, H.J., Ishak, K.G., Thorgeirsson, U.P., Timbrell, J.A., Snodgrass, W.R. and Nelson, S.D. (1976). Isoniazid liver injury: Clinical spectrum, pathology and probable pathogenesis. Ann. Intern. Med. 84: 181-192.

Mohandas, J., Duggin, G.G., Horvath, J.S. and Tiller, D.J. (1981a). Metabolic oxidation of acetaminophen (paracetamol) mediated by cytochrome P-450 mixed-function oxidase and prostaglandin endoperoxide synthetase in rabbit kidney. Toxicol. Appl. Pharmacol. 61: 252-259.

Mohandas, J., Duggin, G.G., Horvath, J.S. and Tiller, D.J. (1981b). Regional differences in peroxidatic activation of paracetamol (acetaminophen) mediated by cytochrome P-450 and prostaglandin endoperoxide synthetase in rabbit kidney. Res. Commun. Chem. Pathol. Pharmacol. 34: 69-80.

Moldeus, P., Andersson, B. and Gergely, V. (1979). Regulation of glucuronidation and sulfate conjugation in isolated hepatocytes. Drug Metab. Disp. 7: 416-419.

Moldeus, P., Andersson, B., Rahimtula, A. and Berggren, M. (1982). Prostaglandin synthetase catalyzed activation of paracetamol. Biochem. Pharmacol. 31: 1363-1368.

Moldeus, P. and Rahimtula, A. (1980). Metabolism of paracetamol to a glutathione conjugate catalyzed by prostaglandin synthetase. Biochem. Biophys. Res. Commun. 96: 469-475.

Mudge, G.H. (1982). Analgesic nephropathy. Renal drug distribution and metabolism. In Nephrotoxic Mechanisms of Drugs and Environmental Toxins (G.A. Porter, ed.), pp. 209-225, Plenum Medical, New York.

Mudge, G.H., Gemborys, M.W. and Duggin, G.G. (1978). Covalent binding of metabolites of acetaminophen to kidney protein and depletion of renal glutathione. J. Pharmacol. Exp. Ther. 206: 218-226.

Murray, T.G. (1982). Analgesic nephropathy. Clinical and epidemiologic factors. In Nephrotoxic Mechanisms of Drugs and Environmental Toxins (G.A. Porter, ed.), pp. 197-208, Plenum Medical, New York.

Murray, T. and Goldberg, M. (1976). Analgesic abuse and renal disease. Ann. Rev. Med. 26: 537-550.

Murray, T.G., Wyllie, R.G., Hill, G.S., Ramsden, P.W. and Heptinstall, R.H. (1972). Experimental papillary necrosis of the kidney. Am. J. Pathol. 67: 285-302.

Nelson, S.D. (1982). Metabolic activation and drug toxicity. J. Med. Chem. 25: 753-765.

Nelson, S.D., Dahlin, D.C., Rauckman, E.J. and Rosen, G.M. (1981). Peroxidase-mediated formation of reactive metabolites of acetaminophen. Mol. Pharmacol. 20: 195-199.

Nelson, S.D., Forte, A.J. and Dahlin, D.C. (1980). Lack of evidence for N-hydroxyacetaminophen as a reactive metabolite of acetaminophen in vitro. Biochem. Pharmacol. 29: 1617-1620.

Nelson, S.D., Forte, A.J., Vaishnav, Y., Mitchell, J.R., Gillette, J.R. and Hinson, J.A. (1981). The formation of arylating and alkylating metabolites of phenacetin in hamsters and hamster liver microsomes. Mol. Pharmacol. 19: 140-145.

Nelson, S.D., Mitchell, J.R., Snodgrass, W.R. and Timbrell, J.A. (1978). Hepatotoxicity and metabolism of iproniazid and isopropylhydrazine. J. Pharmacol. Exp. Ther. 206: 574-585.

Newton, J.F. and Hook, J.B. (1981). The isolated perfused kidney. In Methods in Enzymology (W.B. Jakoby, ed.), Vol. 77, pp. 94-105, Academic Press, New York.

Nordblom, G.D., White, R.E. and Coon, M.J. (1976). Studies on hydroperoxide-dependent substrate hydroxylation by purified liver microsomal cytochrome P-450. Arch. Biochem. Biophys. 175: 524-533.

Nordenfelt, O. (1972). Deaths from renal failure in abusers of phenacetin-containing drugs. Acta Med. Scand. 191: 11-16.

Nugteren, D.H. and Hagelhof, E. (1973). Isolation and properties of intermediates in prostaglandin biosynthesis. Biochim. Biophys. Acta 326: 448.

Olafsson, O., Gudmundsson, K.R. and Brekkan, A. (1966). Migraine, gastritis and renal papillary necrosis: A syndrome in chronic non-obstructive pyelonephritis. Acta Med. Scand. 179: 121-128.

Omura, T. and Sato, R. (1964). The carbon monoxide-binding pigment of liver microsomes. I. Evidence for its hemoprotein nature. J. Biol. Chem. 239: 2370-2378.

Potter, W.Z., Davis, D.C., Mitchell, J.R., Jollow, D.J., Gillette, J.R. and Brodie, B.B. (1974). Acetaminophen-induced hepatic necrosis. III. Cytochrome P-450 mediated covalent binding in vitro. J. Pharmacol. Exp. Ther. 187: 203-210.

Prescott, L.F., Wright, N., Roscoe, P. and Brown, S.S. (1971). Plasma-paracetamol half-life and hepatic necrosis in patients with paracetamol overdosage. Lancet 1: 519-522.

Price, V.F. and Jollow, D.J. (1982). Increased resistance of diabetic rats to acetaminophen-induced hepatotoxicity. J. Pharmacol. Exp. Ther. 220: 504-513.

Proudfoot, A.T. and Wright, N. (1970). Acute paracetamol poisoning. Br. Med. J. 3: 557.

Raaflaub, J. and Dubach, U.C. (1975). On the pharmacokinetics of phenacetin in man. Eur. J. Clin. Pharmacol. 8: 261-265.

Rapp, N.S., Zenser, T.V., Brown, W.W. and Davis, B.B. (1980). Metabolism of benzidine by a prostaglandin mediated process in renal inner medullary slices. J. Pharmacol. Exp. Ther. 215: 401.

Reid, W.D. (1973). Mechanism of renal necrosis induced by bromobenzene or chlorobenzene. Exp. Mol. Pathol. 19: 197-214.

Reitman, S. and Frankel, S. (1957). A colorimetric method for determination of serum glutamic oxalacetic and glutamic pyruvic transaminase. Am. J. Clin. Pathol. 28: 56-63.

Rollins, D.E. and Buckpitt, A.R. (1979). Liver cytosol catalyzed conjugation of reduced glutathione with a reactive metabolite of acetaminophen. Toxicol. Appl. Pharmacol. 47: 331-339.

Ross, B., Tange, J., Emslie, K., Hart, S., Smail, M. and Calder, I. (1980). Paracetamol metabolism by the isolated perfused rat kidney. Kidney Int. 18: 562-570.

Rumach, B.H. (1978). Aspirin versus acetaminophen: A comparative view. Pediatrics 62: 943-946.

Rush, G.F., Wilson, D.M. and Hook, J.B. (1983). Selective induction and inhibition of renal mixed function oxidases in the rat and rabbit. Fund. Appl. Toxicol., in press.

Rutkowski, J.V. and Ferm, V.H. (1982). The teratogenicity of aminophenols (AP) in the Syrian Golden Hamster (SGH). Toxicologist 2: A246.

Samuelsson, B., Goldyne, M., Granstrom, E., Hambery, M., Hammarstrom, S. and Malmsten, C. (1978). Prostaglandin and thromboxanes. Ann. Rev. Biochem. 47: 997.

Samuelsson, B., Granstrom, E., Green, K., Hamberg, M. and Hammarstrom, S. (1975). Prostaglandins. Ann. Rev. Biochem. 44: 669.

Schreiner, G.E. (1978). Drug related nephropathy. Contr. Nephrol. 10: 30-41.

Schut, H.A., Wirth, P.J. and Thorgeirsson, S.S. (1978). Mutagenic activation of N-hydroxy-2-acetylaminofluorene in the Salmonella test system: The role of deacetylation by liver and kidney fractions from mouse and rat. Mol. Pharmacol. 14: 682-692.

Shelly, J.H. (1978). Pharmacological mechanisms of analgesic nephropathy. Kidney Int. 13: 15-26.

Smith, W.L. and Bell, T.G. (1978). Immunohistochemical localization of the prostaglandin forming cyclooxygenase in renal cortex. Am. J. Physiol. 235: F451.

Smith, H.W., Finkelstein, N., Aliminosa, L., Crawford, B. and Graber, M. (1945). The renal clearance of substituted hippuric acid derivatives and other aromatic acids in dog and man. J. Clin. Invest. 25: 388-404.

Smith, G.E. and Griffiths, L.A. (1974). Metabolism of N-acylated and O-alkylated drugs by the intestinal microflora during anaerobic incubation in vitro. Xenobiotica 4: 477-487.

Smith, G.E. and Griffiths, L.A. (1976). Comparative metabolic studies of phenacetin and structurally-related compounds in the rat. Xenobiotica 176: 217-236.

Smith, J.N. and Williams, R.T. (1949a). Studies in detoxication 22. The metabolism of phenacetin (p-ethoxyacetanilide) in the rabbit and a further observation on acetanilide metabolism. Biochem. J. 44: 239-241.

Smith, J.N. and Williams, R.T. (1949b). Studies in detoxication 23. The fate of aniline in the rabbit. Biochem. J. 44: 242.

Spuhler, O. and Zollinger, H.U. (1953). Die chronisch-interstitielle nephritis. Z. Klin. Med. 151: 1-50.

Steel, R.G.D. and Torrie, J.H. (1960). Principles and Procedures of Statistics, McGraw-Hill Book Company, New York.

Stygles, V.G. and Iuliucci, J.D. (1981). Structural and functional alterations in the kidney following intake of nonsteroidal anti-inflammatory agents. In Toxicology of the Kidney (J.B. Hook, ed.), pp. 151-178, Raven Press, New York.

Tange, J.D., Ross, B.D. and Ledingham, J.G.G. (1977). Effects of analgesics and related compounds on renal metabolism in rats. Clin. Sci. Molec. Med. 53: 485-492.

Timbrell, J.A., Mitchell, J.R., Snodgrass, W.R. and Nelson, S.D. (1980). Isoniazid hepatotoxicity: The relationship between covalent binding and metabolism in vivo. J. Pharmacol. Exp. Ther. 213: 364-369.

Wilkinson, S.P., Moodie, H., Arroyo, V.A. and Williams, R. (1977). Frequency of renal impairment of paracetamol overdose compared with other causes of acute liver damage. J. Clin. Path. 30: 141-143.

Williams, R. and Davis, M. (1977). Clinical and experimental aspects of paracetamol hepatotoxicity. Acta Pharmacol. Toxicol. 41: 282.

Wirth, P.J., Dybing, E., Von Bahr, C. and Thorgeirsson, S.S. (1980). Mechanism of N-hydroxyacetylarylamine mutagenicity in the Salmonella test system: Metabolic activation of N-hydroxyphenacetin by liver and kidney fractions from rat, mouse, hamster and man. Mol. Pharmacol. 18: 117-127.

Zenser, T.V., Mattammal, M.B., Brown, W.W. and Davis, B.B. (1979). Cooxygenation by prostaglandin cyclooxygenase from rabbit inner medulla. Kidney Int. 16: 688-694.